Hijacking Germ Cells for Cancer:

Examining a 'Dead End' in Male Germ Cell Development

by

Matthew Simon Cook

Department of Cell Biology
Duke University

Date:_____

Approved:

_____
Blanche Capel, Supervisor

_____
Chris Nicchitta, Chair

_____
Sally Kornbluth

_____
Jack Keene

Dissertation submitted in partial fulfillment of
the requirements for the degree of
Doctor of Philosophy in the Department of
Cell Biology in the Graduate School of
Duke University

2010

ABSTRACT

Hijacking Germ Cells for Cancer:

Examining a 'Dead End' in Male Germ Cell Development

by

Matthew Simon Cook

Department of Cell Biology
Duke University

Date:_____

Approved:

_____
Blanche Capel, Supervisor

_____
Sally Kornbluth

_____
Chris Nicchitta

_____
Jack Keene

An abstract of a dissertation submitted in partial fulfillment of the requirements for the degree of Doctor of Philosophy in the Department of Cell Biology in the Graduate School of Duke University

2010

Abstract

Germ cells represent the immortal line: they are guardians of a totipotent genome and are essential for the genetic survival of an individual organism and ultimately a species. An error at any stage in development (specification, migration, colonization, differentiation, adult maintenance) can lead to one of two disastrous outcomes: (1) germ cell death or (2) unchecked growth and proliferation leading to tumorigenesis. The work in this dissertation utilizes a classic mouse model (*Ter*) resulting in both of these phenotypes to explore the molecular mechanisms important for development of germ cells.

A homozygous nonsense mutation (*Ter*) in murine *Dnd1* (*Dnd1*$^{Ter/Ter}$) results in a significant (but not complete) early loss of primordial germ cells (PGCs) prior to colonization of the gonad in both sexes and all genetic backgrounds tested. The same mutation also leads to testicular teratomas only on the 129/SvJ background. Male mutants on other genetic backgrounds ultimately lose all PGCs with no incidence of teratoma formation. It is not clear how these PGCs are lost, develop into teratomas, or what factors directly control the strain-specific phenotypic variation.

Work here demonstrates that *Dnd1* expression is restricted to germ cells and that the *Ter* mutant defect is cell autonomous. The early loss of germ cells is due in part to BAX-mediated apoptosis which also affects the incidence of tumorigenesis on a mixed

genetic background. Moreover, tumor formation is specific to the male developmental pathway and not dependent on sex chromosome composition of the germ cell (XX vs. XY). Despite normal initiation of the male somatic pathway, mutant germ cells fail to differentiate as pro-spermatogonia and instead prematurely enter meiosis.

Results here also reveal that, on a 129/SvJ background, many mutant germ cells fail to commit to the male differentiation pathway, instead maintain expression of the pluripotency markers, NANOG, SOX2, and OCT4, and initiate teratoma formation at the stage when male germ cells normally enter mitotic arrest. RNA immunoprecipitation experiments reveal that mouse DND1 directly binds a group of transcripts that encode negative regulators of the cell cycle, including $p27^{Kip1}$, which is not translated in $Dnd1^{Ter/Ter}$ germ cells. Additionally, overexpression of DND1 in a teratocarcinoma cell line leads to significant alteration of pathways controlling the G1/S checkpoint and the RB tumor suppressor protein. This strongly suggests that DND1 regulates mitotic arrest in male germ cells through regulation of cell cycle genes, serving as a gatekeeper to prevent the activation of a pluripotent program leading to teratoma formation. Furthermore, strain-specific morphological and expression level differences that may account for sensitivity to tumor development are reported here.

Dedication

This dissertation is dedicated to a friend who should have been here to celebrate this occasion, and take his share in the achievement. Alex, we still miss you. I hope that you would have been proud – I will never forget what your friendship meant to me.

Alexander Ney (1978-2008)

Contents

List of Tables

List of Figures

Acknowledgements

I am stardust – without the big bang and subsequent heterogeneity of matter distribution leading to the 'clumping' that resulted in star formation and fusion of hydrogen into higher elements, I would not be here; and for that I am grateful. Aside from the stars, none of this would have been possible without the fearless mentoring abilities of Blanche Capel, to train this sugar-loving biology student into a real scientist. The advice and support from my committee (Brigid, Jack, Sally, Chris, Robin) has been invaluable. Special thanks to Lindsey for being my partner in crime, and chatting with me constantly on g-chat, even when located only an arm's length behind me. Many thanks to all lab members (Lindsey, Steve, Jonah, Samantha, Danielle, Tony, Iordan, and Jen), for reminding me (mostly) of what "normal" vaguely looks like. Thanks to the former trail-blazers in Blanche's lab (Doug, Leo, Hao, Yuna, Maria, Ashley, Eric) who welcomed me with open arms after joining. A special thanks to the many graduate rotation (David, Matt, Lindsey, Chris), undergraduate (Hilary, Jeff, Jen), and high school (Sarvani) students who survived my mentorship.

A great debt of gratitude goes out to my fellow CMBers and Tox kids for keeping me sane and sharing the fun over the years of graduate school: Frank, Emily, Jon, Keaton, Bidong, Marshall, Nicole, Jeff, Bryan, Kyle, Lindsey, Hilary, Alex, Andy, and Laura. I will love my Duke Chapel Choir friends forever: Hilary, Cass, Daniel, Stu,

Henry, Long, Christian, Will, Alden, Patty, Jonathan, and Amanda. Friends outside of school who kept my feet on the ground: Carlo, James, Tony, Chris, Whitney, Sterling, TJ, Holly, Jason, James, Micah, and Ryan. I owe some of my best friendships and favorite discussions at my house (very late at night) to the heathens forming the core group of Atheist Movie Night: Liz, Nik, John, Joel, Nick, Jeff, John, and Martin ("Transposons *disprove* intelligent design!").

Above all, the deepest debt of gratitude I owe is to my parents, Simon and Donna, without whom I would not be the man I am today. Their love and support have provided me a life of which any reasonable person would be outrageously jealous to claim for themselves. More thanks to my loving sister, who has put up with me over the years, and (I hope) will continue to put up with me for many decades to come. Thanks to my grandparents Norma Cook, Simon Hoy Cooke Sr., and Louise Rogers, as well as extended family: Debra, Bookie, Jed, Tori, and Jeremy.

I would also like to thank my undergraduate mentor, John Stiller, for demonstrating the elegance and power of scientific inquiry, and giving me the motivation to pursue a life that embraces reason.

> Experience without theory is blind, but theory without experience
> is mere intellectual play.
>
> Immanuel Kant (*1724-1804*)

1. Introduction

1.1 Mouse Germ Cell Development

An interesting feature of germ cells is that they are specified at such an early stage in the developmental process that there is no proper gonad formed in which they can reside and carry out their function of gametogenesis. This forces the germ cells to migrate through the developing embryo to reach the gonad, struggling to maintain their identity in a milieu of molecular signals. After arriving in the gonad, mammalian germ cells commit to their sex-specific fate and differentiate as pro-spermatogonia in testes or oocytes in ovaries (for review see (Western, 2009)). Males contain a spermatogonial stem cell that resides in the testis and produces spermatozoa for the lifetime of the organism, whereas females are endowed with a limited number of oocytes that will mature over the course of many months until depleting the original supply. For a timeline of these events see Figure 1.

1.1.1 Specification and Migration

Mammalian primordial germ cells (PGCs) of both sexes are induced to form from somatic progenitors at E6.5 in the epiblast by specific signaling molecules, such as BMP4, patterning the border of the extraembryonic ectoderm (Lawson et al., 1999; Ohinata et al., 2009). This is in contrast to the process of preformation used to specify germ cells in organisms such as *C. elegans* and *Drosophila* (Strome and Lehmann, 2007).

Figure 1 – Timeline of germ cell development. PGCs are specified in the mouse embryo at E6.5, migrate to the gonads, and arrive between E10.0 and E11.5. Until E12.5, EG cells can be efficiently derived from germ cells. After arrival in the gonads, germ cells initiate sex-specific patterns of development. In the ovary they enter meiosis at E13.5 and arrest just after birth at the end of the first prophase. In the testis, germ cells are enclosed in testis cords by E12.5, and arrest in mitosis at E13.5. Mitosis resumes after birth, when mGS cells can be derived from spermatogonia.

Figure 1

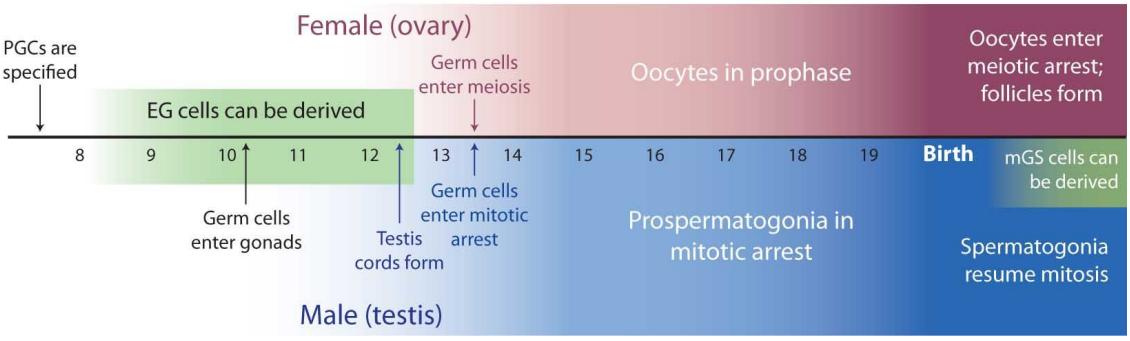
Female (ovary)
PGCs are specified
EG cells can be derived
Germ cells enter meiosis
Oocytes in prophase
Oocytes enter meiotic arrest; follicles form
8
9
10
11
12
13
14
15
16
17
18
19
Birth
mGS cells can be derived
Germ cells enter gonads
Testis cords form
Germ cells enter mitotic arrest
Prospermatogonia in mitotic arrest
Spermatogonia resume mitosis
Male (testis)

Germ cell specification involves (1) the silencing of genes associated with somatic cell differentiation (eg. Hox genes), likely through the action of *Blimp1* and other chromatin modifying complexes (Ancelin et al., 2006; Saitou, 2009), (2) the maintenance of markers associated with pluripotency (*Oct4*, *Nanog*, and *Sox2*), which likely exert global transcriptional control, and (3) the activation of germ cell-specific genes (eg. *Dnd1*, *Tdrd1*, and *Nanos3)*, many of which are RNA-binding proteins (RBPs) involved in translational regulation (Ohinata et al., 2006; Yabuta et al., 2006).

Once specified, germ cells enter the hindgut by E8.5 and migrate along the dorsal aorta until they reach the genital ridge. During this time they proliferate approximately every sixteen hours (Buehr et al., 1993) and require specific survival factors to prevent apoptosis and promote cell division. Several factors known to be required for survival *in vivo* include *c-kit*, *kit-l*, TIAR, *Fgfr2-IIIb*, *Nanos3*, *Dnd1*, and *Mvh* (Beck et al., 1998; Sakurai et al., 1995a; Suzuki et al., 2008; Takeuchi et al., 2005; Tanaka et al., 2000; Zhao and Garbers, 2002). During active migration, guidance cues such as SDF-1 and its receptor CXCR4 (Molyneaux et al., 2003) as well as *c-kit* and *kit-l* (Buehr et al., 1993; Mintz and Russell, 1957), are necessary to keep PGCs from traveling off course. PGCs that migrate to ectopic locations are eliminated by BAX-mediated apoptosis (Stallock et al., 2003). From a founding population of only a few dozen PGCs, thousands will reach the genital ridges to populate the bipotential gonads by E11.5 (Godin et al., 1990).

1.1.2 Colonization and XY-Specific Germ Cell Development

Once PGCs colonize the gonad, they undergo a reprogramming process that leads to their sex-specific differentiation. Survival and commitment of XY germ cells to the male fate is dependent on expression of *Fgf9* in somatic cells (DiNapoli et al., 2006) and *Nanos2* in germ cells (Suzuki and Saga, 2008). Null mutations of these genes, or other downstream genes involved in blocking the activity of retinoic acid, like *Cyp26b1* (Bowles et al., 2006), lead to transient up-regulation of meiotic markers (typical of female germ cells during this stage of fetal development) and subsequent germ cell death.

Between E12.5 and E13.5, male germ cells begin differentiation as pro-spermatogonia marked by expression of *Gm114* (Tang et al., 2008) and *Nanos2* (Suzuki and Saga, 2008), and enter mitotic arrest in G0 until after birth (Matsui, 1998; McLaren, 1984; Western et al., 2008). Genes associated with initiation of mitotic arrest include the cell cycle regulators $p27^{Kip1}$, $p21^{Cip1}$, and $p16^{Ink4a}$ (Western et al., 2008). Interestingly, germline null mutations in the cell cycle gene *Pten* at this stage lead to teratoma development (Kimura et al., 2003). As germ cells exit cell cycle and become quiescent, the pluripotency genes *Nanog* and *Sox2* are downregulated (Durcova-Hills and Capel, 2008). Male germ cells do resume mitosis until after birth (Fig. 1).

The signal responsible for directing male germ cells to mitotically arrest and differentiate as pro-spermatogonia (and repress meiotic initiation) remains unknown but is thought to originate from Sertoli cells (McLaren, 1988; McLaren and Southee, 1997).

Recently, it has been demonstrated that *Sdmg1*, a transmembrane protein expressed only in males, is necessary for proper localization of the secretory SNARE Stx2 and endosome trafficking within Sertoli cells (Best et al., 2008). Importantly, inhibition of this secretion pathway in gonad cultures resulted in the entry of male germ cells into meiosis, often referred to as male-to-female germ cell sex reversal. Further experiments are necessary to determine the molecular identity of the secreted signal.

1.1.3 RNA Binding Proteins in Germ Cell Development

PGC development is tightly controlled both at the transcriptional level, and at the post-transcriptional level, by RNA-binding proteins (RBPs). Critical roles for RBPs in the early germline have been studied extensively in other species (Raz, 2000; Seydoux and Braun, 2006). For example, the RBP Nanos is required for the establishment of the germ cell lineage in *Drosophila* (Forbes and Lehmann, 1998; Lehmann and Nusslein-Volhard, 1991), and is one of the most functionally conserved genes important for germ cell development in most metazoans ranging from sea urchins to humans (Fujii et al., 2006; Jaruzelska et al., 2003); deletion of Nanos results in a failure to adopt a germ cell identity. In the *C. elegans* germline, RBPs regulate the decision between mitosis and meiosis (Kimble and Crittenden, 2005).

RBPs are also associated with the "nuage", "p-bodies" or "germ-cell granules" in various non-mammalian species where they sequester target mRNAs and regulate their stability and/or translation (Seydoux and Braun, 2006). They are also involved in germ

cell regulation in mammals (Fujiwara et al., 1994; Hosokawa et al., 2007; Sada et al., 2009; Suzuki and Saga, 2008; Suzuki et al., 2008; Tanaka et al., 2000). RBPs that are important in germ cell specification and differentiation in mice include Mouse vasa homolog (*Mvh*), *Nanos3*, *Nanos2*, *Tdrd6*, *Tdrd7*, *Boule*, *Pumilio2*, *Tiar*, *Dazl*, and *Dnd1* (Beck et al., 1998; Hosokawa et al., 2007; Lin and Page, 2005; Suzuki and Saga, 2008; Tanaka et al., 2000; Urano et al., 2005; Youngren et al., 2005). Of these RBPs, only mutations in *Dnd1* have resulted in teratoma formation (Noguchi and Noguchi, 1985; Stevens, 1973; Youngren et al., 2005).

RBPs can regulate expression of sets of targets resulting in control over broad cellular functions. For example, the RBP HuR can promote an anti-apoptotic program through its regulation of a host of transcripts involved in cell death and survival (Abdelmohsen et al., 2007; Keene, 2007). RBPs can act as translational regulators of cell cycle in germ cells. It has been established that Nanos and Pumilio function to repress translation of maternally deposited *Cyclin B* in *Drosophila* PGCs (Kadyrova et al., 2007), and it has been more recently documented that GLD-1 translationally represses *Cyclin E* in *C. elegans* germ cells, thus preventing premature mitotic division and embryonic gene activation, ultimately leading to teratoma formation (Biedermann et al., 2009). While many invertebrate studies have determined a mechanism of action for several conserved RBPs, we still have a very limited understanding of the role that RBPs play in the regulation of the mammalian germ cell genome.

1.2 Germ Cells as Stem Cells

While germ cells normally give rise only to male and female gametes, they are carriers of the totipotent information necessary to generate a complete organism. Induced pluripotent cells have now been generated from many cell types (Yamanaka, 2009); however germ cells are an efficient starting population. During their proliferative migratory period, and until about two days after their arrival in the gonad, germ cells explanted to culture and placed under the influence of a specific cocktail of signals readily form embryonic germ cells (EG cells), a pluripotent cell with properties similar to ES cells (Cheng et al., 1994; Donovan and de Miguel, 2003; Labosky et al., 1994a).

However, by approximately E12.5, XX and XY germ cells lose this property coincident with their transition to sex-specific differentiation (Figure 1). Both XX and XY germ cells cease cell divisions at approximately E13.5, a few days after they arrive in the gonad. Female germ cells enter meiosis and arrest at the end of the first prophase. By contrast, XY germ cells enter mitotic arrest and transition to a population of pro-spermatogonia (for review, see (Bowles and Koopman, 2007)). After birth, pro-spermatogonia move to the periphery of testis cords, resume mitosis, and establish the male germline stem cell population of the adult testis (called spermatogonial stem cells, SSCs). SSCs retain the potential to renew their own population, but are normally restricted to give rise only to sperm throughout the lifetime of the male. However, SSCs from the neonatal and adult testis readily form multipotent stem cell lines (mGS cells)

under-specific *in vitro* conditions (Guan et al., 2006; Kanatsu-Shinohara et al., 2004; Kanatsu-Shinohara et al., 2008a). Interestingly, germ cells from mice mutant for the cell cycle regulator, *Trp53*, show a higher efficiency of transformation to mGS cells (Kanatsu-Shinohara et al, 2008) and EG cells can be derived more efficiently from migratory PGCs with a constitutively active form of Akt (Kimura et al., 2008).

The facility with which transitions can be induced suggests a close relationship between the genomic programming of a germ cell and the genomic programming of a multipotent stem cell. A comparison of the transcriptional profiles between GS cells (capable only of renewing the spermatogonial stem cell population) and mGS cells (capable of contributing to all cells of the embryo) revealed differences in the levels of pluripotent transcription factors and in DNA methylation patterns (Kanatsu-Shinohara et al., 2008b). The potential to proliferate indefinitely and escape growth control is normally harnessed in the fetal and adult testis by intrinsic mechanisms within the germ cells and by the somatic cell niche within testis cords. However, the incidence of testicular germ cell tumors in humans is high, highlighting the importance of the regulatory controls that suppress the potential for germ cells to escape to a multipotent state capable of unregulated growth and differentiation.

1.3 Testicular Teratomas

Nowhere is the potential for misregulation of germ cells more evident than in testicular teratomas (Fig. 2). These tumors arise spontaneously in young boys as non-seminomatous germ cell tumors, characterized by the differentiation of a diverse array of cell and tissue types within the tumor, including cartilage, muscle, hair, and glandular tissue as well as a cluster of stem-like cells from which the tumor can be propagated (for review see (Solter, 2006)). These unusual tumors reflect the close relationship between germ cells, stem cells, and tumor cells, and hold important clues about the maintenance of, and transition between, these cell fates.

1.3.1 Teratomas and *Ter* Mice

Germ cell tumors (GCTs) are the most frequent cause of cancer in men between the ages of 15 and 40 (Hussain et al., 2008). Although spontaneous testicular teratomas are virtually non-existent in mice, Leroy Stevens established a substrain of mice in the 1950s (129/SvJ) in which the incidence of spontaneous teratomas is approximately 1% (Stevens and Little, 1954). Teratomas can be experimentally induced by transplantation of a 129/SvJ (129/SvJ) wild type testis, or an egg cylinder stage embryo to an ectopic site, presumably reflecting the vulnerability of wild type germ cells to escape from the controls of their niche and undergo reprogramming, even in the absence of specific defects.

Figure 2 – Bilateral testicular teratoma. (Top) Large bilateral testicular teratomas from a P17 mouse compared to **(Bottom)** a pair of P17 sterile testes. Scale bares represent 1cm.

Figure 2

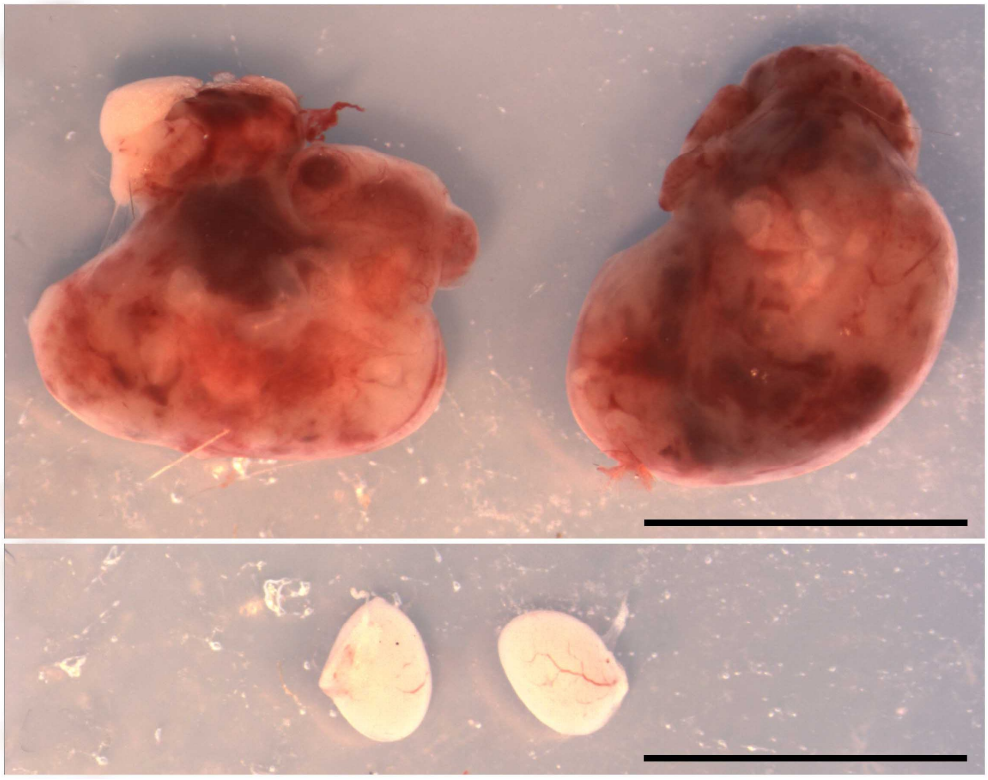

In 1973 Stevens discovered a mutation on the 129/SvJ genetic background (called *Ter*) that raised the incidence of spontaneous teratomas to approximately 30% (Stevens, 1973). It was discovered later that the mutation segregated in Mendelian ratios such that heterozygous and homozygous mice had a tumor incidence of 17% and 94% respectively (Noguchi and Noguchi, 1985). Despite the high incidence on the 129/SvJ background, when *Ter* was crossed onto other inbred strains, such as C57BL/6J, there was no occurrence of testicular teratoma (Sakurai et al., 1995b). Unknown loci on the 129/SvJ X-chromosome, the MOLF chromosome 19, *Trp53*, *eIF2β*, and $Kitl^{Sl}$ have now been implicated as potential modifiers of the tumor phenotype and many of these are being investigated by the Nadeau laboratory (Hammond et al., 2007; Heaney et al., 2009; Lam et al., 2007; Lam and Nadeau, 2003).

Interestingly, the variable penetrance of the tumor phenotype in *Ter* mice of different genetic backgrounds faithfully mimics the etiology of the human disease, where the incidence of germ cell tumors is correlated with ethnicity and other complex genetic influences that have not been explained (Brown et al., 1987; Brown et al., 1986; Hussain et al., 2008; Linger et al., 2007; Looijenga, 2009; Oosterhuis and Looijenga, 2005). Remarkably, the *Ter* mutation has been implicated in a novel mechanism of epigenetic inheritance termed trans-generational epistasis, whereby any of six other genetic modifiers in combination with *Ter* (in either male or female parent) increase susceptibility to teratomas in *Ter*/+ heterozygous offspring (Lam et al., 2007).

1.3.2 Discovering *Dnd1*

The identity of the *Ter* locus was finally mapped to a gene called *Dead end 1* (*Dnd1*), which is expressed in PGCs and only found in vertebrates (Youngren et al., 2005). Importantly, in situ analyses have indicated *Dnd1* expression at all stages of germ cell development (Fig. 3). Although teratomas in 129/SvJ *Ter* ($Dnd1^{Ter/Ter}$) mice are male-specific, both sexes show a severe, but incomplete, loss of PGCs early in development on all genetic backgrounds (Sakurai et al., 1995a). It is not known how PGCs are lost in $Dnd1^{Ter/Ter}$ mutants, or what strain-specific differences contribute to teratoma formation. In zebrafish, where the *Dnd* phenotype was originally characterized, morphant embryos contain PGCs that are specified but never exhibit motile characteristics, and thus fail to migrate to the site of the developing gonad and are lost completely (Weidinger et al., 2003). In mice, although the normal number of PGCs is specified, there is an immediate decline in germ cell population size in mutant embryos compared to wild-type, beginning at the time of migration (approximately E8.5) (Sakurai et al., 1995a). However, unlike the zebrafish phenotype, no migration defect was detected in mice. The cause for decreased population size is unknown: it could be the result of proliferation defects, active cell death, or even differentiation during migration.

Figure 3 – *Dnd1* is expressed in germ cells at several transitional stages of their development. During PGC specification, migration through the hindgut, colonization of the gonad, and maintenance in the adult testis, *Dnd1* transcript is expressed. Current data demonstrate a necessary role for *Dnd1* in the initial expansion of PGCs during migration and for normal development down a male pathway after colonization of the testis. The role of *Dnd1* in adult germ cells remains unclear.

Figure 3

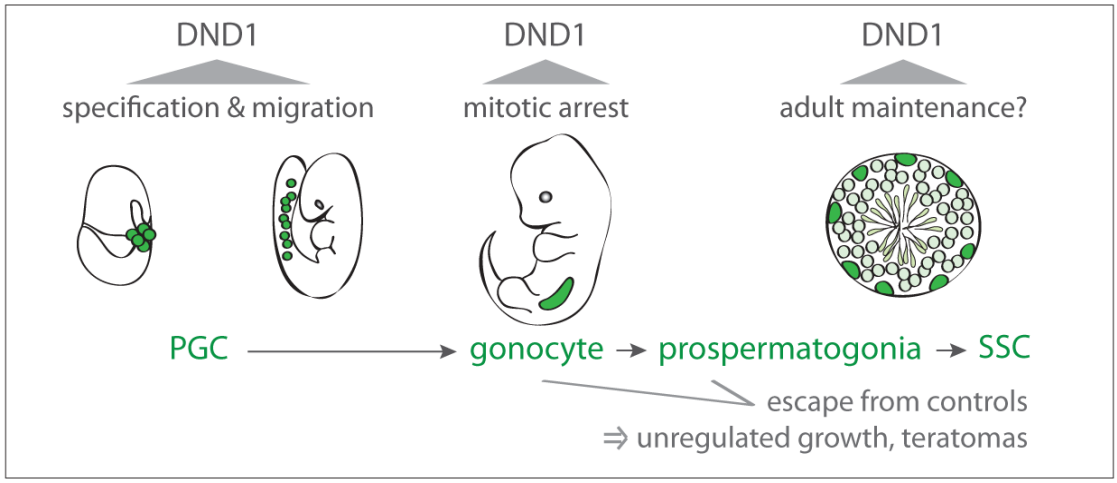
DND1
DND1
DND1
specification & migration
mitotic arrest
adult maintenance?
PGC
gonocyte
prospermatogonia
SSC
escape from controls
⇒ unregulated growth, teratomas

In *Xenopus*, the 3′ untranslated region (UTR) is essential for the differential localization of *Dnd* mRNA to the vegetal pole of oocytes (Horvay et al., 2006). In zebrafish, cis-acting elements within the *Dnd* transcript, including the RNA recognition motif (RRM), are necessary for the translocation of the protein from the nucleus to the germ granules of the cytoplasm (Slanchev et al., 2008). Interestingly, chicken DND is expressed in germ cells only as a nucleoprotein at both embryonic and adult stages (Aramaki et al., 2009). In both *Xenopus* and zebrafish *Dnd* morphant embryos, unlike mutant mice, no germ cells migrate properly or successfully populate the gonad. Additionally, no tumor formation has been reported in either *Xenopus* or zebrafish morphants (Horvay et al., 2006; Slanchev et al., 2008; Weidinger et al., 2003). This suggests that tumor formation in mice may be dependent upon the loss of *Dnd1* in the few mutant germ cells that colonize the gonad, not from the early defect after specification. Additionally, while important for survival/proliferation, the role for *Dnd1* in PGC migration/motility does not appear to be conserved in mice.

By the time germ cells have arrived in the gonad (E11.5), wild-type germ cells number in the thousands while only several dozen persist in the *Dnd1*$^{Ter/Ter}$ gonad. On most genetic backgrounds, adult *Dnd1*$^{Ter/Ter}$ males are completely sterile, with no germ cells remaining and no evidence of teratomas after birth. By contrast, in the 129/SvJ testis, germ cells are either lost or give rise to teratomas in approximately 94% of homozygous mutants during fetal development (Noguchi and Noguchi, 1985). Female

Dnd1$^{Ter/Ter}$ mice on the 129/SvJ background (and all other backgrounds tested) are subfertile but show no incidence of teratoma formation indicating that either the XX germ cell or the ovarian environment is not susceptible to this pathway of teratoma formation.

Recent studies have revealed that human and zebrafish DND1 can control miRNA regulation of gene expression by binding to uridine-rich regions (URRs) in the 3′-UTRs of target mRNAs, and protecting them from miRNA-mediated translational repression (Kedde et al., 2007b). Four mRNA targets of DND1 in human cell lines and zebrafish embryos were identified through a candidate approach. As targets for DND1, the authors functionally identified the zebrafish transcripts *nanos* and *tdrd7*, two RBPs essential for germ cell migration in zebrafish, as well as human *p27*^{Kip1} and *Lats2*, two genes involved in cell cycle regulation (Koprunner et al., 2001; Mishima et al., 2006). These four genes likely represent a small subset of the genes regulated by DND1. There has not been a comprehensive screen to identify the host of targets potentially bound by DND1.

The four targets already identified are potentially important for mammalian germ cell regulation at different stages of development. In mammals, Nanos and Tudor orthologs are expressed and associated with germ cell specification and differentiation (Hosokawa et al., 2007; Suzuki and Saga, 2008; Suzuki et al., 2008). The early *Dnd1*$^{Ter/Ter}$

phenotype resembles the *Nanos3*-null phenotype, but a direct relationship has not been shown.

Because teratoma formation likely involves both cell autonomous and paracrine signaling, it is important to determine whether *Dnd1* expression is restricted to germ cells in the developing gonad, or also extends to the somatic cells that surround germ cells and regulate their development. *In situ* expression studies reveal *Dnd1* transcripts in the genital ridge of developing male and female gonads. In E12.5-E14.5 XY gonads, the expression pattern is limited to testis cords, which contain both Sertoli cells and germ cells (Youngren et al., 2005). One group has shown that the transformed Sertoli cell lines TM4, 15P-1, and MSC1 do not express DND1 (Bhattacharya et al., 2007). However, a conflicting report demonstrated that $Dnd1^{Ter/Ter}$ mutant gonadal somatic cells failed to support cultures of wild-type or mutant germ cells, suggesting a secreted *Ter*-dependent factor necessary for germ cell survival (Takabayashi et al., 2001). It is important to distinguish whether *Dnd1* is indeed expressed in Sertoli cells, or whether mutations in this gene are limited to a cell-autonomous effect on germ cells. Interestingly, mutations in the transcription factor *Dmrt1*, which is expressed in both germ and Sertoli cells, lead to a high incidence of testicular teratomas on a 129/SvJ background (Krentz et al., 2009).

The work in this dissertation will further define the nature of the *Dnd1* defect in $Dnd1^{Ter}$ mice, uncover new putative mRNA targets, and demonstrate a role for this RBP

linking cell cycle and differentiation in the commitment of XY germ cells to a pro-spermatogonial fate. In addition, work here suggests a further role for *Dnd1* in the adult maintenance of germ cells and provides the first evidence for strain-specific differences in morphology and gene expression that possibly account for teratoma susceptibility.

2. Materials and Methods

2.1 Mice, timed matings, and genotyping

Dnd1$^{Ter/+}$ mice were provided by Dr. Joseph Nadeau at Case Western Reserve University and maintained on the 129/SvJ background. *Bax*$^{+/-}$ mice (1-Baxtm1Sjk/J C57BL/6J.129/SvJ) were imported from Jackson Laboratories and maintained on a mixed genetic background (129/SvJ;C57BL/6J). *Dnd1*$^{Ter/+}$ mice were crossed to *Bax*$^{+/-}$ mice and the F1 offspring were intercrossed to maintain the line and obtain double heterozygous animals for timed matings. *Oct4-EGFP* mice were maintained as a homozygous line on a C57BL/6J background. Eventually, all of these alleles were combined and backcrossed at least 10 generations to a pure 129/SvJ or C57BL/6J background. *Sox9-ECFP* mice were maintained as a homozygous line on a C57BL/6 background and outcrossed to CD-1 for timed matings. XY *Sry*^{MYC} mice were maintained on a 129/SvJ strain, crossed to *Dnd1*$^{Ter/+}$ mice to obtain heterozygotes, and the progeny were mated with *Dnd1*$^{Ter/+}$ females. For all timed matings, males and females were setup in the afternoon and the next morning females were checked for plugs and counted as day E0.5 if positive. Tail DNA was extracted using standard methods and genotyped according to previously published protocols (Cook et al., 2009). *Bax* mice were genotyped using the protocol found on the Jax website. *Sry*^{MYC} mice were genotyped by PCR using an annealing temperature of 60^{o}C and running the 130bp product on a 2% agarose gel. *Dnd1*^{Ter} mice were genotyped by PCR using an annealing temperature of 62^{o}C. The PCR product (145bp) was digested

overnight at 37°C with the restriction enzyme DdeI and run on a 4% agarose gel or 7% acrylamide gel. DdeI digestion of DNA from mice with the *Dnd1*^{Ter} mutation produces 123bp and 22bp products.

2.2 Immunofluorescence and histology

Fluorescent immunocytochemistry was performed on whole mount or cryosectioned gonads that were fixed overnight at 4°C in 4% PFA, washed in PBS for whole mount antibody staining, or put through a sucrose gradient (10%, 15%, 20%, 20%:OCT 1:1 overnight at 4°C) before embedding in OCT for sectioning. Antibodies (Rat anti-GCNA1 (kindly provided by George Enders 1:50), Rabbit anti-MVH (Abcam cat. #ab13840 1:500), Rat anti-E-CADHERIN (Zymed Laboratories cat. #13-1900 1:500)), Rabbit anti-NANOG (Cosmo Bio cat. #RCAB0002P-F 1:300), Rabbit anti-SOX2 (Chemicon cat. #Ab5603 1:1000), Rabbit anti-OCT4 (Abcam cat. #ab19857-100 1:500), Rabbit anti-LAMININ (kindly provided by Dr. Harold Erickson 1:500), Rabbit anti-P27^{Kip1} (Santa Cruz cat. #sc-529 1:250), Rabbit anti-Ki67 (NeoMarkers cat. #RM-9106-S 1:500), Rabbit anti-GM114 (generated in our lab (Tang et al., 2008) 1:500), Rabbit anti-SCP3 (Novus cat. #300-231 1:500), Rabbit anti-STRA8 (kindly provided by Dr. Pierre Chambon 1:500), Rabbit anti-DMRT1 (kindly provided by Dr. David Zarkower 1:500), Rabbit anti-phostpho-Histone H3 (Cell Signaling 9701S 1:500), Rabbit anti-SOX9 (Millipore/Chemicon AB5535 1:500), Rat anti-PECAM (BD Pharmingen 553370 1:500),

Rabbit anti-phospho-AKT-308 (Cell Signaling 4056 1:500), Rabbit anti-phospho-AKT-473 (Cell Signaling 4058 1:500), Rabbit anti-CASPASE-3 (BD Pharmingen 557038 1:500), and Rabbit anti-FOXA2 (kindly provided by Dr. Brigid Hogan 1:1000)), were added to the blocking solution (PBS and 0.1% Triton X-100, 3% BSA, and 10% heat-inactivated goat serum) and incubated rocking overnight at 4°C (or stationary for sections). Samples were washed four times over a 30 minute period in washing solution (PBS and 0.1% Triton X-100, 3% BSA, and 1% heat-inactivated goats serum), and then incubated 1 hour at room temperature in blocking solution with Cy2-, Cy3-, or Cy5-conjugated secondary antibodies (1:500; Jackson Immunoresearch). Samples were then washed four times for 30 minutes total in washing solution, then mounted in DABCO and imaged on a Zeiss LSM510 confocal microscope. For histology, gonads were dissected and fixed in Bouin's solution overnight, then washed thoroughly in 70% ethanol. After embedding in paraffin, gonads were sectioned (5um), stained with haematoxylin and eosin, and mounted in DABCO.

2.3 Flow cytometry, RNA extraction, and RT-PCR

Gonads at the specified stages were dissected and separated from the mesonephros, collected on ice in PBS, and trypsinized at 37°C for 15 minutes. The trypsin was removed and 500uL of Dulbecco's Modified Eagle Medium was added to stop the reaction. The tissue was drawn through a 27 ½ gauge needle to break up cells,

then put over a cell strainer and spun down briefly to collect the flow through. The suspension was subjected to fluorescence activated cell sorting (FACS) at a core facility, which allows for the isolation of populations of cells based on the presence of a fluorescent label. ECFP-positive or (EGFP-positive) and negative cell fractions were obtained in PBS and centrifuged to pellet the cells. The PBS was aspirated and a total RNA extraction was performed using TRIzol® (Invitrogen) and chlorophorm with a 100% isopropanol precipitation and 75% ethanol wash. For whole tissue RNA extraction, gonads were dissected from the mesonephros and either stored in RNALater or immediately put in TRIzol as described above. cDNA was generated from RNA using the iScript™ cDNA Synthesis Kit (Bio-Rad) according to the manufacturer's protocol. For the end-point RT-PCR, thermal cycler reactions were performed on each cDNA fraction using primers for *Dnd1, Sox9*, *Oct4*, and *HPRT* using an annealing temperature of 62°C for 29 cycles. Each primer set was designed to span an intron and one primer from each set to overlap an exon-exon boundary by at least 7-nucleotides on each side. Sequences for these primers can be found in Table 1. The products were run on a 2% agarose gel and imaged using a Bio-Rad gel-doc and Quantity One software imaging system.

2.4 qRT-PCR

Quantitative RT-PCR was used to determine relative expression levels of transcripts in XY gonads of different genotypes and strain backgrounds. Gonad

dissection, RNA extraction, and cDNA synthesis have all been described previously (Cook et al., 2009). For qPCR each analysis was performed in triplicate in a total volume of 20uL reaction mix containing 1.25uL cDNA template, 10uL 2X SensiMix*Plus* SYBR® (Quantace, cat# QT615-02), 4.75uL RNase-free water, and 4uL 1uM gene-specific forward/reverse primers (200nM final concentration each). qPCR was performed on an iCycler™ Thermal Cycler (Bio-Rad, cat# 170-8720). Cycling conditions for all primers were as follows: 95°C for 3 min (one cycle); 95°C for 15 sec, 62°C for 30 sec, 72°C for 30 sec (40 cycles); and 72°C for 5 min (one cycle). Specific sequences for all primers can be found in Table 1. Primer sets were tested for efficiency and found to work optimally with the delta-Ct method. Target gene Ct thresholds were determined and normalized to *Hprt, Oct4*, or *Canx*.

2.5 miRNA Analysis

The *mir*Vana™ miRNA Isolation Kit (Ambion cat# AM1560, AM1561) and *mir*Vana™ qRT-PCR miRNA Detection Kit (Ambion cat# AM1558) were used to extract and detect small RNAs. E14.5 CD-1 testes were dissected and stored in RNA*later*™ (Qiagen cat# 1018087) until 20 pairs had been obtained. Small RNAs were extracted from these testes and an E12.5 liver, and miR-221, miR-222, and 5S rRNA were detected by qRT-PCR using the kit according to the manufacturer's protocol.

Table 1 – List of all primers used for RT- and qRT-PCR.

Table 1		
Gene	Forward	Reverse
Akt1	5′-CATCCCTTCCTTACGGCCCT-3′	5′-CATGAGGTTCTCCAGCTTCAGGT-3′
Akt2	5′-TTCCTTACAGCCCTCAAGTATGCC-3′	5′-GATCCTCCGTGAAGACTCGCTC-3′
Akt3	5′-CAGAGGAAAGAGAAGAGTGGACGG-3′	5′-GGGTTGTAGACGCATCCATCTC-3′
Bax	5′-TACAGGGTTTCATCCAGGATCGAG-3′	5′-GCAATCATCCTCTGCAGCTCC-3′
Cyclin E1	5′-GCCCTCTGACCATTGTGTCC-3′	5′-GCACCACTGATAACCTGAGACCT-3′
Cyclin E2	5′-AGAAAGCTTCAGGTTTGGAATGGG-3′	5′-CTCTTTGGTGGTGTCATAATGCCT-3′
Cyp26b1	5′-AGGAGCTGAAGGATGGAACCC-3′	5′-TGACCTCCTTGATGACACAGTCC-3′
Dhh	5′- GCCTGATGACAGAGCGTTGC-3′	5′- GAGTGAATCCTGTGCGTGGTG-3′
Dmrt1	5′-GGAAACCAGTGGCAGATGAAGAC-3′	5′-AGGACGCAGACTCACATTCCA-3′
Dnd1	5′-GCCCTGGTAGAAGGTCAGTCAC-3′	5′-GCCCTGTTCCTAAACACTTGGTC-3′
Fgf9	5′-CAGGGAACCAGGAAAGACCA-3′	5′-GAGGTAGAGTCCACTGTCCAC-3′
Gapdh	5′-AGGTCGGTGTGAACGGATTTG-3′	5′-TGTAGACCATGTAGTTGAGGTCA-3′
Gm114	5′-ACTGTTTCAGTTCAGCTTGGGAG-3′	5′-GCTTTCGTGCCTTGACAAAGGA-3′
Hprt1	5′-TGGACTGATTATGGACAGGACTGAA-3′	5′-TCCAGCAGGTCAGCAAAGAACT-3′
Lats2	5′-CCGCTTCTACATTGCAGAGTTGAC-3′	5′-CTGTCTCATGTGGTTCCCTTTCTG-3′
Mvh	5′-TACTGTCAGACGCTCAACAGGA-3′	5′-ATTCAACGTGTGCTTGCCCT-3′
Nanog	5′-TGAGCTATAAGCAGGTTAAGAC-3′	5′-CAATGGATGCTGGGATACTC-3′
Nanos2	5′-GACCATCCATCTATCTTCACCT-3′	5′-CCTCCTCTAGTTCCTGTAACC-3′
Nanos3	5′-CCGTGCCATCTATCAGTCCC-3′	5′-CATCCTGTGTCTTTGCCTTGTC-3′
Oct4	5′-GGAGGAAGCCGACAACAATGA-3′	5′-TCCACCTCACACGGTTCTCAA-3′
P21^{Cip1}	5′-GCCTTGTCGCTGTCTTGCAC-3′	5′-CTCCTGACCCACAGCAGAAGAG-3′
P27^{Kip1}	5′-GGTTAGCGGAGCAGTGTCCA-3′	5′-ATGTCCATTCAATGGAGTCAGCGA-3′
PRB	5′-AGAAGGTCTGCCAACACCCA-3′	5′-GTTCGAGTGGAAGTCATTTCTGCC-3′
Pten	5′-AACTTGCAATCCTCAGTTTGTGGT-3′	5′-GAGGTTTCCTCTGGTCCTGGT-3′
Sox2	5′-TGGACTGCGAACTGGAGAAGG-3′	5′-TGCGTTAATTTGGATGGGATTGGT-3′
Sox9	5′-GCGGAGCTCAGCAAGACTCTG-3′	5′-ATCGGGGTGGTCTTTCTTGTG-3′
Trp53	5′-TCACTCCAGCTACCTGAAGACC-3′	5′-AGTCATAAGACAGCAAGGAGAGGG-3′
Zfp42	5′-TGGAATCAAAGCTCCTGCACAC-3′	5′-TGCCTCGTCTTGCTTTAGGGT-3′

2.6 Cell culture, Western blot analysis, and RNA immunoprecipitation

Mouse 3T3 cells were transfected with vectors encoding GFP, GFP-DND1α, TAP, or TAP-DND1α. For GFP imaging cells were fixed in 4% PFA, washed in PBS, stained for two hours with Propidium Iodide (PI), washed in PBS, and mounted in DABCO for imaging on a Zeiss 510 Meta confocal microscope. For RNA Immunoprecipitation (RIP) and Western blot analysis, 3T3 cells were lysed 24 hours after transfection in appropriate lysis buffer. For Western blot analysis, extracts were separated on a 4-20% gradient SDS-PAGE gel and transferred to nitrocellulose. Rabbit anti-TAP (Open Biosystems WB 1:10,000) was used as a primary antibody and a horseradish peroxidase-conjugated anti-rabbit antibody was used for secondary at 1:5000. Western blots were developed with ECL (Amersham™) and exposed to film (Kodak). RIP was performed as published previously (Keene et al., 2006). Briefly, lysed cells were immediately frozen at -80°C to prevent adventitious binding. IgG Sepharose beads (Amersham) were washed three times in wash buffer and 100uL lysate was added to 850uL NT2 buffer, 2uL RNaseOUT (Invitrogen), 2uL VRCs (Sigma), 10uL 1M DTT, and 40uL 0.5M EDTA. After two hours of incubation at room temperature the beads were pelleted and washed six times with wash buffer. TRIzol was added directly to the beads to perform an RNA extraction followed by cDNA synthesis and qRT-PCR as described above.

2.7 Microarray and analysis

P19 cells were transfected via Lipofectamine 2000 (Invitrogen®) with a construct encoding either GFP-DND1 or GFP alone. After 24 hours of recovery, cells were collected and RNA was extracted using the RNeasy Mini Kit (Qiagen). After quality assessment using a NanoDrop (Thermo-Scientific), RNA was provided to the Duke array core facility to run an Affymetrix® Mouse Gene 1.0 ST array. Three biological replicates were run for each construct and data was downloaded into Microsoft Excel for analysis with ArrayTools.

2.8 In situ hybridization

Gonads were dissected, fixed in 4% paraformadlehyde (PFA) overnight at 4°C, washed in 0.1% Tween-20/PBS, dehydrated in 100% methanol and stored at -20°C until used. Full-length *Dnd1*, cloned into pGEM®-T Easy vector (Promega) was used as a probe. In situ hybridization on gonads was performed as described previously (Henrique et al., 1995; Kim et al., 2006). A digoxigenin labeled RNA probe for *Dnd1* was detected using an alkaline phosphatase-conjugated anti-digoxigenin antibody.

2.9 Gonad cultures

CD-1 gonads with mesonephroi attached were dissected at E13.5 and placed in media containing 10% FBS and either given concentrations of an inhibitor or equal

amounts of DMSO for control. Cultures were carried out in 30uL volumes and in humidified chambers at 37°C with 5% CO_2. LY294002 (EMD) is a potent inhibitor of PI3Kinase (which also blocks Akt signaling) and was used at concentrations of 25 or 100uM. Akt Inhibitor V (or Tricibirine - EMD) is a selectively potent inhibitor only of Akt1/2/3 and was used at 1, 10, and 100uM concentrations. Cultures lasted 24 or 48 hours before gonads were removed from the media, fixed, and then processed according to the immunostaining procedures listed above.

2.10 Busulfan treatment

CD-1 pregnant females were given a 150 mg/kg (~4.5 mg/mouse) dose of Busulfan. 30 mg Busulfan was dissolved in 500uL 95°C DMSO and combined with an equal volume of 95°C water, then cooled to 37°C before intraperitoneal injection at E10.5. Mice were dissected at E14.5 and germ cell depletion was confirmed by alkaline phosphatase staining of one pair of gonads from the litter. Remaining gonads pairs were processed for *in situ* hybridization.

3. Defining the *Dnd1*^{Ter} Defect

3.1 Introduction

To understand the molecular mechanism by which *Dnd1* prevents teratoma formation, it is important to know the exact context and cell type in which it is playing a role. After mapping the *Ter* mutation to *Dnd1* (Youngren et al., 2005), several immediate questions emerged: Is *Dnd1* expressed in Sertoli cells? Is tumor formation in mutants dependent on the presence of a Y-chromosome or the male developmental pathway? Is the somatic program affected in mutant testes? How are the germ cells initially lost in mutants? Are other known pathways that are important in teratoma formation misregulated in *Dnd1* mutants? The following section will answer these questions and better define the *Dnd1*^{Ter} defect.

3.2 Summary

The use of transgenic reporter lines to isolate cell populations of the testis confirms that *Dnd1* is exclusively expressed in germ cells, not Sertoli cells, of the developing gonad. Interestingly, *Dnd1*$^{Ter/Ter}$ XX germ cells that develop within a testis give rise to the same neoplastic clusters as mutant XY germ cells in a testis, indicating that tumor formation is specific to the testis environment, not to XY germ cells. Importantly, the male somatic program is initiated normally with robust expression of SOX9 and other essential male differentiation genes. To determine the mechanism underlying early PGC loss, *Dnd1*$^{Ter/Ter}$ embryos were crossed to a *Bax*-null background where germ cells were partially rescued. Surprisingly, on a mixed genetic background, rescued male germ cells also generate fully developed teratomas at a high rate. Double mutant females on a mixed background do not develop teratomas, but are fertile and produce viable offspring. Although mutations in *Dmrt1* also result in testicular teratomas, *Dmrt1* is not misregulated in *Dnd1*$^{Ter/Ter}$ mutants. Finally, while others have reported a possible role for *Dnd1* in embryonic viability on the 129/SvJ background, our colony shows no such susceptibility.

3.3 Results

3.3.1 Dnd1 expression is restricted to germ cells

In situ expression patterns of *Dnd1* in the embryonic testis have revealed transcript in the developing testis cords, but did not distinguish definitively whether it was expressed in both Sertoli and germ cells (Youngren et al., 2005). Interestingly, previous experiments indicated that somatic cells might be altered in *Dnd1*$^{Ter/Ter}$ testes, suggesting that *Dnd1* may be expressed in the soma (Takabayashi et al., 2001). *Dmrt1*, which when mutated can also give rise to testicular teratomas, is expressed in both Sertoli and germ cells (Krentz et al., 2009). It is important to distinguish the expression pattern of *Dnd1* to determine the cell type that is directly affected by the defect and possibly causing tumor formation.

To determine whether *Dnd1* expression is restricted to germ cells or is also characteristic of Sertoli cells, a chemotherapeutic agent, busulfan, was injected into pregnant females to eliminate germ cells from the developing embryonic gonads by E14.5. We then compared the *Dnd1* expression pattern to that of uninjected E14.5 testes (Fig. 4A,C). After busulfan treatment, expression of *Dnd1* was eliminated in the testis (Fig. 4B,D), suggesting that *Dnd1* is either not expressed in Sertoli cells or requires the presence of germ cells.

Figure 4 - Expression of *Dnd1* is restricted to germ cells of the developing testis. *Dnd1 in situ* expression in a whole mount **(A,B)** and sectioned **(C,D)** E14.5 WT testis is restricted to testis cords, and disappears in a Busulfan treated testis **(B,D)**. Busulfan is a chemical that eliminates germ cells. **(E,F)** RT-PCR on *Sox9-ECFP* positive and negative cells, sorted from E12.5-E15.5 gonads. *Dnd1* expression is only detected in the ECFP-negative fraction (containing the *Oct4* positive germ cell population) and is excluded from the pure Sertoli cell fractions (exclusively *Sox9* positive).

Figure 4

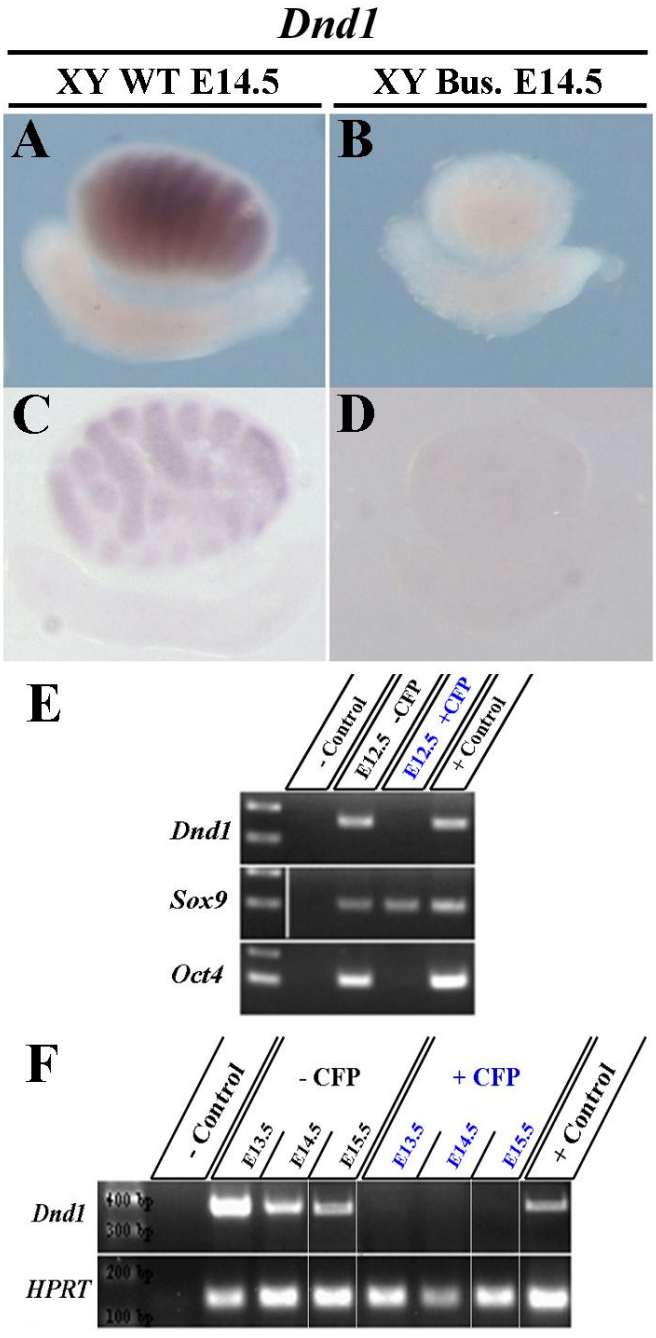
Dnd1
XY WT E14.5
XY Bus. E14.5
A
B
C
D
E
- Control
E12.5 -CFP
E12.5 +CFP
+ Control
Dnd1
Sox9
Oct4
F
- Control
- CFP
+ CFP
E13.5
E14.5
E15.5
E13.5
E14.5
E15.5
+ Control
Dnd1
400 bp
300 bp
HPRT
200 bp
100 bp

To investigate this question further we made use of the transgenic reporter line, *Sox9-ECFP*. The *Sox9-ECFP* line contains an ECFP reporter driven by a *Sox9* enhancer element (Sekido and Lovell-Badge, 2008), and is-specific to Sertoli cells in the gonad. RT-PCR analysis of sorted cells between stages E12.5 and E15.5 revealed *Dnd1* expression in the ECFP-negative pool that contains *Oct4* expressing cells (germ cells), but not in the ECFP-positive (Sertoli cell only) pool (Fig. 4E,F). Note that cell sorting did not eliminate all *Sox9*-positive cells from the negative pool (e.g., *Sox9*-positive cells remain in the *Sox9-ECFP*-negative pool). However, the *Sox9-ECFP*-positive pool is pure and contains no *Oct4*-expressing cells (Fig. 4E). These experiments indicate that *Dnd1* transcript is located within germ cells, and not in Sertoli cells. This suggests that the primary defect in $Dnd1^{Ter/Ter}$ mutant gonads is only in germ cells.

3.3.2 Neoplasia formation is specific to the male developmental pathway

The fact that testes and not ovaries form teratomas in $Dnd1^{Ter/Ter}$ embryos indicates that there is something specific either to XY germ cells or to the male pathway of development that predisposes mutant germ cells to transformation. To distinguish between these possibilities, 129/SvJ (129/SvJ) XY Sry^{MYC} males were crossed to 129/SvJ $Dnd1^{Ter/+}$ heterozygous females. Sry^{MYC} mice contain an autosomal MYC-tagged SRY protein that causes female-to-male sex reversal (Sekido et al., 2004). Intercrosses between XX $Dnd1^{Ter/+}$ heterozygotes and XY Sry^{MYC}; $Dnd1^{Ter/+}$ heterozygotes produced sex-reversed XX $Dnd1^{Ter/Ter}$ testes.

Figure 5 – XX germ cells in an XX *Sry*^{MYC} testis form neoplastic clusters like XY germ cells in a testis. XY germ cells are MVH positive (green) in an E18.5 control XY testis **(A)**, and in an XX *Sry*^{MYC} (sex-reversed) testis **(B)** although their numbers are somewhat reduced. **(C)** At E18.5, the XY *Dnd1*$^{Ter/Ter}$ testis lacks MVH-positive cells, but an E-cadherin-positive (red) neoplastic cluster is detected. These clusters typically give rise to nascent teratomas. **(D)** At E18.5 the XX *Sry*^{MYC} *Dnd1*$^{Ter/Ter}$ testis also lacks MVH-positive germ cells but contains a similar E-cadherin positive neoplastic cluster. All testis samples are on a 129/SvJ background. Scale bars represent 50μm.

Figure 5

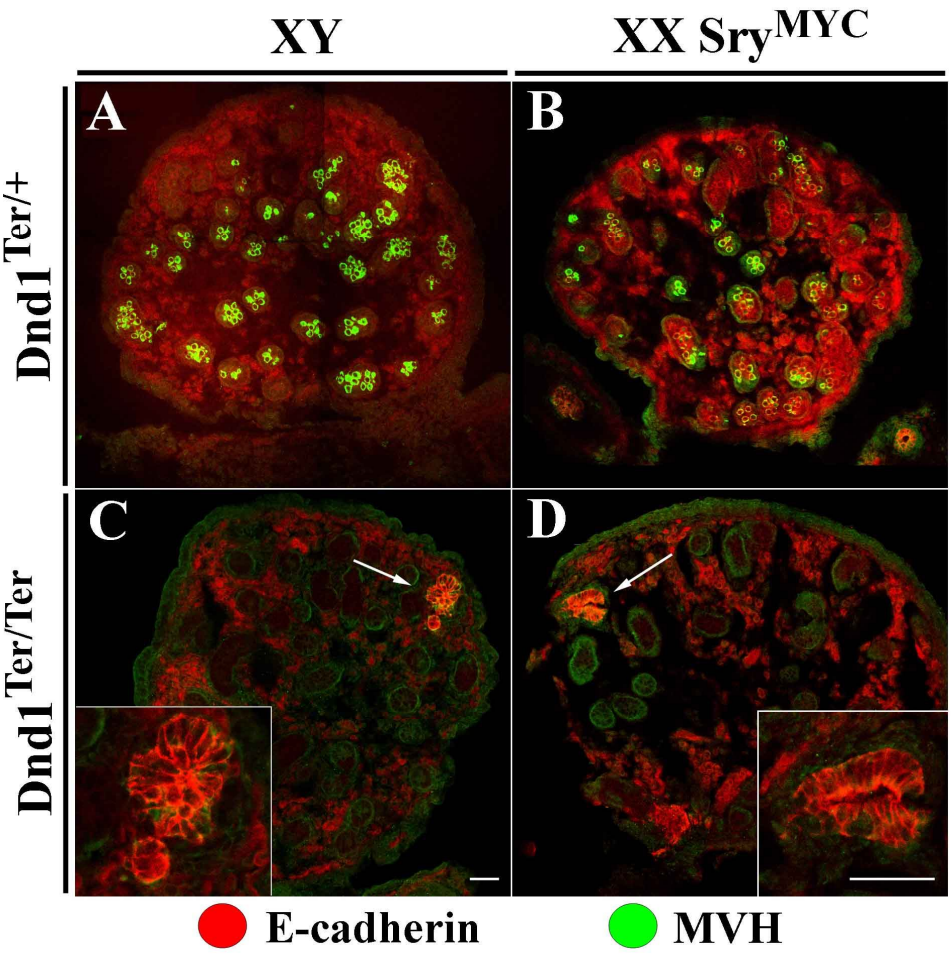

Normally, mutant XY germ cells on a 129/SvJ background give rise to transforming germ cell clusters. These clusters have previously been identified histologically (Rivers and Hamilton, 1986).

These clusters are detectable based on morphology and immunofluorescent staining for E-cadherin by E18.5 (Fig. 5C arrow and inset). Examination of mutant XX germ cells in a sex-reversed testis at this stage also revealed similar neoplasias (Fig. 5D arrow and inset). This indicates that the initiation of teratoma formation is dependent upon a male developmental pathway and not the sex chromosomes of the PGCs. Despite the presence of XX neoplasias (n=2/3 at E18.5) that resembled the early stage of teratoma formation in XY testicular germ cells, we never saw mature teratomas after birth in XX *Sry*^{MYC}; *Dnd1*$^{Ter/Ter}$ mice (n=0/10 at P14 and later). Few germ cells persist in sex-reversed controls compared to normal testis controls at later developmental stages and after birth (data not shown). As XX germ cells are usually lost perinatally in XX sex-reversed males (McLaren, 1984), it is possible that germ cell loss and other testis cord defects reported for XX sex-reversed testes (Ishii et al., 2007) prevent formation of fully-developed teratomas even though early neoplasias can be identified.

3.3.3 The male somatic program is initiated normally

Dnd1$^{Ter/Ter}$ germ cells form teratomas only in testes, not in ovaries. The susceptibility to teratoma initiation in *Dnd1*$^{Ter/Ter}$ gonads seems to be specific to the male developmental pathway and not to sex chromosome composition. This suggests that

there may be a defect in the male somatic program that leads to tumorigenesis. The fact that *Dnd1* is only expressed in germ cells (Fig. 4) suggests that any impairment of the somatic program would be indirectly caused by the *Dnd1*^{Ter} mutation, possibly resulting from a significant decrease in germ cell number. In fact, a previous report revealed that media conditioned from mutant somatic cells causes increased apoptosis in wildtype germ cell cultures (Takabayashi et al., 2001).

To determine whether initiation of the male somatic pathway is misregulated in mutant testes we examined expression of SOX9, a key regulator of the male somatic pathway. We found that, despite the significant loss of germ cells by E14.5, SOX9 expression was unaffected (Fig. 6B,D green) and somatic cell morphological development occurred normally. This is consistent with the model demonstrating that defects intrinsic to germ cells lead to the developmental disruptions in *Dnd1*$^{Ter/Ter}$ mutants. Interestingly, the majority of mutant germ cells (though not all) are found in the developing rete testis (Fig. 6D red), which may reflect a failure of the smaller germ cell population to expand to more distal regions of the testis.

Figure 6 – The male somatic program is initiated normally in mutant gonads. E-CAD (red) labels germ cells. **(A,C)** E14.5 129/SvJ control testes contain SOX9 (green) expressing cells, demarcating Sertoli cells, in distinct testis cord structures surrounding germ cells. **(B,D)** E14.5 129/SvJ *Dnd1*$^{Ter/Ter}$ testes also contain normal-looking SOX9-expressing Sertoli cells that reside in testis cords and surround the few remaining germ cells (red) located predominantly in the developing rete. Scale bars represent 50μm. **(E)** Mutant gonads have a significant decrease in *Mvh* and *Oct* expression compared to controls because of the loss in germ cells. *Dmrt1* expression is also reduced but not eliminated due to its expression in Sertoli cells as well. **(F)** Compared to controls, mutant gonads express similar levels of important male somatic markers such as *Sox9*, *Cyp26b1*, *Fgf9*, and *Dhh*.

Figure 6

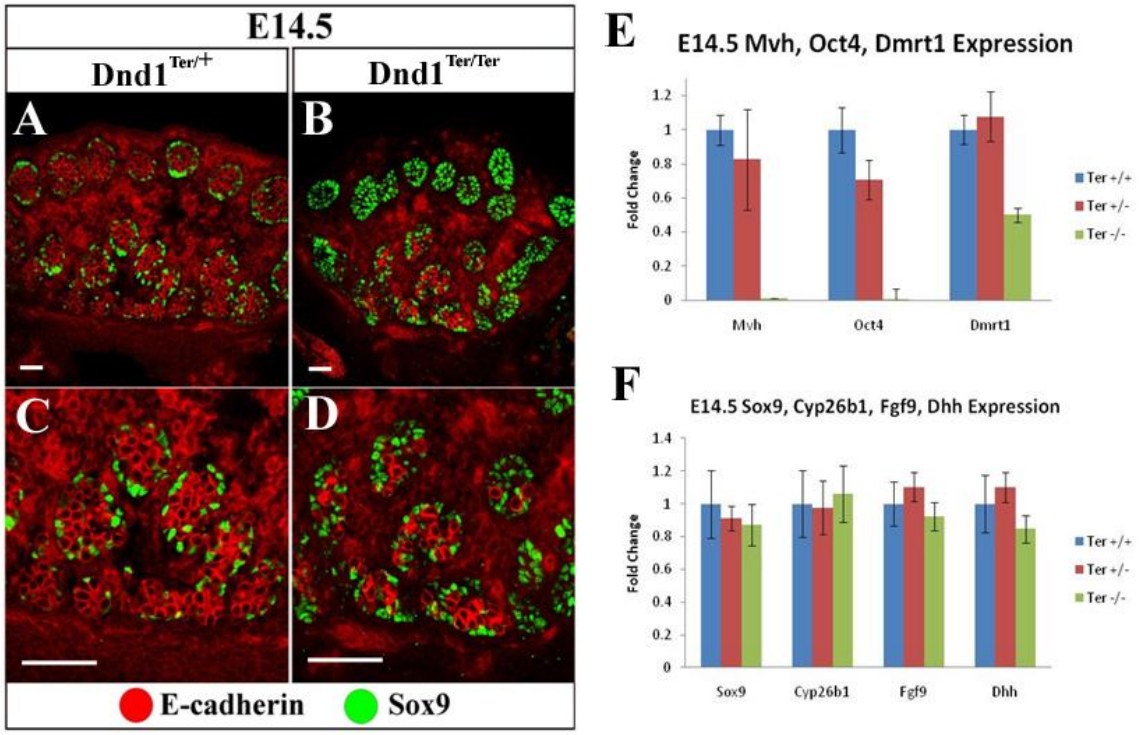
E14.5
Dnd1 Ter/+
Dnd1 Ter/Ter
A
B
C
D
E-cadherin
Sox9
E
E14.5 Mvh, Oct4, Dmrt1 Expression
Fold Change
1.2
1
0.8
0.6
0.4
0.2
0
Mvh
Oct4
Dmrt1
Ter +/+
Ter +/-
Ter -/-
F
E14.5 Sox9, Cyp26b1, Fgf9, Dhh Expression
Fold Change
1.4
1.2
1
0.8
0.6
0.4
0.2
0
Sox9
Cyp26b1
Fgf9
Dhh
Ter +/+
Ter +/-
Ter -/-

To explore the possibility that the expression of other essential differentiation genes may be affected in mutant gonads, E14.5 control and mutant testes were dissected for qRT-PCR. Expression levels of germ cell-specific markers such as *Mvh* and *Oct4* are significantly decreased in mutant gonads compared to controls, and the expression of *Dmrt1*, which is transcribed in both Sertoli and germ cells, is decreased by half (Fig. 6E). Transcript levels of *Sox9*, *Cyp26b1*, *Fgf9*, and *Dhh* were not significantly altered in mutant gonads compared to controls (Fig. 6E). These data suggest that male somatic development initiates normally in mutant gonads.

3.3.4 Bax-mediated apoptosis affects early germ cell loss and incidence of testicular teratomas

Dnd1$^{Ter/Ter}$ embryos suffer a significant reduction in the number of germ cells arriving in the gonads of both sexes on all backgrounds tested (Sakurai et al., 1995a). However, the fate of male and female mutant germ cells diverges after colonization of the gonad. The few mutant XX germ cells that successfully migrate to the gonad are maintained in the ovary and give rise to mature oocytes, albeit in greatly reduced numbers. Adult mutant females have small ovaries and are sub-fertile, but can produce offspring at low rates when crossed with wild-type males (Noguchi and Noguchi, 1985). By contrast, mutant XY germ cells colonize the testis but transform on the 129/SvJ background, giving rise to testicular teratomas at a rate of approximately 95% (Fig. 2). On other backgrounds, XY germ cells are lost completely by perinatal stages.

Examination of a mixed background *Dnd1*$^{Ter/Ter}$ testis revealed that by postnatal day eleven (P11), no germ cells could be detected by analysis with antibodies against mouse Vasa homolog (MVH) or germ cell nuclear antigen 1 (GCNA1) (data not shown).

It is unknown why this drastic phenotypic variation occurs between strain backgrounds. An initial hypothesis was that the tumor susceptibility phenotype could be positively correlated with the number of germ cells colonizing the gonads in *Dnd1*$^{Ter/Ter}$ embryos. Previously, alkaline phosphatase stains had been carried out on mutant C57BL/6J gonads to identify and count PGC numbers (Sakurai et al., 1995a). However, upon examination of PGC numbers in 129/SvJ mutants it was obvious that there was no significant difference in germ cell population size in mutant gonads between these different backgrounds. This indicates that the mechanism underlying early loss of germ cells is similar to both backgrounds and suggests that the strain-specific tumor phenotype is not affected by the number of colonizing germ cells, but rather by other strain-specific properties.

The early PGC loss common to mutants of all backgrounds is not well-understood. Although the correct number of PGCs is specified in *Dnd1*$^{Ter/Ter}$ mice, as early as E8.5, a difference can be noted in the number of migrating germ cells entering the hindgut between mutants and wild-type, based on alkaline phosphatase staining (Sakurai et al., 1995a). Germ cell loss is exacerbated during migration, as only a few dozen germ cells reach the *Dnd1*$^{Ter/Ter}$ gonad (compare Fig. 7A and 7C). However,

reports have been inconclusive in determining whether differences in mutant germ cell number are due to active cell death, lack of proliferation, or differentiation during migration. To investigate whether cell death plays a role in early germ cell loss of mutants, the *Dnd1*^{Ter} mice were crossed to mice with a mutation that genetically blocks one apoptotic pathway.

Based on data showing that blocking BAX-mediated apoptosis rescues PGCs in other germ cell-deficient mutants (Stallock et al., 2003; Suzuki et al., 2008), the *Bax* mutation (1-Baxtm1Sjk/J C57BL/6J.129/SvJ) was crossed onto *Dnd1*^{Ter} mice. To this end, *Bax* heterozygotes on a mixed genetic background (129/SvJ;C57BL/6J;CD1) were mated to *Dnd1* heterozygotes of the 129/SvJ background to obtain double heterozygotes. These offspring were intercrossed to produce compound double mutants on a mixed background. *Dnd1*$^{Ter/Ter}$;*Bax*$^{-/-}$ double mutants showed a significant germ cell rescue (~50%) by stage E13.5 on a mixed background (Fig. 7G) and in both sexes (Fig. 8), indicating that Bax-mediated apoptosis is an important mechanism of initial germ cell loss in *Dnd1*$^{Ter/Ter}$ mutants. However, the rescued phenotype is not complete indicating that there may be other BAX-independent cell death pathways involved, defects in proliferation, or aberrant differentiation contributing to the loss of mutant germ cells.

Figure 7 – *Dnd1*$^{Ter/Ter}$;*Bax*$^{-/-}$ double mutant testes have more germ cells and males develop testicular teratomas on a mixed genetic background. (A) Germ cells (immunostained with MVH in green) are grouped inside testis cords in a wildtype testis at E13.5. Germ cell numbers are greatly reduced in a *Dnd1*$^{Ter/Ter}$ testis **(C)**, and somewhat increased in a *Dnd1*$^{Ter/+}$ mouse carrying two loss of function alleles of *Bax* **(E)**. **(G)** A *Dnd1*$^{Ter/Ter}$;Bax$^{-/-}$ double mutant testis shows a significant increase in germ cell number compared to C. Scale bars represent 50μm. **(B)** P8 wildtype testes. On a mixed genetic background, *Dnd1*$^{Ter/Ter}$ mutant testes are reduced in size as a result of germ cell loss **(D** as compared to **B)**. Loss of *Bax* on a *Dnd1*$^{+/+}$ background leads to an increase in testis size **(F)**, whereas loss of *Bax* on a *Dnd1*$^{Ter/Ter}$ background results in teratoma formation **(H)**. Scale bars represent 0.5cm.

Figure 7

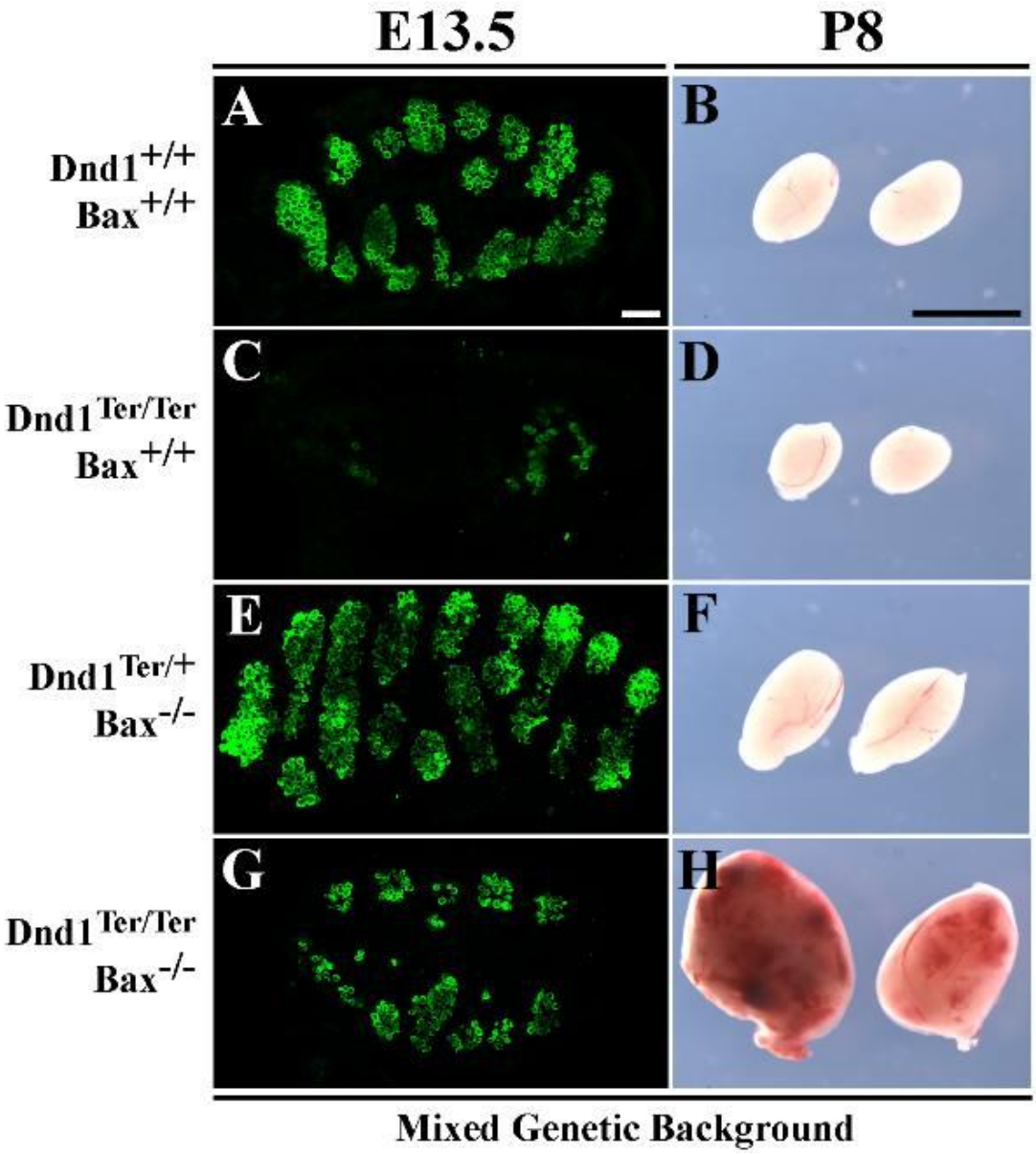
E13.5
P8
A
B
C
D
E
F
G
H
Dnd1+/+
Bax+/+
Dnd1Ter/Ter
Bax+/+
Dnd1Ter/+
Bax-/-
Dnd1Ter/Ter
Bax-/-
Mixed Genetic Background

Figure 8 – *Dnd1*$^{Ter/Ter}$*;Bax*$^{-/-}$ double mutant ovaries have more germ cells. (A,D) E15.5 and E17.5 **c**ontrol ovaries contain a normal number of germ cells as shown by MVH staining (green). **(B,E)** E15.5 and E17.5 *Dnd1*$^{Ter/Ter}$ have a significant decrease in germ cells. **(C,F)** E15.5 and E17.5 double mutant ovaries have rescued many germ cells (green) compared to *Dnd1*$^{Ter/Ter}$ mutants alone.

Figure 8

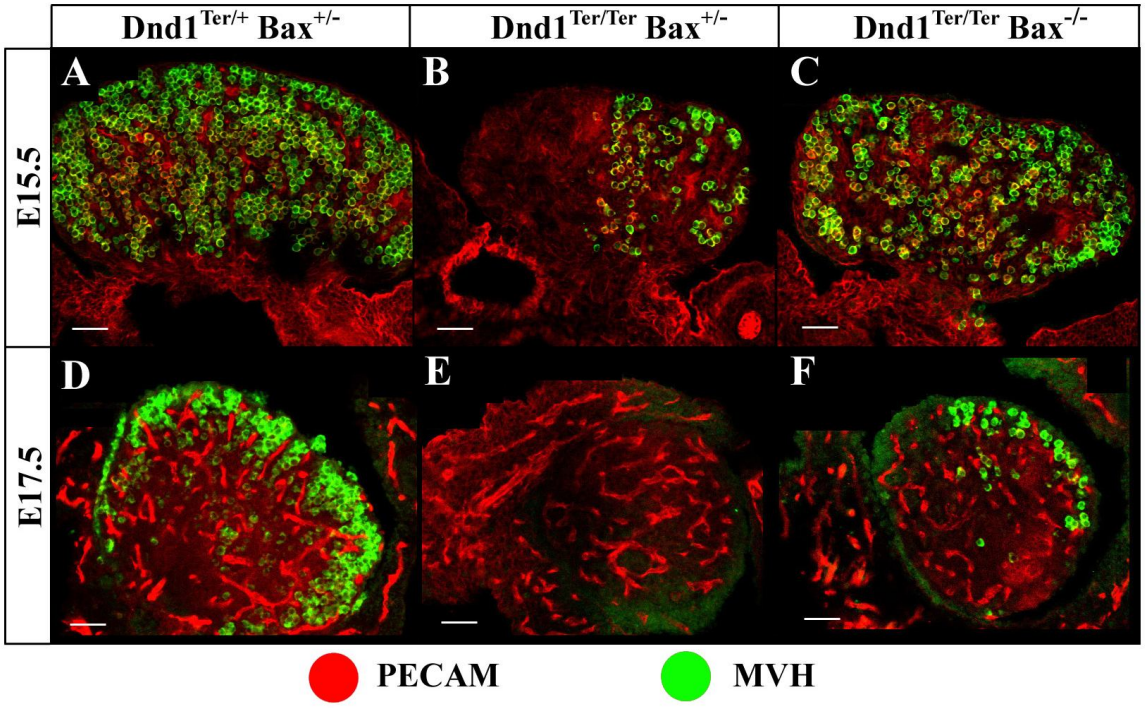
Dnd1Ter/+ Bax+/-
Dnd1Ter/Ter Bax+/-
Dnd1Ter/Ter Bax-/-
E15.5
E17.5
A
B
C
D
E
F
PECAM
MVH

In *Dnd1*$^{Ter/Ter}$ males, few germ cells colonize the gonad, but those that do either transform on a 129/SvJ genetic background or undergo cell death resulting in testes completely devoid of germ cells by birth on other genetic backgrounds. We investigated whether rescuing early germ cell loss on a *Bax* mutant background leads to the formation of teratomas in a non-129/SvJ testis with increased numbers of mutant germ cells. Surprisingly, on a mixed genetic background, we found that double mutant male samples exhibited typical testicular teratomas (Fig. 7H) at a high rate, as compared to single *Dnd1*$^{Ter/Ter}$ mutant testes (Fig. 7D) on a similar background, which are normally devoid of germ cells by the time of birth.

To determine whether double mutants on a pure C57BL/6J background could also develop mature testicular teratomas, both alleles were backcrossed over 10 generations to C57BL/6J and then intercrossed to generate double mutant males. While the incidence of teratoma formation in mice on a mixed background was slightly lower than that reported for a pure 129/SvJ background (89%), no tumors developed on a pure C57BL/6J background (Table 2). The double mutants that did not develop teratomas lost their germ cells entirely. Interestingly, 40% of *Dnd1*$^{Ter/Ter}$*;Bax*$^{+/-}$ mice on a mixed background developed teratomas, although smaller in size and typically unilateral. As a control, *Dnd1*$^{Ter/Ter}$*;Bax*$^{+/+}$ samples on mixed and pure C57BL/6J backgrounds were examined and none developed teratomas by P20 (Table 2). At this stage, all XY gonads from this group were completely devoid of germ cells.

These experiments suggest that while mutant germ cells on the 129/SvJ background efficiently generate teratomas, mutant germ cells on other backgrounds also have this capacity, but are less efficient at undergoing the transformation event, or are normally cleared more efficiently by competing mechanisms of cell death.

In *Dnd1*$^{Ter/Ter}$ mutants, the significant early loss of germ cells results in sub-fertile females (Noguchi and Noguchi, 1985). The few germ cells that colonize the gonad survive throughout ovarian development. However, the ovaries are small and contain very few oocytes (Fig. 9A). Rescuing the early germ cell loss on a *Bax* mutant background resulted in double mutant females that maintained many more oocytes than *Dnd1*$^{Ter/Ter}$ single mutants alone, as determined by histological analysis (Fig. 9B). Additionally, these double mutant females were fertile and produced viable, fertile offspring when out-crossed to CD-1 mice (data not shown). As reported previously for the single mutants, there was no incidence of ovarian teratoma in double mutant females (Noguchi et al., 1996).

Table 2 - Teratoma penetrance in double mutant gonads on mixed and C57BL/6J genetic backgrounds.

Table 2

	Mixed	C57BL/6J
$Bax^{-/-}$ $Dnd1^{Ter/Ter}$	89% (n=28)	0% (n=9)
$Bax^{+/-}$ $Dnd1^{Ter/Ter}$	42% (n=36)	0% (n=8)
$Bax^{+/+}$ $Dnd1^{Ter/Ter}$	0% (n=12)	0% (n=22)

Figure 9 - *Dnd1*$^{Ter/Ter}$*;Bax*$^{-/-}$ ovaries have more mature oocytes than *Dnd1*$^{Ter/Ter}$ ovaries.

Representative sections from the thickest part of **(A)** a P16 *Dnd1*$^{Ter/Ter}$ ovary and **(B)** a P18 *Dnd1*$^{Ter/Ter}$*;Bax*$^{-/-}$ ovary stained with hematoxylin and eosin. Scale bars represent 100μm.

Figure 9

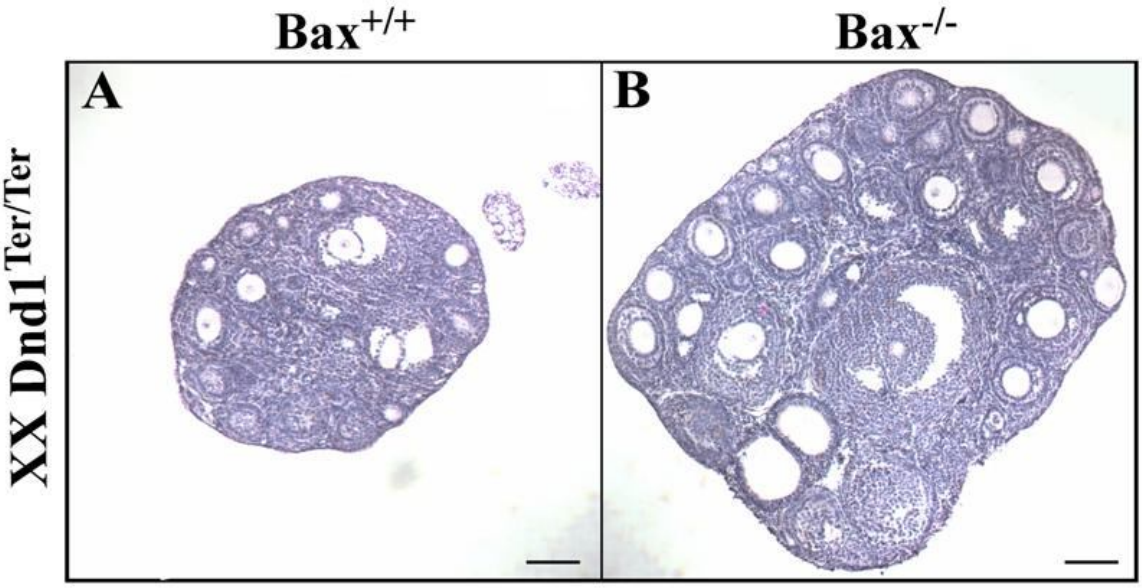

3.3.5 Teratoma formation is independent of Dmrt1

There are a few other mutations besides *Dnd1*^{Ter} that are known to predispose mice to testicular teratomas. One of these is loss of function of the transcription factor *Dmrt1* (Krentz et al., 2009). Originally identified in invertebrates as a gene important in sex determination, the mammalian orthologue is also involved in postnatal differentiation of the testis (Raymond, 2000). Loss of *Dmrt1*, which is expressed in both Sertoli and germ cells, leads to a high incidence of testicular teratomas only on the 129/SvJ background. Further analysis demonstrates that its expression is only required in germ cells to prevent tumor formation (Krentz et al., 2009).

To determine whether *Dmrt1* is misregulated in *Dnd1*$^{Ter/Ter}$ testes, mutant gonads were examined for expression of *Dmrt1*. Compared to controls, *Dnd1*$^{Ter/Ter}$;*Bax*$^{-/-}$ double mutant testes on a mixed background, which have a high incidence of tumors, show no aberrant expression of *Dmrt1* compared to controls (Fig. 10). This suggests that the pathway of tumor formation for *Dnd1* mutants is independent of *Dmrt1*.

3.3.6 Loss of *Dnd1* does not affect embryonic viability

While only germ cells express *Dnd1* in the developing gonad, *in situ* analyses detect transcript in other tissues of the developing embryo (Youngren et al., 2005) and ESTs have been identified in different organs of the adult including the heart and brain. Since loss of *Dnd1* in PGCs can lead to BAX-mediated apoptosis, it is possible that loss of

expression in other tissues could also lead to cell death. Corroborating this, a previous report observed a role for DND1 in embryonic viability (Bhattacharya et al., 2007). It was shown that loss of *Dnd1* on a 129/SvJ background, but not on a C57BL/6J background, leads to embryonic lethality.

Five hundred progeny from *Dnd1*$^{Ter/+}$ 129/SvJ crosses were examined and the ratios of wild-type, heterozygous, and homozygous mutants were calculated (Table 3). The proportions fell within Mendelian ratios, with a P-value greater than 0.975. These data indicate that, in our colony on a 129/SvJ genetic background, the *Dnd1*^{Ter} mutation does not affect embryonic viability.

Figure 10 – *Dmrt1* expression in *Dnd1*$^{Ter/Ter}$;*Bax*$^{-/-}$ double mutant gonads. (A,C) Control germ cells (E-CADHERIN in red) robustly express DMRT1 (green). **(B,D)** Mutant germ cells (E-CADHERIN in red) still express DMRT1 (green). Scale bars represent 50μm.

Figure 10

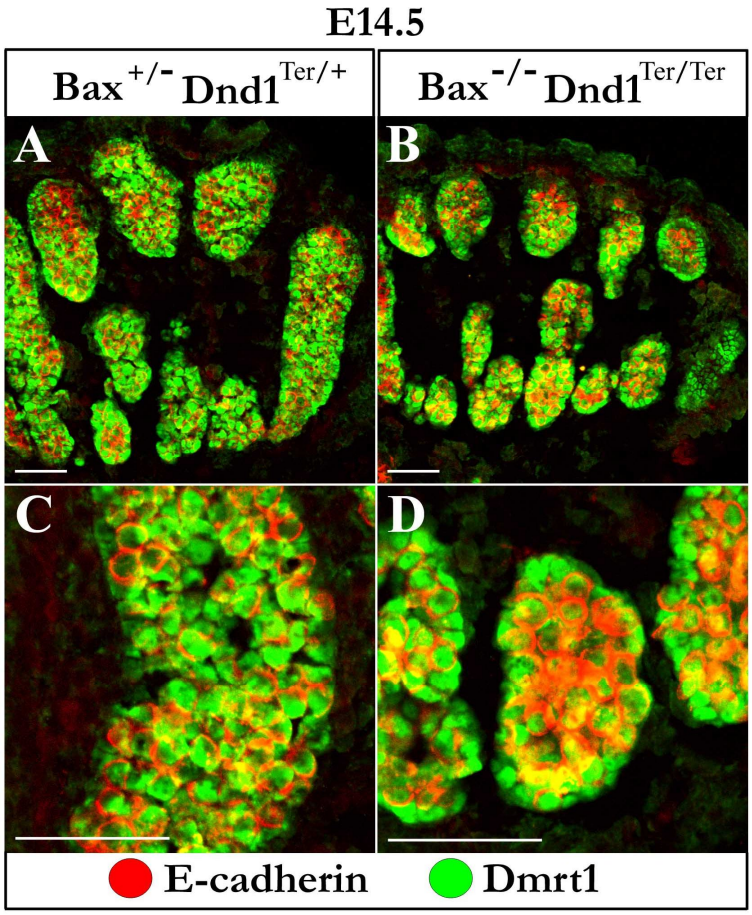

Table 3 - Comparison of genotypes from 129/SvJ–*Ter* derived progeny.

Table 3

	Genotype			*Total no. examined*	X^2	*P*
	+/+	**Ter/+**	**Ter/Ter**			
Observed	124	249	127	500	0.044	0.978
Expected	125	250	125			

3.4 Discussion

Testicular teratomas in *Dnd1*$^{Ter/Ter}$ mice are believed to arise from misregulated germ cells during development of the fetal gonad. Findings in this chapter reveal that *Dnd1* is expressed in germ cells and not in Sertoli cells between E12.5-15.5, the time period when teratoma formation begins in *Dnd1*$^{Ter/Ter}$ mutants (Rivers and Hamilton, 1986). This expression pattern indicates that the direct effects of the *Dnd1*^{Ter} mutation occur in germ cells, and not in the somatic supporting cell lineage. Teratomas arise from defects in the intrinsic cellular program in germ cells, within the context of the strain-specific background. It is not yet clear whether genetic background affects the frequency or degree of misregulation of the intrinsic germ cell program, whether it affects the somatic environment and its ability to regulate or clear mutant germ cells, or whether it affects both.

Interestingly no ovarian teratomas have been documented in *Dnd1*$^{Ter/Ter}$ mutants. Not only do tumors not develop in mutant females, but the few germ cells colonizing the ovary survive, eventually giving rise to mature oocytes, and mutant females are classified as subfertile (Noguchi and Noguchi, 1985). This suggests that (1) the early *Dnd1* defect that causes the loss of germ cells is not sufficient for teratoma initiation and (2) there is a second critical role for *Dnd1* in germ cells during normal male development after colonization of the gonad.

To distinguish whether tumor formation is dependent on the male pathway or having a Y-chromosome, XX sex-reversed mutants were analyzed and found to show initiation of the same neoplasias as XY mutant controls. This supports a model where susceptibility is dependent on the male developmental pathway, as Leroy Stevens first reported when transplanting embryonic gonads in the 1970s (Stevens, 1970a, b).

If the male developmental pathway is susceptible, is it possible that the somatic program is not initiated normally? Previous reports suggested that the mutant male somatic environment is not normal, and that there is a secreted TER-factor that is necessary to prevent apoptosis of germ cells (Takabayashi et al., 2001). Data reported here do not support this idea. Specifically, SOX9 expression is robust, male morphological development is normal, and expression levels of other essential male somatic markers (including those known to regulate mitotic arrest) are not significantly altered in mutant gonads. Additionally, the mechanism of tumor formation appears to be independent of the function of *Dmrt1* as expression is not misregulated in mutant testes. Together, these data indicate that tumor formation results from an intrinsic defect in mutant germ cells that arise **after** colonization of the XY gonad and during normal male somatic development.

Dnd1$^{Ter/Ter}$ mice display two very distinct phenotypes: (1) initial loss of germ cells common to both sexes on all genetic backgrounds and (2) male-specific teratoma formation only on the 129/SvJ genetic background. The germ cell loss phenotype is

similar to the *Nanos3* null phenotype (Suzuki et al., 2008). Like DND1, NANOS3 is a conserved RNA binding protein expressed in PGCs after specification. A null mutation in *Nanos3* leads to the loss of a high proportion of germ cells prior to their arrival in the gonad, similar to *Dnd1* mutants. Also like the *Nanos3* mutants, blocking BAX-mediated apoptosis only partially rescues the germ cell loss. This suggests that other mechanisms may contribute to germ cell loss in both mutants, including BAX-independent cell death, lack of proliferation, or even trans-differentiation of germ cells during migration. It was found that the *Nanos3* null germ cells did not trans-differentiate or have proliferation defects during migration (Suzuki et al., 2008), however, this has not been investigated in *Dnd1* mutants.

Zebrafish DND binds the 3'UTR of *Nanos* in primordial germ cells to promote translation by protecting the transcript from miRNA-mediated repression (Kedde et al., 2007a). Based on the high conservation of *Nanos* in organisms from *C. elegans* to *H. sapiens*, it is possible that a similar mechanism of early misregulation of the murine *Nanos3* transcript (functionally homologous to zebrafish *Nanos*) leads to the early germ cell loss phenotype of $Dnd1^{Ter/Ter}$ mutants (Kedde and Agami, 2008; Saga, 2008).

Bax rescue significantly increases the number of oocytes in adult females, which makes them more fertile than $Dnd1^{Ter/Ter}$ single mutant ovaries. These females produce viable, fertile offspring, indicating that PGCs rescued in *Bax* mutants are not significantly impaired, at least with respect to the female developmental pathway. This

further supports the notion that teratomas arise during the male developmental program as the result of a secondary function of DND1 within germ cells in the fetal testis.

The 129/SvJ-specific phenotype of testicular teratoma formation in *Dnd1*$^{Ter/Ter}$ mice has been particularly enigmatic since the early 1970s. Very few germ cells colonize the gonad, sometimes none, but those that arrive frequently transition into teratomas, or are lost by birth. The possibility that the number of colonizing germ cells might be higher in 129/SvJ mice and directly related to the incidence of teratomas is not supported by the evidence that there is virtually no difference in initial colonizing germ cell numbers between strain backgrounds. Therefore this is not a viable option to explain the inherent strain difference in susceptibility. Additionally, double mutants on a pure C57BL/6J background rescue the early germ cell loss yet none develop testicular teratomas suggesting that germ cell number cannot be the most important limiting factor in tumor formation.

Nonetheless, we found that if the number of mutant germ cells in the *Dnd1*$^{Ter/Ter}$ testis is increased by blocking BAX-mediated apoptosis, teratomas arise on a **mixed** genetic background at a rate of 89% and at a rate of 40% in *Bax* heterozygotes (although smaller and typically unilateral). In *Bax* homozygous mutants, it seemed likely that the increased number of germ cells might uncover transformation events that normally occur at a low frequency on mixed genetic backgrounds. However, in heterozygous *Bax*

mutants, where we detect no difference in germ cell number, it seems more plausible that loss of the *Bax* pathway may compromise the capacity of the mixed background fetal testis to clear misregulated germ cells. Even so, homozygous mutation of *Bax* does not lead to an increased incidence of teratomas in the absence of mutation in *Dnd1*.

Although BAX may normally contribute to the elimination of mutant germ cells from the fetal testis, it is obviously not the only mechanism for clearing defective germ cells, as mutant germ cells are still cleared in some mixed background and all C57BL/6J double homozygous mutants (Table 2), indicating that when the strain-specific components necessary for transformation are not present, mutant germ cells cannot continue to develop in the male pathway and will be eliminated eventually by some form of cell death.

Germ cell number may be important for penetrance of a tumor phenotype on mixed genetic backgrounds. However, increased numbers of germ cells did not result in tumor formation in double mutants on a pure C57BL/6J background, indicating that differences specific to C57BL/6J block tumor formation even when many more mutant germ cells are present in the gonad. Other possible strain-specific differences that contribute to tumor susceptibility will be explored more thoroughly in the next chapter.

While expression of *Dnd1* is important for germ cell development, little is known about its function in other tissues. ESTs and other expression analyses indicate that *Dnd1* is expressed in various organs such as heart and brain, suggesting other possible

roles for *Dnd1* in development and adult life. Here five hundred adult mice from heterozygous crosses in our colony were examined and no evidence was found for a negative impact of the *Dnd1*^{Ter} mutation on embryonic viability on a 129/SvJ genetic background. The difference between our finding and a previous report demonstrating a role for *Dnd1* in embryonic viability on the 129/SvJ background (Bhattacharya et al., 2007) could be due to sub-strain differences that have arisen since separation of the two colonies. Importantly, it has been shown that the 129/SvJ strain is a contaminated strain and different isolated colonies are not be expected to show the same penetrance of various established phenotypes (Threadgill et al., 1997).

The baseline data and tools developed in this chapter laid the groundwork to explore the molecular role for DND1 in germ cells. To elucidate the underlying cause of transformation in *Dnd1*$^{Ter/Ter}$ germ cells, a full molecular analysis of the transition of mutant germ cells into nascent teratomas was needed. Importantly, the *Dnd1*$^{Ter/Ter}$*;Bax*$^{-/-}$ double mutant is a tool that can be used to compare mutant germ cells undergoing transformation to those that are not. A critical event that occurs during the period of male germ cell development when teratomas arise is mitotic arrest. Mitotic arrest is presumably not occurring in mutant germ cells based on the large size of the tumors that form and previous findings that proliferation is not arrested in *Dnd1*$^{Ter/Ter}$ mutants (Rivers and Hamilton, 1986). Among targets of DND1 recently identified in human cell lines are several cell cycle regulators that are involved in mitotic arrest in the fetal testis

(Kedde et al., 2007a; Western et al., 2008). The next chapter will determine whether misregulation of mitotic arrest plays a direct role in tumorigenesis or aberrant development of germ cells in *Dnd1*$^{Ter/Ter}$ mice and whether there are strain differences. *Dnd1* may represent a link between cell cycle and pluripotency in developing germ cells.

4. DND1 Regulates Pluripotency, Cell Cycle, and Male Differentiation in Germ Cells of the Fetal Testis

4.1 Introduction

Based on work in the previous chapter it is clear that *Dnd1* is poised to perform an essential role in male germ cell development soon after colonization of the gonad. Data indicate that tumor formation results from an intrinsic defect in mutant germ cells **after** colonizing the gonad and during normal male somatic development. Determining how *Dnd1* regulates normal male germ cell development and blocks teratoma formation is of important clinical interest and is the main focus of the following chapter. These findings result from basic questions and hypotheses surrounding the *Dnd1*^{Ter} mouse model: What marks the neoplastic transition in *Dnd1*$^{Ter/Ter}$ mutants on a 129/SvJ background? Does tumorigenesis on a mixed genetic background occur in a similar manner? To what extent do male germ cells fail to differentiate in mutants? How is cell cycle misregulated in mutant germ cells? What strain-specific differences account for susceptibility in *Dnd1*^{Ter} mice? The following section will address these questions and demonstrate a role for *Dnd1* in male germ cell development as a regulator of pluripotency, differentiation, and cell cycle.

4.2 Summary

Immunofluorescence data demonstrate that mutant germ cells on a 129/SvJ background fail to upregulate markers of differentiation and instead maintain pluripotency genes as they transition into early neoplasias. qRT-PCR of mutant gonads reveals the downregulation of important male differentiation genes such as *Nanos2*, which leads to the ectopic upregulation of meiotic initiation genes such as *Scp3* and *Stra8*. Additionally, mouse DND1 directly binds a group of transcripts that encode negative regulators of the cell cycle, including $p27^{Kip1}$, which is not translated in $Dnd1^{Ter/Ter}$ germ cells. As a result, mutant germ cells fail to mitotically arrest in G0, regardless of strain background. However, double mutants on a C57BL/6J background do not undergo active cell divisions whereas on a mixed background active mitoses are still detected. Overexpression of *Dnd1* in cultured cells results in gene expression changes to related cell cycle pathways. Finally, strain-specific pluripotency gene expression and morphological differences in testis cord structure and germ cell number possibly account for susceptibility to tumorigenesis.

4.3 Results

4.3.1 129/SvJ mutant germ cells maintain pluripotent markers and fail to differentiate during neoplasia formation

It is clear that XY mutant germ cells do not differentiate normally prior to teratoma formation. To investigate the differentiation status of mutant germ cells, various markers of germ cell development were examined between E11.5 and birth on both 129/SvJ, mixed, and C57BL/6J genetic backgrounds. Wildtype migratory PGCs express the markers of pluripotency, OCT4, NANOG, and SOX2, and can be induced to form pluripotent EG cells with high efficiency (Durcova-Hills et al., 2001; Labosky et al., 1994a, b). The efficiency of EG cell induction declines sharply after E12.5, coincident with the down-regulation of NANOG and SOX2 expression, which occurs in males as germ cells begin sex-specific differentiation into prospermatogonia within developing testis cord structures (Durcova-Hills and Capel, 2008). However, in 129/SvJ *Dnd1*$^{Ter/Ter}$ testes, clusters of cells that are histologically distinct from wildtype prospermatogonia appear within E15.5 cords (Rivers and Hamilton, 1986).

By late fetal stages, large masses can be found growing and differentiating within mutant testes. To determine how the expression of germ cell markers is correlated with this neoplastic transition, immunocytochemistry markers were used to examine pluripotency and differentiation in 129/SvJ mutant germ cells during the period spanning colonization of the gonad at E11.5 to birth. A comprehensive summary of this data can be found in Figure 11.

Between E11.5 and E13.5, mutant germ cells on a 129/SvJ background express the cell membrane protein E-CADHERIN (E-CAD), up-regulate the conserved RNA binding protein mouse vasa homolog (MVH), and express the pluripotency markers NANOG, SOX2, and OCT4 similar to wildtype germ cells (Fig. 12A,E,I,M arrows, respectively). At this stage there is no morphological distinction between mutant and wildtype germ cells other than a significant decrease in population size in *Dnd1*$^{Ter/Ter}$ gonads. By E16.5 wildtype male germ cells have entered mitotic arrest, down-regulated NANOG and SOX2, and initiated commitment to the male pathway. In contrast, 129/SvJ mutants contain morphologically distinct clusters of cells lacking MVH and maintaining expression of E-CAD, NANOG, SOX2, and OCT4 (Fig. 12B,F,J,N), even in the smallest clusters and solitary germ cells (Fig. 12B,F,J,N arrowheads). As late as E16.5, clusters of E-CAD positive cells are present along with isolated germ cells that express low levels of MVH (Fig. 12B inset arrowheads) and are NANOG and SOX2 positive (Fig. 12F,J arrowheads). Between E17.5 and perinatal stages, no MVH positive, morphologically wildtype germ cells were detected outside a tumor (Fig. 12C, Fig. 13A,B, and data not shown).

Figure 11 – Summary of expression data in 129/SvJ *Dnd1*$^{Ter/Ter}$ germ cells (red) compared to wildtype germ cells (blue) during their transition into nascent teratomas. Area highlighted in yellow indicates the period when mitotic arrest normally occurs.

Figure 11

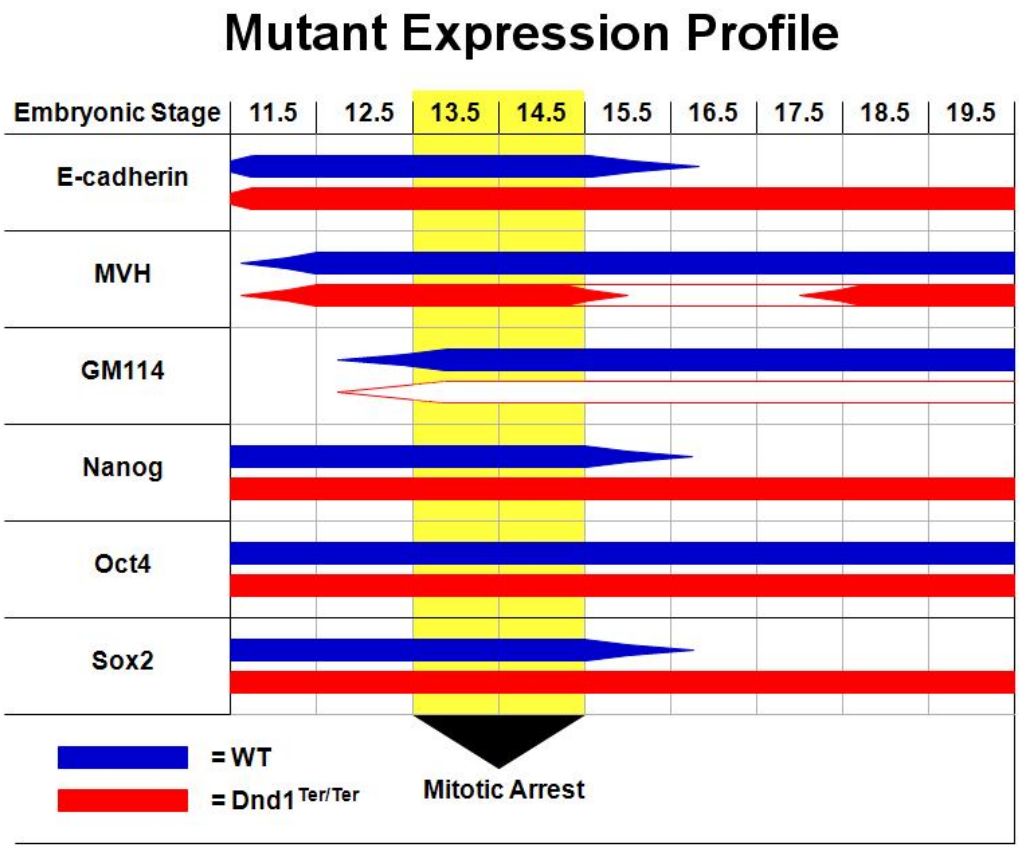
Mutant Expression Profile
Embryonic Stage
11.5
12.5
13.5
14.5
15.5
16.5
17.5
18.5
19.5
E-cadherin
MVH
GM114
Nanog
Oct4
Sox2
= WT
= Dnd1 Ter/Ter
Mitotic Arrest

Figure 12 – Transformation of mutant germ cells involves morphological changes, transient expression of MVH, and maintenance of expression of the pluripotent markers NANOG, SOX2, and OCT4. E-CADHERIN (red). *Dnd1*$^{Ter/Ter}$ 129/SvJ (A-C,E-G,I-K,M-O). Arrows indicate mutant germ cells expressing MVH **(A)**, NANOG **(E)**, SOX2 **(I)**, and OCT4 **(M)** similar to wildtype germ cells at E13.5. By E16.5, 129/SvJ mutant germ cells change morphologically to form E-CAD positive clusters that are no longer MVH positive **(B)** yet maintain expression of NANOG **(F)**, SOX2 **(J)**, and OCT4 **(N)**, unlike wildtype germ cells. At this stage there are still a few morphologically wildtype germ cells that appear to be isolated and have faint or no MVH expression **(B inset arrowheads)** but still express the pluripotent markers **(F,J,N arrowheads)**. As the neoplasias increase in size, they lack MVH (**C**), and pluripotent markers are regionally restricted **(G,K,O)**. **Dnd1$^{Ter/Ter}$;Bax$^{-/-}$ Mixed background (D,H,L,P)**. At E17.5, arrows indicate morphologically distinct clusters of cells that aberrantly express MVH **(D)** and maintain expression of NANOG **(H)**, SOX2 **(L)**, and OCT4 **(P)**. Arrowheads indicate morphologically wildtype germ cells that maintain expression of MVH **(D)** and OCT4 **(P)** but lack NANOG **(H)** and SOX2 **(L)**, similar to wildtype germ cells at this stage. Scale bars represent 50μm.

Figure 12

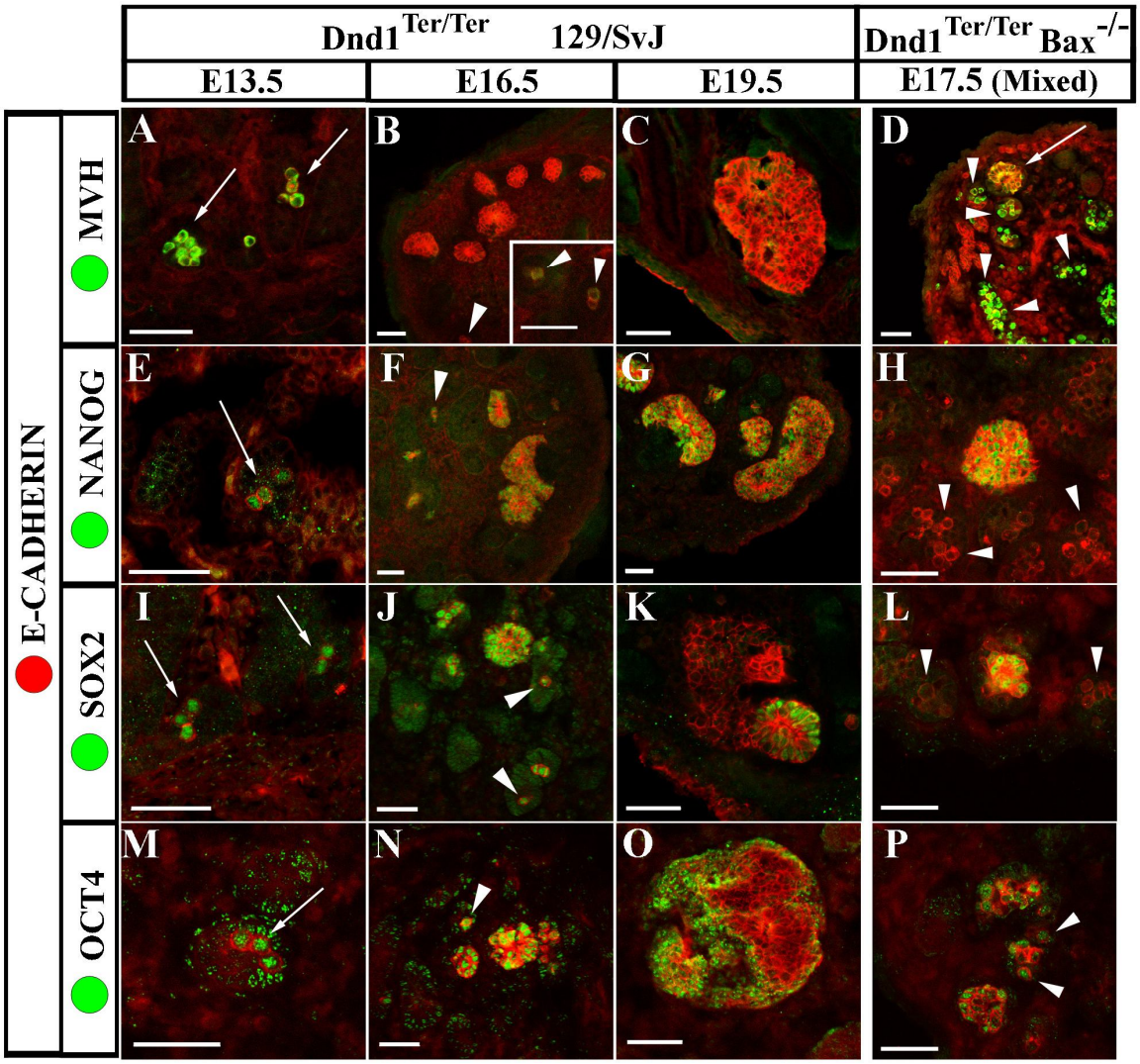
Dnd1 Ter/Ter 129/SvJ
Dnd1 Ter/Ter Bax -/-
E13.5
E16.5
E19.5
E17.5 (Mixed)
E-CADHERIN
MVH
NANOG
SOX2
OCT4
A
B
C
D
E
F
G
H
I
J
K
L
M
N
O
P

Between E19.5 and perinatal stages, mutant testes contain very large E-CAD positive masses (Fig. 13). Using LAMININ-A (LAM) to mark cord boundaries, E-CAD positive masses are observed at the edge of broken LAM positive structures, spilling into the interstitium (Fig. 13G) revealing their origin from within the cords. During these tumor stages, NANOG, SOX2, and OCT4 positive cells are still present but are restricted to a subset of cells in the teratoma (Fig. 12G,K,O, respectively), correlating to the embryonal carcinoma (EC) compartment often associated with developing teratocarcinomas (Rivers and Hamilton, 1986). Morphological changes are accompanied by molecular expression changes indicating differentiation or specification of certain cell types. MVH positive cells reappear at various locations in the larger growths (Fig. 13 A,B). NANOG and SOX2 detected in serial sections at these stages show very similar expression profiles restricted to-specific clusters of cells (Fig. 13 C,E) that never overlap with MVH positive cells (Fig. 13 B,D,F). Further signs of differentiation are evident in P1 samples immunostained with the transcription factor and pan endodermal marker FOXA2 (Fig. 14).

The transition into E-CAD positive neoplasias and maintenance of pluripotent markers was also observed in mutants carrying the *Oct4-EGFP* reporter transgene. The *Oct4-EGFP* line contains an EGFP reporter driven by an *Oct4* enhancer element (Ohbo et al., 2003), and is normally specific to germ cells in the gonad.

Figure 13 – Growth in nascent teratomas. At E19.5 MVH expression is sometimes detected in a subset of cells in the developing teratoma **(A,B)**. Serial sections of mutant testes at E19.5 reveal overlapping expression patterns of NANOG and SOX2 **(C,E and D,F)** which never overlap with expression of MVH **(B,D,F)**. Nascent tumors arise within cords but escape from testis cord boundaries, marked by Laminin (green) **(G,H)**. Testis cord boundaries **(G arrowheads)** are broken at E19.5 **(G arrow)** and neoplasias (red cells, E-CAD) escape and can grow to very large sizes in the interstitium **(G,H)**. Scale bars represent 50μm.

Figure 13

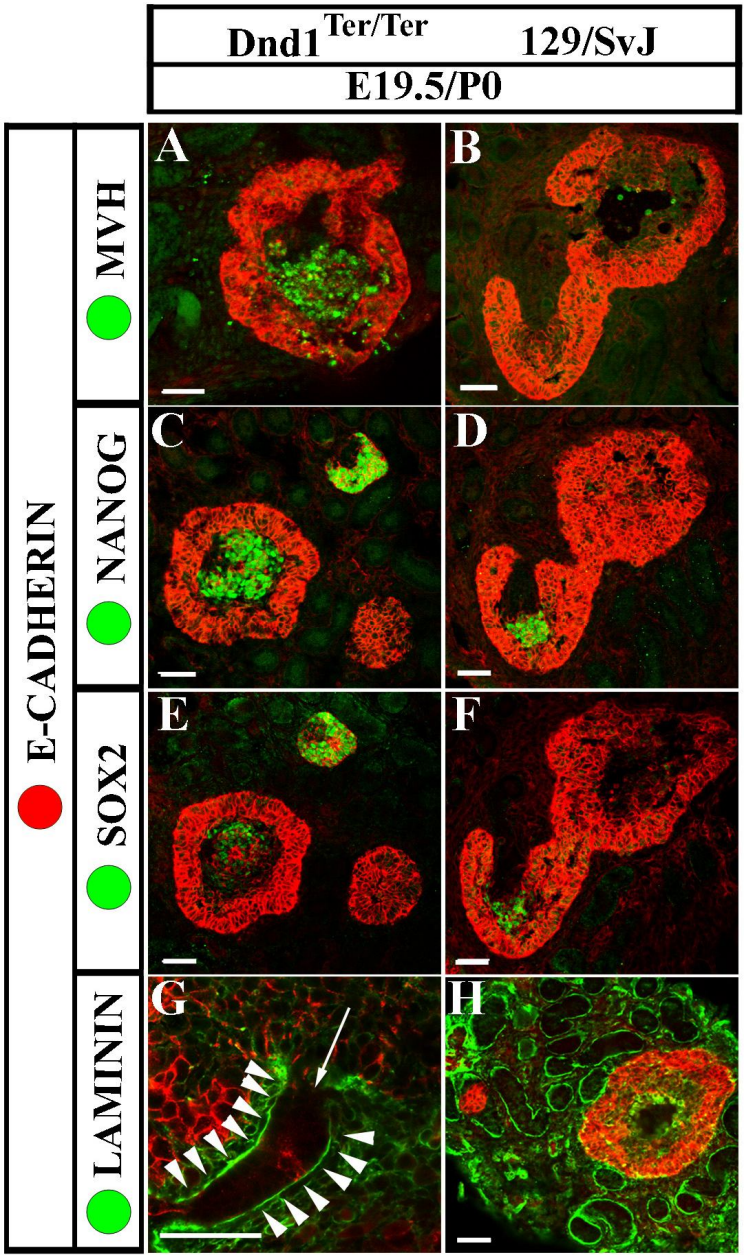
Dnd1 Ter/Ter
129/SvJ
E19.5/P0
E-CADHERIN
MVH
NANOG
SOX2
LAMININ
A
B
C
D
E
F
G
H

Figure 14 – Differentiation in nascent teratomas. Serial sections of E-CAD-positive (red) differentiating teratomas. In addition to cell clusters co-expressing NANOG and SOX2 (see Fig. 12), SOX2 (green, left panel) also labels differentiating cells that morphologically resemble neuroectoderm tissue (arrowheads). The pan-endodermal marker FOXA2 (green, right panel) labels many cells in a differentiating teratoma. Scale bars represent 50μm.

Figure 14

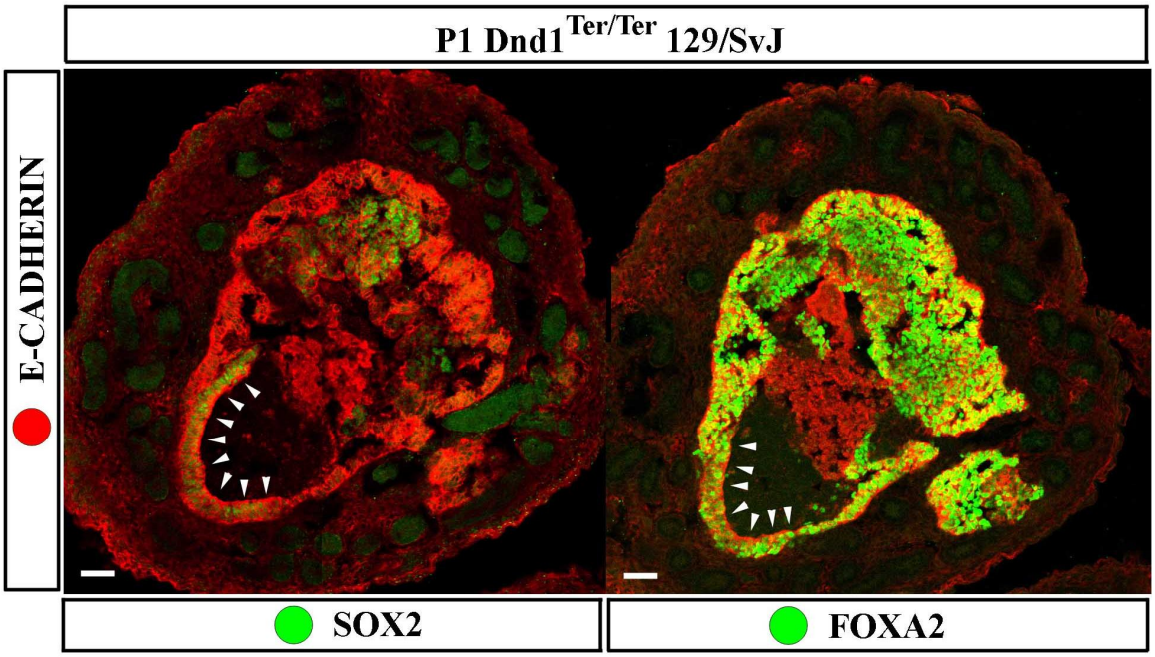

Figure 15 – Transformation in *Oct4-EGFP* positive mutant testes. (A-D) E15.5 *Dnd1*$^{Ter/Ter}$ mutant testis. E-CAD positive (red) neoplasias begin to form which are GFP (green) and NANOG (blue) positive. Even cells that morphologically resemble wildtype germ cells are NANOG positive at this stage (unlike wildtype cells). Presumably most (or all) of these mutant germ cells transform in mutants. (E-H) E19.5 *Dnd1*$^{Ter/+}$ heterozygote with a neoplasia. At this stage most germ cells are GFP-positive, NANOG-negative, and still look morphologically normal (arrowheads). The E-CAD positive neoplasia has escaped from the testis cords and grown much larger. Expression of GFP and NANOG are only expressed in pockets of cells within the growing tumor (arrows).

Figure 15

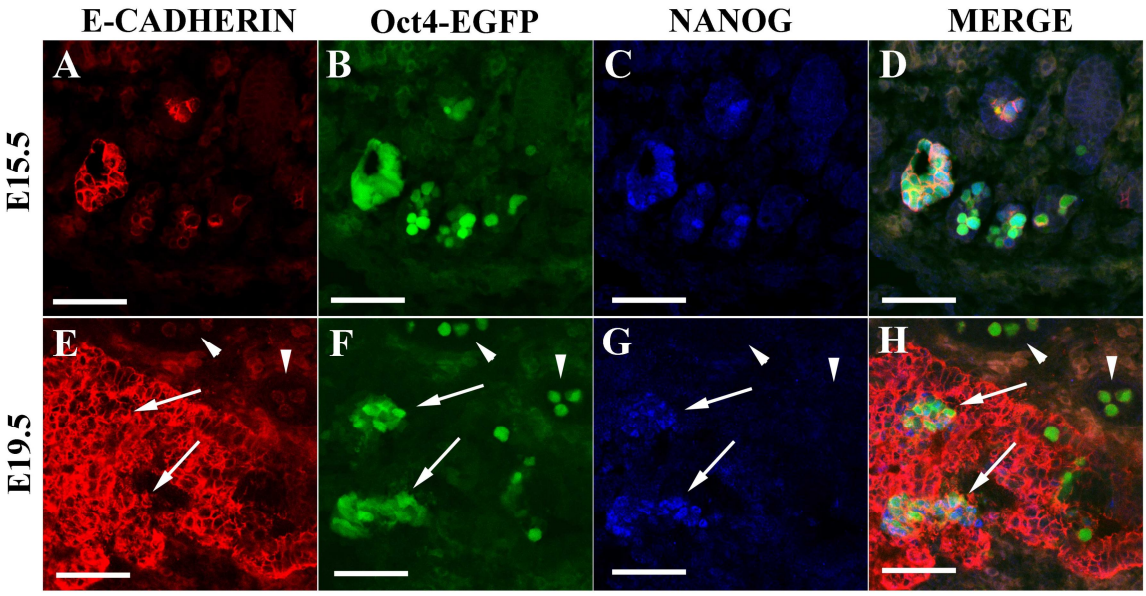

At E15.5 NANOG expression was detected throughout the growing neoplasia and in individual cells that still morphologically resemble wildtype germ cells (Fig. 15C). By E19.5, a *Dnd1*$^{Ter/+}$ heterozygous testis also contained a growing neoplasia but without the significant loss in germ cells (Fig. 15E-H). Untransformed germ cells are GFP-positive and NANOG-negative (Fig. 15 arrowheads). The E-CAD neoplasia is very large at this stage, and GFP and NANOG expression are not found throughout the entire growth but are restricted to pockets of cells within the nascent tumor (Fig. 15 arrows).

When the *Dnd1*^{Ter} mutation is crossed onto other inbred strain backgrounds, testicular teratomas do not develop and instead, all germ cells of the testis are eventually lost (Noguchi et al., 1996; Stevens, 1981). By blocking cell death using a homozygous *Bax*-null allele, the initial PGC loss observed in *Dnd1*$^{Ter/Ter}$ embryos was rescued (Fig. 7). Under these conditions, testicular teratomas arose on mixed genetic backgrounds. However, whether the pattern of tumorigenesis was similar to the pattern in 129/SvJ mutants, and whether the majority of rescued germ cells underwent neoplasia formation, as do the majority of mutant germ cells on the 129/SvJ background, was unclear.

To clarify these questions, *Dnd1*$^{Ter/Ter}$;*Bax*$^{-/-}$ mixed background mutants were collected for immunocytochemical analysis. Like 129/SvJ, *Dnd1*$^{Ter/Ter}$;*Bax*$^{-/-}$ double mutant germ cells on a mixed background express MVH, NANOG, SOX2, OCT4, and lack GM114 expression after colonization of the gonad (Fig. 16). At E17.5 mixed background

double mutants also contain E-CAD positive neoplasias (Fig. 12D arrow) that express NANOG, SOX2, and OCT4 (Fig. 12H,L,P). However, many germ cells were morphologically normal, MVH positive, and NANOG and SOX2 negative (Fig. 12D,H,L,P arrowheads). Only a fraction of *Dnd1*$^{Ter/Ter}$;*Bax*$^{-/-}$ germ cells present at this stage in mixed background mutants transition into neoplasias. This is similar to the situation in 129/SvJ *Dnd1*$^{Ter/+}$ (heterozygous) embryos, where the vast majority of germ cells develop normally, but a few transition to teratomas (Fig. 15E-H and Fig. 17). The stochastic nature of neoplasia formation in these two instances suggests a dose/threshold effect that is subject to strain background influences.

Figure 16 – Mutant germ cells (red, E-CAD) on a mixed genetic background express MVH and SOX2 but not GM114, similar to 129/SvJ mutants. (A-C) Wildtype E13.5 testes and **(D-F)** double-mutant testes stained with MVH **(A,D)**, SOX2 **(B,E)**, and GM114 **(C,F)**. Scale bars represent 50μm**.**

Figure 16

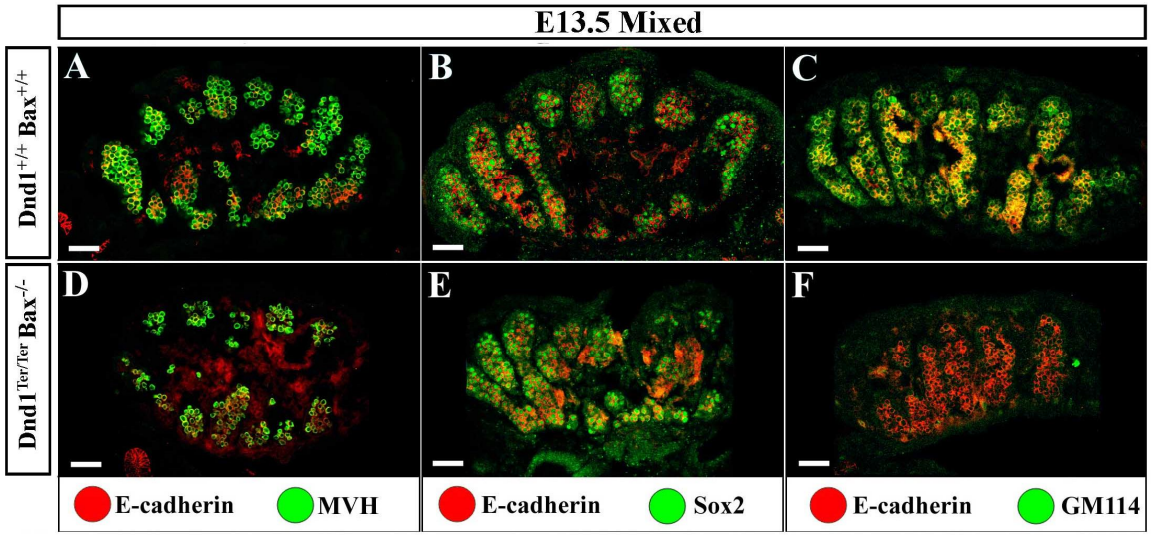
E13.5 Mixed
Dnd1+/+ Bax+/+
Dnd1Ter/Ter Bax-/-
A
B
C
D
E
F
E-cadherin
MVH
E-cadherin
Sox2
E-cadherin
GM114

Figure 17 – Tumorigenesis in 129/SvJ heterozygotes. In 129/SvJ *Dnd1*$^{Ter/+}$ testes, germ cells (E-CAD, red) sometimes form teratomas, positive for Ki67 (green, arrow), whereas most germ cells are negative for Ki67, and presumably arrested in G0 (arrowhead). Scale bars represent 50μm.

Figure 17

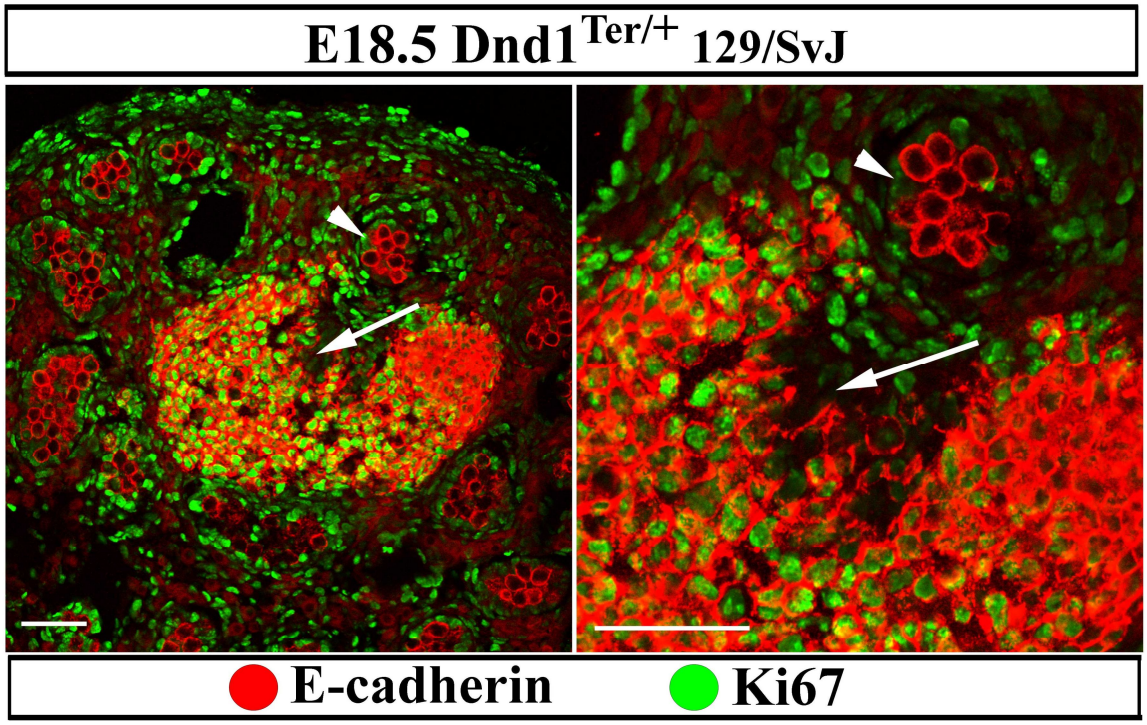

4.3.2 Germ cell transcripts are misregulated in mutant gonads

To determine whether transcripts for *Nanos* genes and other pluripotency and differentiation markers are misregulated in *Dnd1*$^{Ter/Ter}$ germ cells, we isolated mRNA from whole gonads dissected at E13.5 from *Dnd1*$^{Ter/+}$;*Bax*$^{+/-}$ intercrosses on a mixed background. We generated cDNA and used quantitative RT-PCR to measure expression levels of germ cell-specific genes normalized to a germ cell-specific transcript (Fig. 18A). To validate this approach we included two experimental controls. First, *Oct4* (a germ cell-specific gene) was normalized to a ubiquitous gene, *Hprt1*, to determine whether *Oct4* expression levels reflected the number of rescued germ cells as determined by immunofluorescence in *Dnd1*$^{Ter/Ter}$;*Bax*$^{-/-}$ mutants reported previously (Fig. 7A,C,E,G). *Oct4* expression was reduced ($p<0.005$) in *Dnd1*$^{Ter/Ter}$ gonads, consistent with the presence of many fewer germ cells (Fig. 18B third bar), while there was a slight increase in *Oct4* expression in *Dnd1*$^{+/+}$;*Bax*$^{-/-}$ gonads, reflecting the presence of more germ cells compared to wildtype and double mutant testes (Fig. 18B).

Second, expression of *Dnd1* (which, within the gonad, is-specific to germ cells) was analyzed in wildtype, *Bax* mutant, and double mutant gonads. *Dnd1*$^{Ter/Ter}$ single mutants were omitted from this and following analyses because the persistence of so few germ cells led to highly variable and inconclusive results. *Dnd1* expression was down-regulated almost 3-fold ($p<0.001$) in germ cells from double mutant gonads (Fig. 17C Double mutant) compared to controls (Fig. 18C Control), as expected from

nonsense-mediated decay due to the mutation (Youngren et al., 2005). Based on these validations, we concluded that normalization of germ cell-specific genes to *Oct4* expression accounts for differences in germ cell numbers in the mutants and provides a more reliable normalization than a general housekeeping gene like *Hprt1*.

Consistent with the immunocytochemical results showing maintenance of pluripotent markers, *Nanog* was up-regulated ($p<0.005$) in double mutants (Fig. 18D). In contrast, *Mvh* expression was down-regulated more than 2.5-fold ($p<0.001$) in $Dnd1^{Ter/Ter};Bax^{-/-}$ germ cells (Fig. 18E) (despite the presence of MVH protein in 129/SvJ and mixed background $Dnd1^{Ter/Ter}$ mutants at this stage (Fig. 12A and Fig. 16D)). *Nanos3* expression was down-regulated more than 2-fold ($p<0.0005$) (Fig. 18F), whereas *Nanos2* expression was down-regulated more than 10-fold ($p<0.0005$) in double mutants (Fig. 18G). *Nanos3* expression may be affected much earlier, when primordial germ cells are specified. *Nanos3* mutants show a similar loss of PGCs at early migratory stages (Suzuki et al., 2008; Tsuda et al., 2003). The significant decrease in *Nanos2* expression is consistent with the up-regulation of meiotic markers in mutant germ cells (Fig. 19). Another germ cell-specific gene, *Gm114*, showed no significant difference in transcript expression level in double mutants (Fig. 18H); however, GM114 protein was not detected in $Dnd1^{Ter/Ter}$ 129/SvJ germ cells (Fig. 18J inset) or in $Dnd1^{Ter/Ter};Bax^{-/-}$ mixed background germ cells (Fig. 18J) throughout development (Fig. 11), indicating potential translational regulation of this gene.

Figure 18 – Mutant germ cells have altered expression profiles of pluripotent and differentiation genes at E13.5. (A) Schematic representation of tissue collection for qRT-PCR analysis. The numeral indicates how many pairs of each genotype were collected. **(B)** *Oct4* expression levels mimic germ cell number estimates by immunofluorescence as previously published (see cartoon in A and Fig. 7). **(C)** Double-mutants express lower levels of *Dnd1* because the *Ter* mutation is a premature stop codon that activates nonsense-mediated decay. Double-mutant germ cells show up-regulation of **(D)** *Nanog* and a decrease in **(E)** *Mvh*, **(F)** *Nanos3*, and **(G)** *Nanos2* transcript levels compared to controls. **(H)** There is no significant difference in *Gm114* transcript levels in double-mutants. **(I)** GM114 (green) labels wildtype germ cells (E-CAD, red) at E13.5. **(J)** Double-mutant germ cells fail to express GM114 (green) on a mixed background or in $Dnd1^{Ter/Ter}$ mutants on a 129/SvJ background (inset arrows). MNE = mean normalized expression. Each bar represents the standard error of the mean (SEM) of at least three biological replicates. * $p<0.05$; *** $p<0.005$; **** $p<0.001$; ***** $p<0.0005$; ****** $p<0.0001$. Scale bars represent 50μm.

Figure 18

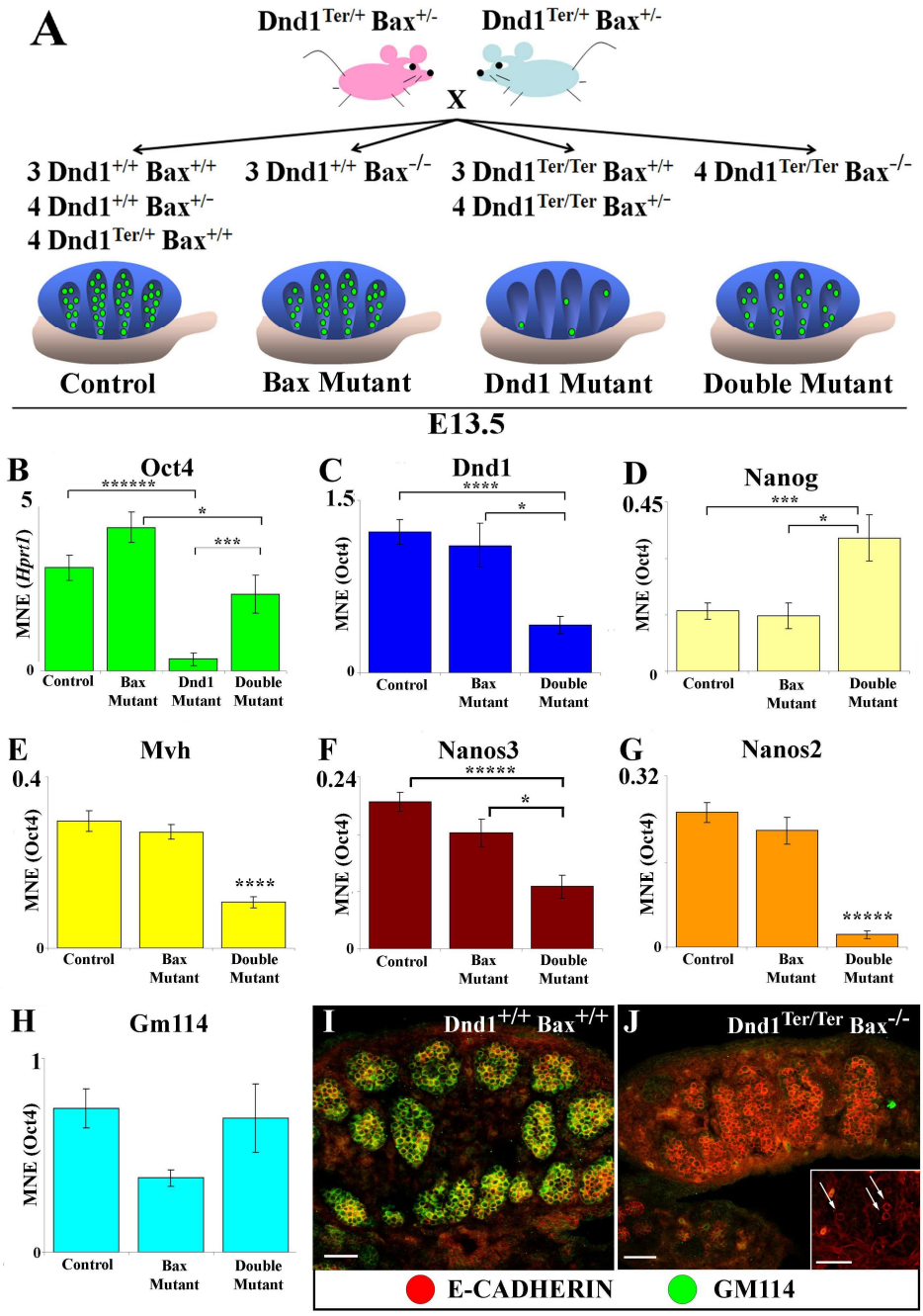
A
Dnd1 Ter/+ Bax +/-
Dnd1 Ter/+ Bax +/-
X
3 Dnd1 +/+ Bax +/+
4 Dnd1 +/+ Bax +/-
4 Dnd1 Ter/+ Bax +/+
3 Dnd1 +/+ Bax -/-
3 Dnd1 Ter/Ter Bax +/+
4 Dnd1 Ter/Ter Bax +/-
4 Dnd1 Ter/Ter Bax -/-
Control
Bax Mutant
Dnd1 Mutant
Double Mutant
E13.5
B Oct4
MNE (Hprt1)
C Dnd1
MNE (Oct4)
D Nanog
MNE (Oct4)
E Mvh
MNE (Oct4)
F Nanos3
MNE (Oct4)
G Nanos2
MNE (Oct4)
H Gm114
MNE (Oct4)
Control
Bax Mutant
Dnd1 Mutant
Double Mutant
I Dnd1 +/+ Bax +/+
J Dnd1 Ter/Ter Bax -/-
E-CADHERIN
GM114

4.3.3 Mutant germ cells prematurely upregulate meiotic markers

Unlike XX germ cells, wildtype XY germ cells do not normally enter meiosis until after birth. This is dependent on the somatic expression of *Cyp26B1* from E11.5-E13.5, which degrades the meiosis-inducing factor retinoic acid (RA) in the testis (Bowles et al., 2006), and germ cell-specific expression of *Nanos2* from E13.5 until after birth (Suzuki and Saga, 2008). Loss of either *Cyp26b1* or *Nanos2* leads to precocious up-regulation of the meiotic markers STRA8 and SCP3 in mutant male germ cells. Based on our previous results, levels of *Cyp26b1* are normal in mutants (Fig. 6F). However, it has been shown in zebrafish that DND targets the *nanos* transcript and promotes translation (Kedde et al., 2007a). In mice, $Dnd1^{Ter/Ter}$ mutant germ cells have a significant reduction in *Nanos2* (Fig. 18G). To test whether these pathways are disrupted in mutants, we examined $Dnd1^{Ter/Ter}$ and $Dnd1^{Ter/Ter};Bax^{-/-}$ germ cells on 129/SvJ and mixed backgrounds for expression of STRA8 and SCP3.

Similar to *Nanos2* mouse mutants, *Dnd1* mutants showed up-regulation of both STRA8 and SCP3 in male germ cells beginning at E16.5 on all genetic backgrounds we investigated (Fig. 19). On the 129/SvJ background, $Dnd1^{Ter/Ter}$ germ cells do not express these meiotic markers at E14.5 (Fig. 19A). By E16.5 many germ cells have formed E-CADHERIN (E-CAD) positive neoplasias. A few morphologically normal cells still present at this stage express SCP3 (Fig. 19B). However, cells within the neoplasias were never positive (Fig. 19C). This result is consistent with results on other genetic

backgrounds. SCP3 was also detected in germ cells of E17.5 *Dnd1*$^{Ter/Ter}$ mutants on a mixed background wildtype for *Bax* (Fig. 19D), and in *Dnd1*$^{Ter/Ter}$;*Bax*$^{-/-}$ double mutant germ cells (Fig. 19E) where STRA8 was also detected at E17.5 (Fig. 19F). However, small clusters of E-CAD positive cells and developing neoplasias were never positive (Fig. 19 arrowheads). SCP3 and STRA8 were also detected in mutants on a C57BL/6J background (data not shown). Overall these results are similar to results in *Nanos2* mutants (Suzuki and Saga, 2008), and suggest that mutant germ cells, regardless of strain background, are not committed to the pro-spermatogonial fate, most likely due to defects intrinsic to germ cells and not to the somatic program.

Figure 19 – Mutant germ cells ectopically express meiotic markers SCP3 and STRA8. **(A)** E14.5 129/SvJ *Dnd1*$^{Ter/Ter}$ germ cells do not express SCP3 (green). **(B)** E16.5 morphologically wildtype germ cells express SCP3 (green). **(C)** E18.5 neoplasias (E-CAD positive) do not express SCP3. **(D)** On a mixed genetic background wildtype for *Bax* (where germ cells do not normally transform) at E17.5, many, but not all, germ cells express SCP3 (green). **(E)** Double-mutant *Dnd1*$^{Ter/Ter}$*;Bax*$^{-/-}$ germ cells also express SCP3 and **(F)** STRA8, but only in morphologically wildtype germ cells and never in neoplasias (arrowheads). Scale bars represent 50μm.

Figure 19

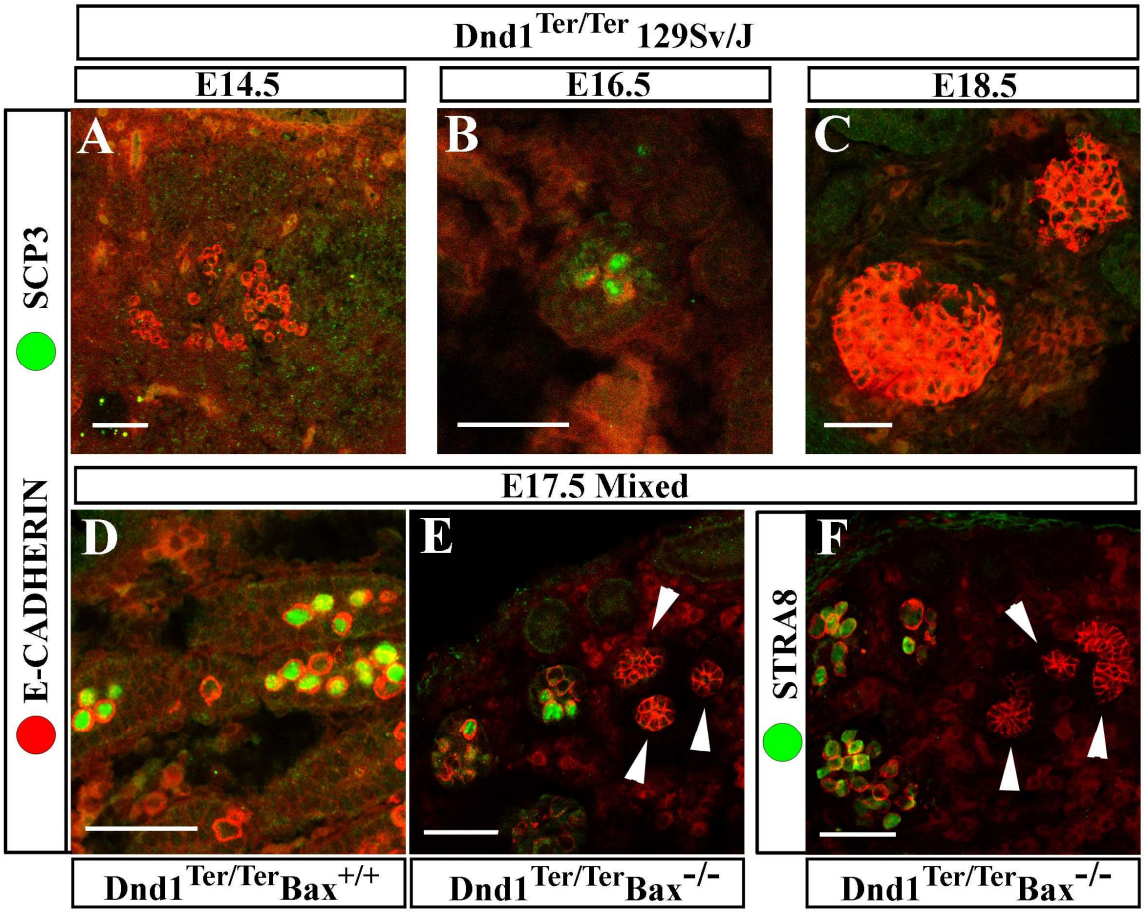
Dnd1Ter/Ter 129Sv/J
E14.5
E16.5
E18.5
A
B
C
SCP3
E-CADHERIN
E17.5 Mixed
D
E
F
STRA8
Dnd1Ter/TerBax+/+
Dnd1Ter/TerBax-/-
Dnd1Ter/TerBax-/-

4.3.4 Mutant germ cells fail to enter mitotic arrest in G0

Maintenance of expression of pluripotent markers and the growth of E-CAD positive clusters in *Dnd1*$^{Ter/Ter}$ germ cells on a 129/SvJ background occur after the stage when wildtype male germ cells typically enter mitotic arrest (Fig. 11 highlighted portion) (McLaren, 2001). In the normal course of events in the fetal testis, *p27*^{Kip1} transcript is up-regulated in germ cells by E13.5 (Western et al., 2008) and protein expression is abundant by E14.5 (Fig. 20 A,B). p27^{Kip1} is a tumor suppressor and cell cycle regulator that inhibits CyclinE/cdk2 complexes, thus preventing phosphorylation of pRB and activating the G1/S checkpoint by inhibition of E2F transcription factors important for cell division (Massague, 2004; Western et al., 2008). As male germ cells up-regulate p27^{Kip1}, they transition into a G1/G0 arrest of cell cycle and no longer express the active cell cycle marker Ki67 (Fig. 20C,D).

Human DND1 can bind *p27*^{Kip1} transcript and protect it from miRNA-mediated translational repression by miR-221/222 (Kedde et al., 2007a). Both miR-221 and miR-222 were detected in developing E14.5 mouse testes (Fig. 20I). This suggests that loss of DND1 in mutant germ cells could lead to miRNA-mediated repression of *p27*^{Kip1} translation and continuation of cell division. Supporting this model, *Dnd1*$^{Ter/Ter}$*;Bax*$^{-/-}$ germ cells fail to up-regulate protein expression of P27^{Kip1} by E14.5 (Fig. 20E,F) and remain Ki67 positive at E14.5 (Fig. 20G,H) and later (data not shown). This was also true of *Dnd1*$^{Ter/Ter}$*;Bax*$^{+/+}$ germ cells on both pure 129/SvJ, mixed, and C57BL/6J backgrounds

(data not shown), indicating that the failure to arrest in G0 is not a strain-specific phenotype, and cannot account for the increased susceptibility to teratoma formation in the 129/SvJ strain. Strikingly, somatic expression of $p27^{Kip1}$ transcript is not significantly down-regulated in mutants at E13.5 (Fig. 20J), suggesting that the loss of protein observed in mutant germ cells is due to a translational defect. Interestingly, in $Dnd1^{Ter/+}$ heterozygotes on a 129/SvJ background, the vast majority of germ cells develop normally and enter mitotic arrest (Fig. 17 arrowhead). However, one (or possibly a few) escape proper regulation and form E-CAD and Ki67-positive neoplasias (Fig. 17 arrows), suggesting dosage effects of DND1 to which the 129/SvJ strain is particularly susceptible.

Figure 20 – Mutant germ cells translationally misregulate *p27^{Kip1}* and fail to enter mitotic arrest. (A,B) Control E14.5 *Dnd1$^{Ter/+}$;Bax$^{+/-}$* germ cells (E-CAD red) express p27^{Kip1} (green) and **(C,D)** lack expression of Ki67 (green). **(E,F)** Mutant *Dnd1$^{Ter/Ter}$;Bax$^{-/-}$* germ cells (E-CAD red) fail to express p27^{Kip1} and **(G,H)** maintain robust expression of Ki67. **(I)** qRT-PCR of miR-221 and miR-222 (the miRNAs that target *p27^{Kip1}*) normalized to 5S rRNA in E14.5 testis (dark gray) and E12.5 liver (light gray). **(J)** Transcript levels of *p27^{Kip1}* are not significantly different in double-mutant gonads (right bar) compared to wildtype (left bar) or *Bax* mutant (middle bar) controls. Each bar represents the SEM of at least three biological replicates. Scale bars represent 50μm.

Figure 20

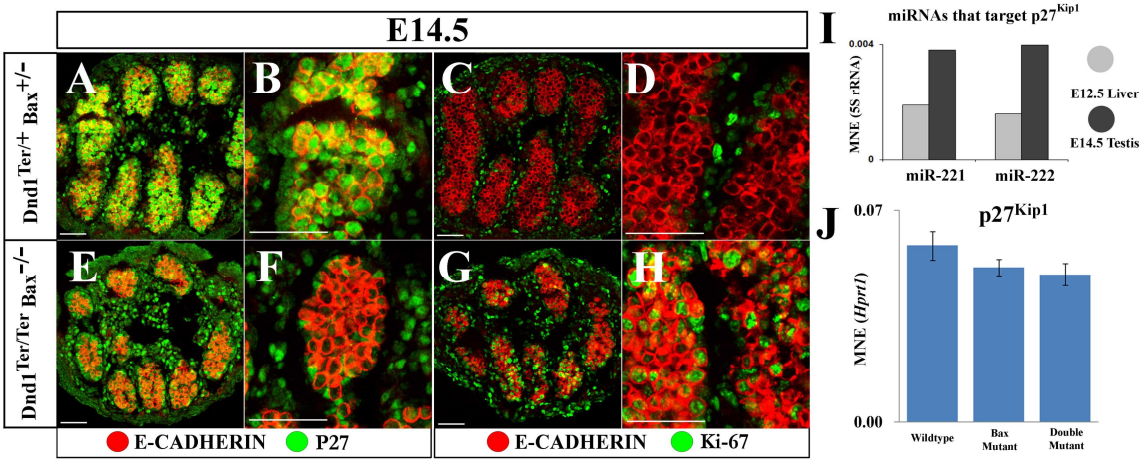
E14.5
A
B
C
D
E
F
G
H
Dnd1Ter/+ Bax+/-
Dnd1Ter/Ter Bax-/-
E-CADHERIN
P27
E-CADHERIN
Ki-67
I
miRNAs that target p27Kip1
MNE (5S rRNA)
0.004
0
E12.5 Liver
E14.5 Testis
miR-221
miR-222
J
p27Kip1
MNE (Hprt1)
0.07
0.00
Wildtype
Bax Mutant
Double Mutant

4.3.5 DND1 binds targets important for germ cell mitotic arrest

The translational misregulation of $p27^{Kip1}$ in $Dnd1^{Ter/Ter}$ germ cells indicates an important role for DND1 during a critical transition. DND1 likely targets other cell cycle regulators in addition to $p27^{Kip1}$. To test this hypothesis, and verify conservation of function of the human protein binding to targets $p27^{Kip1}$ and *Lats2*, both TAP- and GFP-tagged DND1α were over-expressed in mouse 3T3 cells. We verified that full length TAP-DND1α protein was produced by Western blot (Fig. 21A), and found that GFP-DND1α localized to perinuclear granules (Fig. 21B), as reported previously for this cell type and in zebrafish germ cells (Bhattacharya et al., 2007; Slanchev et al., 2008).

To determine whether mouse DND1 binds $p27^{Kip1}$ and *Lats2*, an RNA immunoprecipitation (RIP) was performed (Keene et al., 2006) from 3T3 cells followed by reverse transcriptase (RT-) and quantitative PCR (qRT-PCR). TAP-DND1α was enriched for both $p27^{Kip1}$ and *Lats2* compared to the TAP-tag alone (Fig. 21C). We also examined a set of candidate cell cycle regulator genes that are endogenously expressed in 3T3 cells and are relevant for germ cell mitotic arrest (Kimura et al., 2003; Western et al., 2008). These genes were examined by qRT-PCR, normalized to *Hprt1*, and compared to cells transfected with the TAP-tag alone (*Gapdh* represents a negative control that is not enriched). Enrichment was noted for a series of cell cycle inhibitors including $p21^{Cip1}$, $p27^{Kip1}$, *Lats2*, *pRB*, *p53*, and *Pten* (Fig. 21C left bracket). Each of these was statistically significant compared to *Gapdh*. Positive regulators of cell cycle such as *Cyclin E1*, *Cyclin*

E2, *Akt1*, and *Akt3* were not enriched, though *Akt2* was somewhat enriched (Fig. 21C middle bracket).

4.3.6 DND1 influences gene expression of key cell cycle pathways in cell culture

The ability of DND1 to bind a set of targets that represent cell cycle inhibitors suggests that it may function as a master regulator of mitotic arrest in male germ cells and could possibly affect cell cycle regulation in cell lines in culture. While DND1 does not appear to directly antagonize pluripotency in teratocarcinoma cell lines P19 and F9 (see Appendix 6.2), its effects on cell cycle may be more subtle. To obtain a comprehensive perspective of the functional effects of DND1, TAP or TAP-DND1α was over-expressed in P19 cells, RNA was extracted, and microarrays were performed in biological triplicate to measure the global effects on gene expression.

Based on gene ontology (GO) and transcription factor gene set comparison analyses, several pathways showed alterations at a level of statistical significance of $p<0.005$ by the Efron-Tibshirani's GSA test (Fig. 22). Altered these pathways included the G1/S and G2/M checkpoints, the RB tumor suppressor, and Cdc25 and Chk1 regulatory pathways (Fig. 22C). Additionally, the c-Myc, E2F-1, and E2F-2 transcription factor networks were significantly altered in P19 cells over-expressing DND1. These data suggest that DND1 can globally affect levels of mRNA of a group of cell cycle regulators.

Figure 21 – DND1 binds a set of functionally related targets that are cell cycle regulators. (A) TAP-DND1α migrates at the predicted size of about 50 kDa (right lane) in a Western blot of 3T3 cells. **(B)** GFP-DND1α (green, lower panel) localizes to perinuclear granules compared to GFP alone (top panel) in 3T3 cells. Scale bars represent 20μm. **(C)** Chart representing qRT-PCR results from RIP experiments using TAP-DND1α in 3T3 cells compared to the TAP tag alone and normalized to *Hprt1*. Each gene represents fold enrichment compared to the control. n= the number of independent RIP replicates. Each bar represents the SEM of at least three replicates. * $p<0.05$.

Figure 21

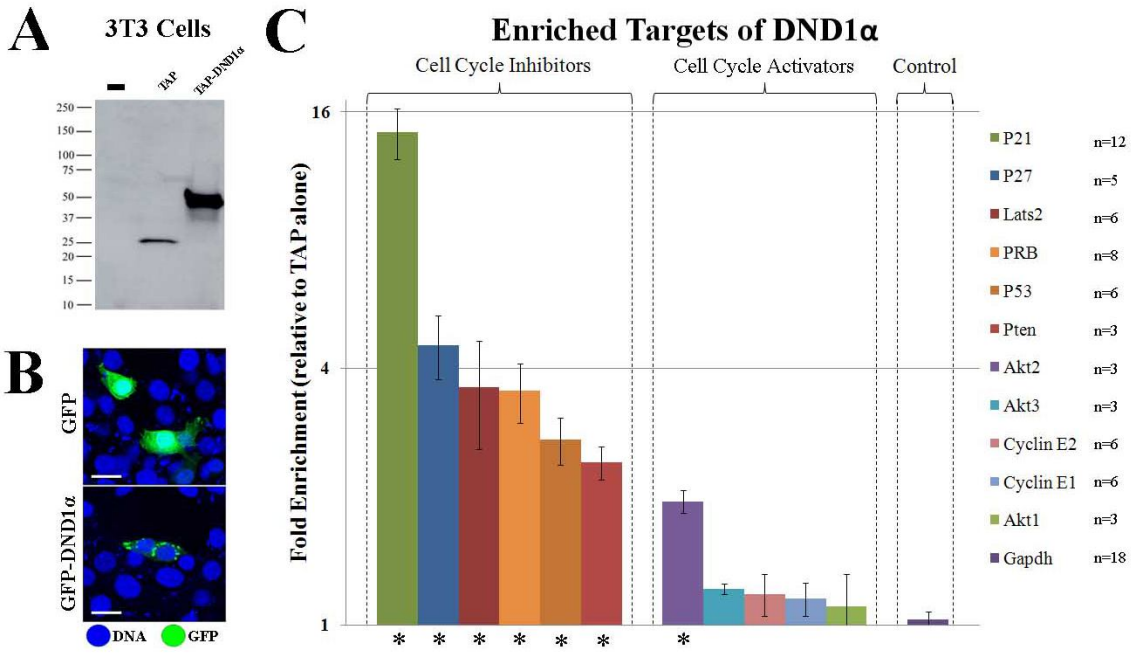
A
3T3 Cells
-
TAP
TAP-DND1α
250
150
100
75
50
37
25
20
15
10
B
GFP
GFP-DND1α
DNA
GFP
C
Enriched Targets of DND1α
Cell Cycle Inhibitors
Cell Cycle Activators
Control
Fold Enrichment (relative to TAP alone)
16
4
1
P21 n=12
P27 n=5
Lats2 n=6
PRB n=8
P53 n=6
Pten n=3
Akt2 n=3
Akt3 n=3
Cyclin E2 n=6
Cyclin E1 n=6
Akt1 n=3
Gapdh n=18

Figure 22 – Overexpression of DND1 results in gene expression changes to important cell cycle checkpoint pathways. **(A)** Fold expression change plot of the total gene set with over-expression of DND1 compared to controls. **(B)** Volcano plot of all genes with p-Value significance plotted on the Y-axis. Genes that were significantly altered with a $p<0.05$ are colored in blue. **(C)** Table of a subset of pathways and transcription factor sets that were significantly altered in cells over-expressing DND1. All passed an Efron-Tibshirani GSA test with a $p<0.005$.

Figure 22

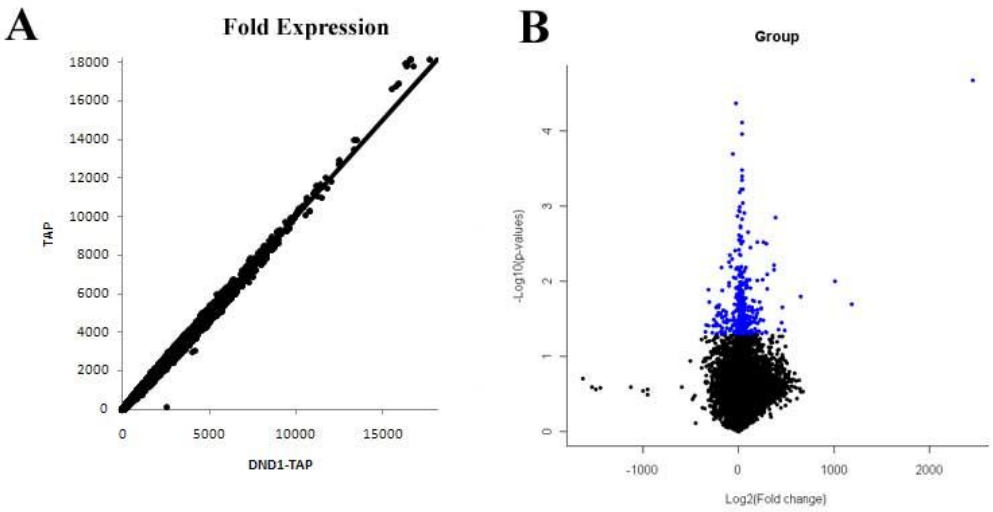

C

Pathway description	Number of genes	Efron-Tibshirani's GSA test p-value
Cell Cycle: G1/S Check Point	25	< 0.005
Cell Cycle: G2/M Checkpoint	22	< 0.005
RB Tumor Suppressor/Checkpoint Signaling in response to DNA damage	11	< 0.005
cdc25 and chk1 Regulatory Pathway in response to DNA damage	7	< 0.005

Transcription factor gene set	Number of genes	Efron-Tibshirani's GSA test p-value
c-Myc_T00140	31	< 0.005
E2F-1_T09126	25	< 0.005
E2F-2_T03526	22	< 0.005

4.3.7 Mutants on the C57BL/6J strain still arrest

Interestingly, *Dnd1*$^{Ter/Ter}$;*Bax*$^{-/-}$ double mutant gonads develop testicular teratomas at a high rate (89%) on a mixed genetic background, yet none (0%) have arisen on a pure C57BL/6J background (Table 2). Despite this obvious phenotypic difference, all mutant germ cells remain Ki67 positive and do not arrest in G0, regardless of strain background (Fig. 20). However, as germ cells do not grow into tumors on a C57BL/6J background, it is possible that C57BL/6J germ cells can compensate for the failure to arrest at G0, and achieve mitotic arrest at another stage of the cell cycle, thus preventing the growth of tumors.

Dnd1$^{Ter/Ter}$;*Bax*$^{-/-}$ double mutants on both mixed and C57BL/6J backgrounds fail to enter G0 as late as E17.5 and remain positive for Ki-67 (Fig. 23A-B,E-F). To test whether double mutant germ cells on a C57BL/6J background were still arrested at some other point in cell cycle, testes were stained with a marker for active cell divisions, phospho-histone H3 (pHH3). Strikingly, many double mutant germ cells on a mixed background were positive for pHH3, while no mutant germ cells on a C57BL/6J background stained positive (Fig. 23C-D,G-H). This finding suggests that C57BL/6J germ cells can compensate for the loss of P27^{Kip1} and arrest at another stage of the cell cycle.

Figure 23 – Double mutant C57BL/6J germ cells still arrest. E17.5 double mutant gonads from mixed and C57BL/6J backgrounds are compared to each other and to controls. **(A,E)** Control germ cells (red) are negative for Ki67 (green) because they have exited cell cycle and arrested in G0. **(B,F)** Double mutant germ cells (red) on both mixed and C57BL/6J backgrounds remain in cycle and are Ki67 positive (green). **(C,G)** Control germ cells (red) are negative for pHH3 (green) because they have exited cell cycle and are not undergoing active mitoses. Double mutant germ cells (red) on a mixed background **(D)** remain pHH3 positive whereas double mutant germ cells on a C57BL/6J background **(H)** are negative. This indicates that mixed background double mutant germ cells continue to divide while those on a C57BL/6J background successfully arrest at another stage in cell cycle. E-CAD marks germ cells in **A, B, C, D**, and **G**. Oct4-EGFP marks germ cells in **E**, **F**, and **H**. Scale bars represent 50μm.

Figure 23

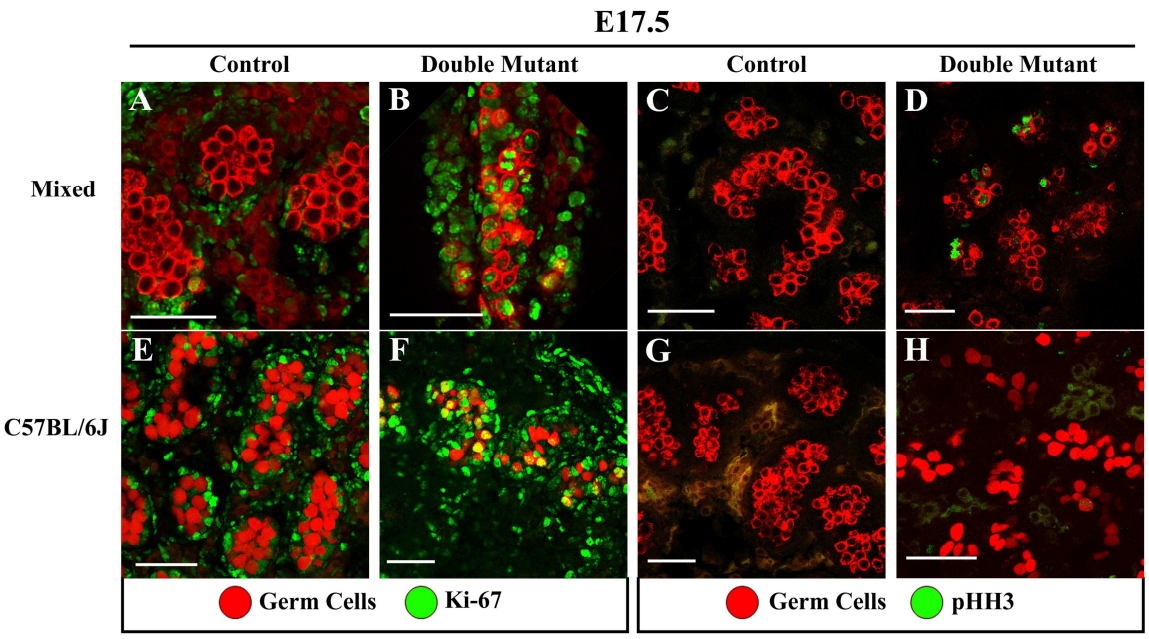
E17.5
Control
Double Mutant
Control
Double Mutant
Mixed
C57BL/6J
A
B
C
D
E
F
G
H
Germ Cells
Ki-67
Germ Cells
pHH3

4.3.8 Strain-specific differences

Surprisingly, germ cells on a *Dnd1*$^{Ter/Ter}$;*Bax*$^{-/-}$ mixed background remain Ki67 positive yet most do not form tumors. In fact, most germ cells down-regulate expression of the pluripotent markers, NANOG, SOX2, and OCT4. This situation is in contrast to the case in 129/SvJ *Dnd1*$^{Ter/Ter}$ mutants, where virtually all germ cells fail to down-regulate pluripotent markers. This difference may be due to a difference in the level of the pluripotent program in 129/SvJ relative to other strains.

To investigate whether there are basic expression level differences in important pluripotent and germ cell differentiation makers, qRT-PCR was performed on gonads from both 129/SvJ and C57BL/6J background. Wild type 129/SvJ XY gonads express significantly higher levels of the pluripotent genes *Oct4*, *Sox2*, and *Nanog* compared to C57BL/6J gonads during stages prior to mitotic arrest (Fig. 24A-C). Levels of other germ cell markers, *Mvh*, *Gm114*, and *Nanos3* (Fig. 24E,F,H), are not significantly different between strains at these stages. A higher expression of pluripotency genes could explain the spontaneous incidence of teratomas in 129/SvJ mice, as it is also easiest to derive embryonic stem cell lines from this strain (Batlle-Morera et al., 2008). It has also been demonstrated that ectopically over-expressing pluripotent genes within *in vivo* tissues can drive tumorigenesis of that cell type (Gidekel et al., 2003). The increased transcriptional levels of pluripotency genes of 129/SvJ germ cells might contribute to tumor susceptibility.

Two-fold higher expression of *Dnd1* and *Nanos2* in 129/SvJ gonads compared to C57BL/6J gonads may be important for counterbalancing the high levels of pluripotent gene expression to regulate mitotic arrest (Fig. 24D,G). The finding that some germ cells in *Dnd1*$^{Ter/+}$ 129/SvJ heterozygotes also transform suggests that the level of DND1 expression is critical to achieve mitotic arrest. The idea of a critical balance between levels of pluripotent genes and DND1 may also explain why a fraction of rescued germ cells in *Dnd1*$^{Ter/Ter}$;*Bax*$^{-/-}$ testes on mixed genetic backgrounds transform. Within the population, there may be different intermediate levels of expression of pluripotent markers and DND1 such that some individual germ cells meet the required threshold, and others do not.

To determine whether significant morphological differences exist between the strains, embryonic testes were dissected from 129/SvJ and C57BL/6J mice at E13.5-E15.5 and stained with a germ cell marker. Unexpectedly, 129/SvJ testes (Fig. 25A-C) have about half the number of testis cords compared to those of C57BL/6J (Fig. 25D-F) yet appear to contain many more germ cells (Fig. 25). To validate the immunofluorescent images suggesting more germ cells in the 129/SvJ testes, *Oct4-EGFP* reporter lines were crossed to pure 129/SvJ and C57BL/6J backgrounds for FACS sorting at stages E13.5-E15.5. Wildtype *Oct4-EGFP* positive gonads were dissociated and flow sorted to count germ cells. A comparison of 129/SvJ to C57BL/6J testes revealed approximately two-fold more germ cells in the 129/SvJ strain (Fig. 26). Additionally, mixed 129.B6 *Oct4-EGFP*

positive F2 wildtype testes maintained numbers of germ cells intermediate to each of the pure strains. Whether there is higher expression of pluripotency genes in isolated germ cells on a 129/SvJ background compared to C57BL/6J has yet to be determined.

Figure 24 – 129/SvJ express higher levels of pluripotent markers than C57BL/6J gonads. (A) *Oct4*, **(B)** *Sox2*, **(C)** *Nanog*, **(D)** *Dnd1*, **(E)** *Mvh*, **(F)** *Gm114*, **(G)** *Nanos2*, **(H)** *Nanos3*, and **(I)** *Bax* transcript levels from E12.5 to E16.5 for each strain indicated (129/SvJ=blue; C57BL/6J=red; Mixed=purple dot). Mixed background represents 129.B6.CD1 interbred and from the same experiments as shown in Figure 3. MNE = mean normalized expression. * $p<0.05$; ** $p<0.01$; *** $p<0.001$; **** $p<0.001$; ***** $p<0.0005$.

Figure 24

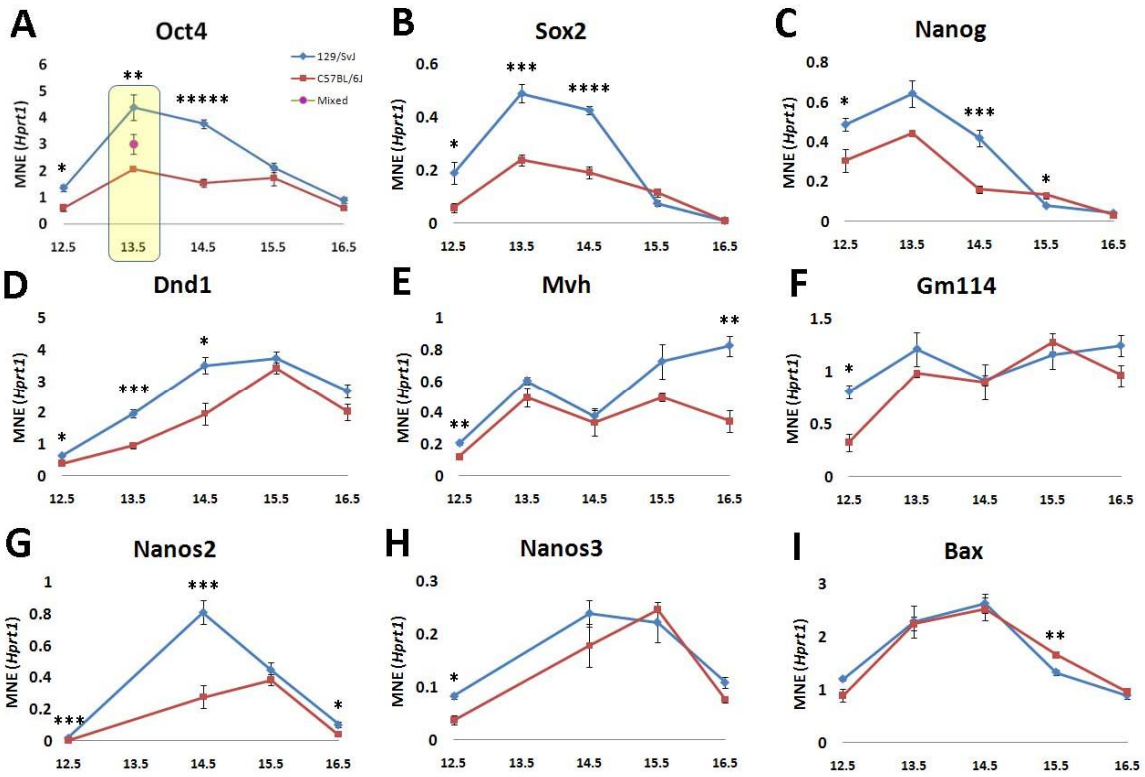
A
Oct4
129/SvJ
C57BL/6J
Mixed
MNE (Hprt1)
B
Sox2
C
Nanog
D
Dnd1
E
Mvh
F
Gm114
G
Nanos2
H
Nanos3
I
Bax
12.5
13.5
14.5
15.5
16.5

Figure 25 – Morphological comparison of 129/SvJ and C57BL/6J testes. (A-C) 129/SvJ testes compared to **(D-F)** C57BL/6J testes at **(A,D)** E13.5, **(B,E)** E14.5, and **(C,F)** E15.5. 129/SvJ testes have fewer testis cords with larger diameters than C57BL/6J testes. Additionally, there appear to be more germ cells (red) in 129/SvJ testes at all stages tested. Scale bars represent 100μm.

Figure 25

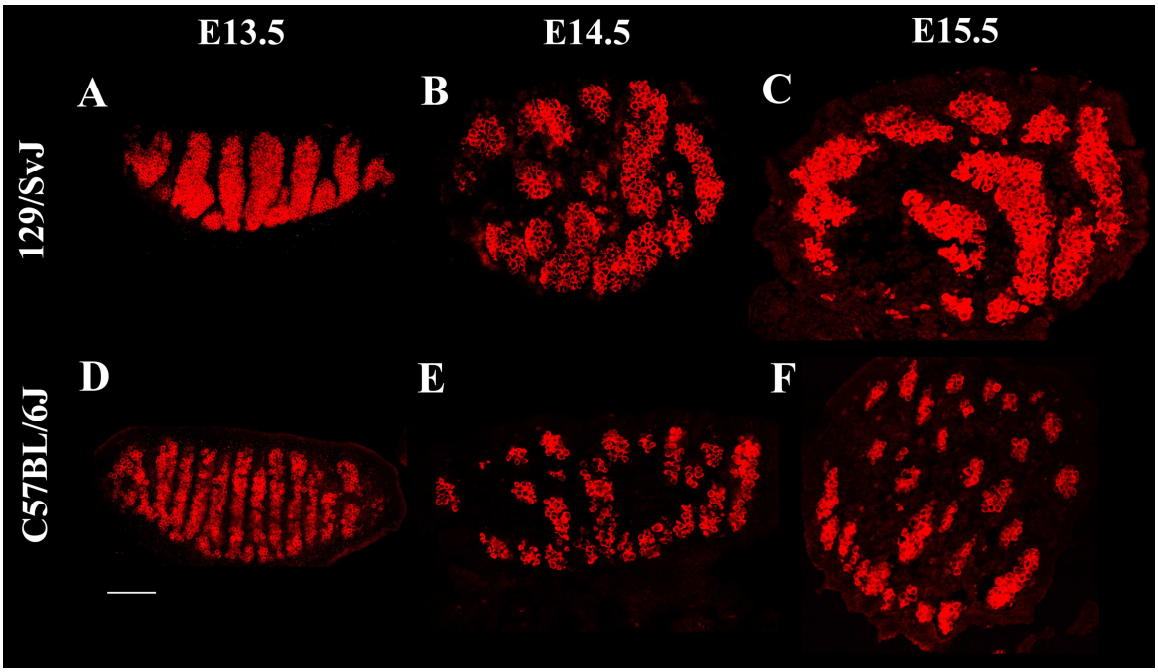

Figure 26 – 129/SvJ testes contain more germ cells than those from C57BL/6J. 129/SvJ testes (green line) contain approximately twice as many germ cells as C57BL/6J testes (blue line) from E13.5 to E15.5. 129.B6 F2 hybrids (red line) contain an intermediate number of germ cells. The data for the E13.5 time point for 129/SvJ is missing.

Figure 26

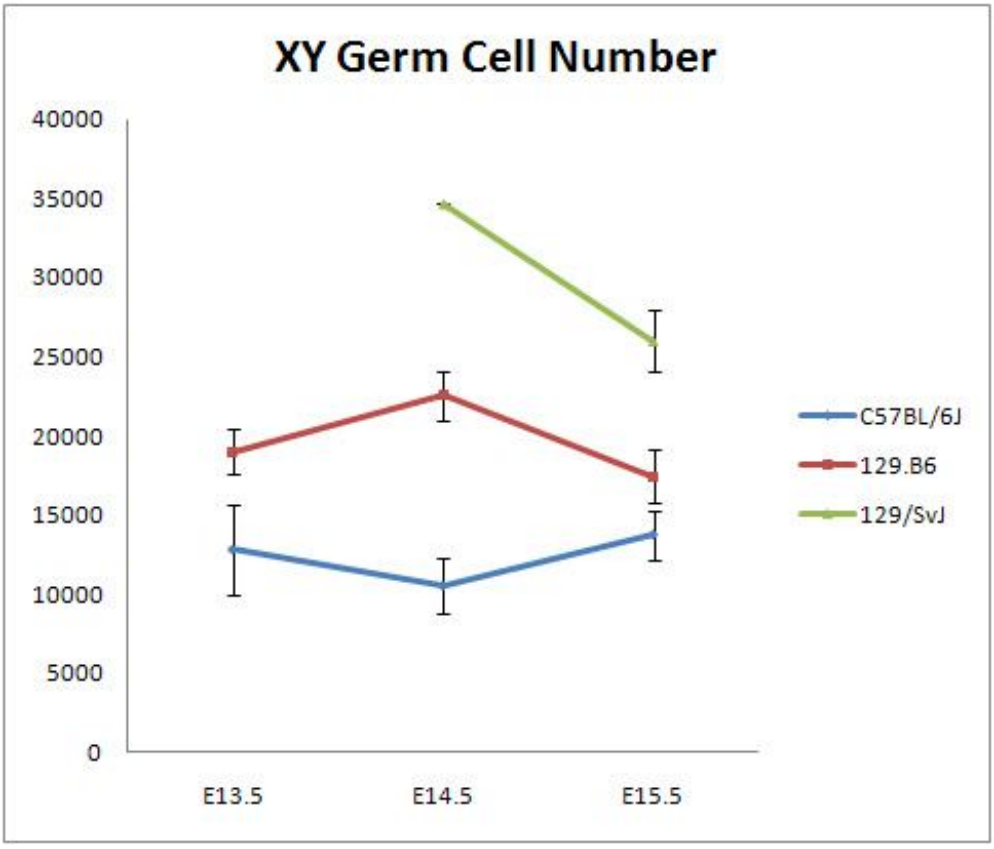
XY Germ Cell Number
40000
35000
30000
25000
20000
15000
10000
5000
0
E13.5
E14.5
E15.5
C57BL/6J
129.B6
129/SvJ

4.4 Discussion

Classic histological analyses of *Dnd1*$^{Ter/Ter}$ 129/SvJ testes documented the timing and remarkable diversity of tissue types that differentiate in developing testicular teratomas (Rivers and Hamilton, 1986; Stevens, 1973). The capacity to recapitulate many cell types of the organism reflects the underlying pluripotent state of the cells from which the tumors are derived. When the *Dnd1*^{Ter} mutation is crossed onto other inbred strain backgrounds, testicular teratomas do not develop and instead, all germ cells of the testis are eventually lost (Noguchi et al., 1996; Stevens, 1981). However, by blocking cell death using a homozygous *Bax*-null allele, we partially rescued germ cell loss in *Dnd1*$^{Ter/Ter}$ embryos (Fig. 7). Under these conditions, testicular teratomas develop at a high rate on mixed genetic backgrounds. However, double mutant ovaries are normal; females are fertile and give rise to viable, fertile offspring (Fig. 9). This suggests that the teratoma phenotype does not simply result from early defects in mutant primordial germ cells but from a later, specific defect(s) in differentiation of pro-spermatogonia in which DND1 plays a critical role.

We have shown here by RIP that mouse DND1 binds the transcript *p27*^{Kip1}. *Dnd1*$^{Ter/Ter}$ germ cells lacking DND1 protein also lack P27^{Kip1} protein (Fig. 20 E,F), although transcript level is not significantly altered (Fig. 20J). The finding that miRNAs (miR-221/222) that target *p27*^{Kip1} transcript are expressed in E14.5 testes (Fig. 20I) suggests that translational misregulation of *p27*^{Kip1} leads to loss of the protein in mutants,

preventing entry into mitotic arrest. We also show that DND1 binds transcripts encoding the cell cycle inhibitors P21^{Cip1} and PTEN. *p21^{Cip1}* is also implicated in germ cell mitotic arrest (Western et al., 2008) and conditional deletion of *Pten* in germ cells leads to testicular teratoma formation with complete penetrance on all genetic backgrounds tested (Kimura et al., 2003). Interestingly, these proteins are up-regulated in mitotically arresting germ cells even though the miRNAs that target these transcripts are up-regulated concurrently (Hayashi et al., 2008). To reconcile this biological conundrum, evidence is provided here for a model suggested previously (Western, 2009) where DND1 acts as a translational promoter of a set of relevant cell cycle inhibitors, protecting them from miRNA-mediated translational repression (Fig. 27). The finding that DND1 binds a functionally related set of targets for cell cycle inhibition is interesting, and parallels other RBP studies that have led to the development of an RNA regulon model, where a single RBP controls the translation of a functionally related set of target transcripts important for cell signaling, survival, or metabolism (Keene, 2007). In addition to its role of translational regulation, it seems that DND1 can also affect gene expression at the level of transcription. Microarray analysis of overexpression experiments revealed that these same important cell cycle pathways were significantly altered, indicating that DND1 can functionally perturb cell cycle.

Figure 27 – Model for DND1 function during differentiation and mitotic arrest of male germ cells.

Figure 27

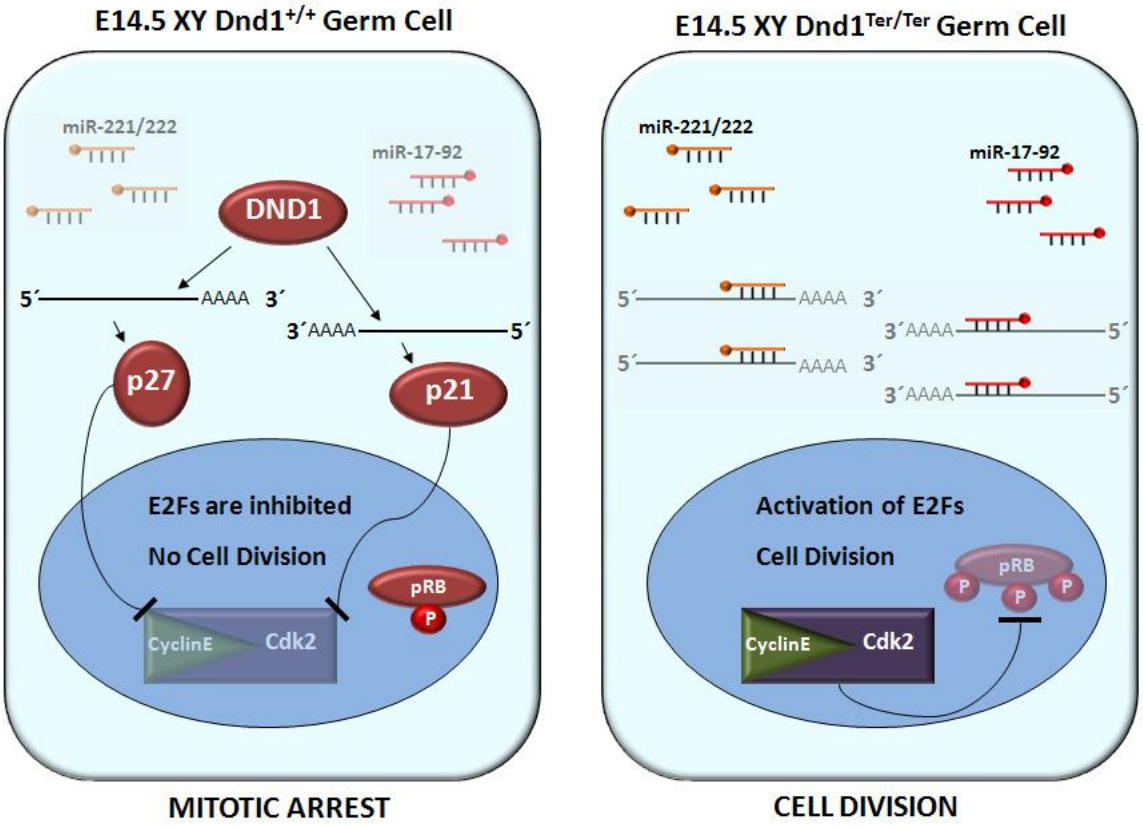
E14.5 XY Dnd1+/+ Germ Cell
miR-221/222
miR-17-92
DND1
5´
AAAA 3´
3´AAAA
5´
p27
p21
E2Fs are inhibited
No Cell Division
pRB
P
CyclinE
Cdk2
MITOTIC ARREST
E14.5 XY Dnd1Ter/Ter Germ Cell
miR-221/222
miR-17-92
5´
AAAA 3´
3´AAAA
5´
5´
AAAA 3´
3´AAAA
5´
Activation of E2Fs
Cell Division
pRB
P
P
P
CyclinE
Cdk2
CELL DIVISION

Although there is no orthologue of *Dnd1* in *Drosophila* or *C. elegans*, other RBPs act as translational regulators of cell cycle in germ cells. It has been established that Nanos and Pumilio function to repress translation of maternally deposited *Cyclin B* in *Drosophila* PGCs (Kadyrova et al., 2007), and it has been more recently documented that GLD-1 translationally represses *Cyclin E* in *C. elegans* germ cells, thus preventing premature mitotic division and embryonic gene activation, ultimately leading to teratoma formation (Biedermann et al., 2009). DND1 is unusual because it is one of the few RBPs that regulate cell cycle by promoting, instead of repressing, translation of targets.

Another novel target for DND1 may be *Gm114*. GM114 protein was absent at all stages of fetal development in $Dnd1^{Ter/Ter}$ germ cells on all genetic backgrounds, even though transcript levels were not significantly affected at E13.5 (Fig. 18H). This suggests that translation of *Gm114* transcript is positively regulated by DND1 or another RBP. Although GM114 is one of the first markers of male-specific germline development, no functional role for this protein is known (Tang et al., 2008). Recently it was reported that the *Drosophila* orthologue from which *Gm114* was identified, *Bag of marbles* (*Bam*), negatively regulates the translation of *E-cadherin* and is inhibited by the translation initiation factor eIF4A (Shen et al., 2009). In mice, the translation initiation factor eIF2S2 suppresses testicular germ cell tumor development (Heaney et al., 2009). It will be

interesting to determine whether GM114 also regulates E-cadherin and interacts with eIF2S2 in mice.

The significant decrease in *Nanos2* expression indicates another critical role for DND1 in regulating differentiation of germ cells as pro-spermatogonia. *Nanos2* may be a direct or indirect target of mouse DND1. Zebrafish DND1 binds to a uridine-rich region in the 3'UTR of zebrafish *nanos* and protects it from miR-430 inhibition during PGC development (Kedde et al., 2007a). Consistent with conservation of this mechanism in mammals, the 3'UTR of *Nanos2* is essential for up-regulation of protein in mouse fetal male germ cells (Tsuda et al., 2006). In *Dnd1* mutants, it is still not clear whether up-regulation of meiotic markers, which may result from loss of *Nanos2*, is an antecedent to cell death or possibly to tumor formation. However, expression of STRA8 and SCP3 was never detected within cells of developing teratomas, arguing against the second possibility. Alternatively, expression of meiotic markers may indicate that XY germ cells have failed to respond to male signals and defaulted to the female developmental pathway. Further experiments are necessary to determine whether mouse DND1 directly regulates *Nanos2* (or *Nanos3*) transcript, and also if these proteins, which are also RBPs, have an important interaction with DND1 protein in developing germ cells.

Despite the clear role DND1 plays in regulating mouse germ cell mitotic arrest and commitment to the male pathway, failure to enter G0 and subsequent up-regulation of meiotic markers are not strain-specific phenotypes. This means that another

susceptibility factor for teratoma formation must exist. In *Dnd1* mutants, loss of *Bax* increases the number of surviving germ cells by gonadal stages and raises the incidence of teratoma formation on a mixed, but not C57Bl/6J, genetic background, indicating that cell death contributes to the clearance of misregulated germ cells at specification/migration stages and could be an important determinant of whether or not teratomas form. However, in $Dnd1^{Ter/Ter};Bax^{-/-}$ testes on a mixed genetic background, the frequency of individual germ cells that undergo neoplasia formation is lower (Fig. 12D,H,L,P) than in $Dnd1^{Ter/Ter}$ testes from the 129/SvJ strain, where virtually all germ cells transform. Surprisingly, mutant germ cells on a 129/SvJ, mixed, and C57BL/6J background remain Ki67 positive even though most do not form neoplasias. It is possible that many germ cells transition to a stable state on backgrounds other than 129/SvJ, even though $p27^{Kip1}$ is not expressed, mitotic arrest at G0 does not occur, and spermatogonial differentiation is not achieved. Supporting this hypothesis is evidence demonstrating that rescued mutant germ cells on a C57BL/6J background are not pHH3-positive while those on a mixed background are still undergoing active mitoses (Fig. 23). The strain-specific factor that allows C57BL/6J mutant germ cells to achieve cell cycle arrest is unknown, but we hypothesize that it is essential to the prevention of teratoma formation on this non-susceptible background.

Other strain-specific differences are also likely to be important. Both morphological and/or molecular strain-specific differences could exist that predispose

the 129/SvJ background to teratoma formation. A recent report highlighted the differences in the somatic transcriptional networks between E11.5 gonads of C57BL/6J and 129/SvJ strains, explaining the particular susceptibility of male-to-female sex reversal observed for C57BL/6J mice (Munger, 2009). It is possible that a similar phenomenon explains 129/SvJ susceptibility to teratoma development. It seems likely that two events are required: continuation of cell division and acquisition of a pluripotent state. The formation of ES cell lines is also dependent on these criteria. The ability to derive ES cells varies between strains, with 129/SvJ being the easiest, and C57BL/6J being more difficult. The same group showed that strain differences in ES cell derivation are due to differences in signaling pathways that affect an intrinsic ability to maintain pluripotency (Batlle-Morera et al., 2008). Interestingly, a recent report that *Dmrt1* mutants also develop testicular teratomas (independently of *Dnd1*) revealed that only 129/SvJ, not C57BL/6J, mutant germ cells had up-regulated the gene *Eras* (*ES-expressing Ras*) seven-fold compared to wild type cells of either strain (Krentz, 2009). Future studies examining both somatic and germ cell-specific transcriptional differences between strains will be informative in defining defects in germ cell programming and teratoma susceptibility on the 129/SvJ background.

Surprisingly, the morphology of the 129/SvJ testis is different from that of the C57BL/6J testis (Fig. 25). Though only containing about half as many, the diameter of a 129/SvJ testis cord is about twice that of C57BL/6J. This could possibly affect tumor

susceptibility if there is a factor secreted by Sertoli cells that is much stronger in 129/SvJ because it must travel a greater distance to reach all of the germ cells in the cord, such that with only a few germ cells present a saturation point is reached and the mutant cells transform. More experiments will be necessary to determine if these sorts of morphological differences contribute to the phenotypic variance in tumor sensitivity.

This chapter shows that loss of *Dnd1* leads to aberrant expression of male germ cell-specific differentiation genes and a failure to arrest at G0 on all genetic backgrounds. The unifying characteristic of transforming germ cells in $Dnd1^{Ter/Ter}$ testes that distinguishes them from non-transforming cells is the maintenance of expression of the pluripotency markers OCT4, SOX2, and NANOG. OCT4 is normally expressed throughout wildtype germ cell development, though SOX2 and NANOG are down-regulated as germ cells enter mitotic arrest. The 129/SvJ strain has a two-fold higher expression of the pluripotent markers than C57BL/6J during this period when germ cells normally exit cell cycle. However, this could be a result of having approximately twice as many germ cells. Performing gene expression analysis on isolated populations of germ cells from each strain will be necessary to conclusively show that there are significant expression level differences in these critical pluripotency markers during the window of susceptibility. Interestingly, levels of *Dnd1* were also two-fold higher in the 129/SvJ compared to C57BL/6J gonads. If this is true in isolated germ cell populations,

these results would suggest that the level of *Dnd1* relative to the level of the pluripotency program is critical to block transformation.

The transition from a migratory PGC program (expressing high levels of pluripotent markers) to differentiation as pro-spermatogonia is dependent on regulation of the cell cycle provided by DND1. It is unclear whether DND1 can directly affect pluripotent gene expression, act to promote spermatogonial differentiation, or both. Regardless, it is the first RBP identified that links the cell cycle and differentiation of male germ cells during this important reprogramming process. Further experiments are necessary to determine if DND1 can directly antagonize pluripotency, whether its effects on cell cycle influence the differentiation process, and how it may regulate epigenetic reprogramming. New research identifying the global set of targets for DND1 at all stages of germ cell development may uncover novel regulatory functions for this RBP and reveal links between programming of the pluripotent genome, cell cycle, and tumor biology.

5. Future Directions

Based on many genetic studies, RNA-binding proteins (RBPs) play a critical role in the regulation of germ cells, but it is not clear why this mechanism (regulation of translation) plays such a central role in germ cells. Based on the loss of function phenotype (the formation of teratomas), DND1 appears to occupy a pivotal position in the hierarchy of genes that maintains the underlying pluripotency of the germ cell genome while repressing unregulated growth and differentiation. This role as "gatekeeper" between these cell states is one of the most critical roles in cell biology.

There are still many unanswered questions regarding the role of DND1 in the reprogramming of male germ cells and teratoma formation: What is the role of Dnd1 at PGC specification? What is the sub-cellular localization of DND1 throughout all stages of germ cell development? What is the role of *Dnd1* in the adult germ cell? What is the complete set of mRNA targets for DND1? What other proteins can DND1 interact with?

Now that we have a basic understanding of why *Dnd1* is important for male germ cells as they colonize the gonad, we can use the tools generated throughout the course of this work and exploit the strain-specific differences to get a better idea of the most important genes regulating this transition.

Figure 28 – Purified GST-DND1α protein from bacteria. Two elutions of purified protein (E1 and E2) are compared to control standards of BSA.

Figure 28

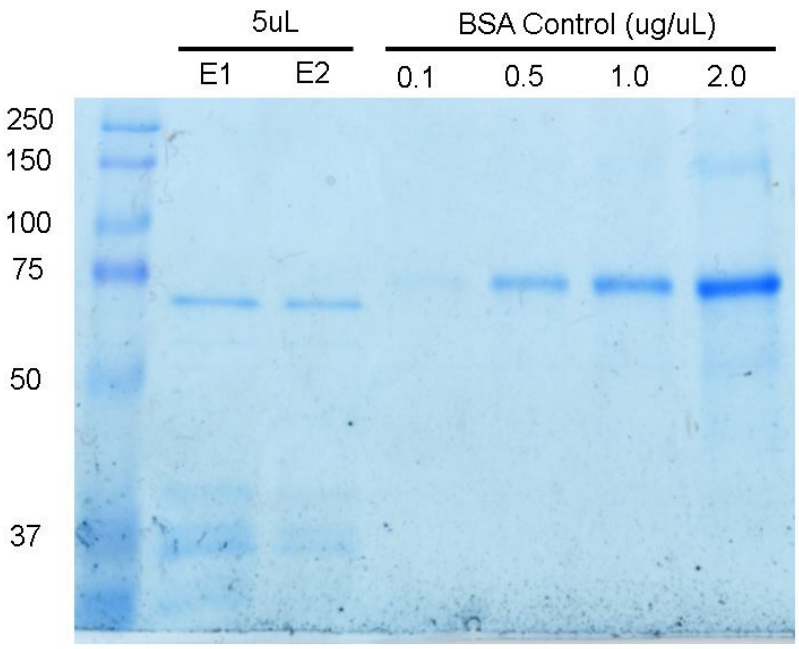

I am currently in the process of generating an antibody to DND1 that can be used to identify subcellular localization in vivo, verify protein partners by immunoprecipitation (IP), and perform endogenous RNA-immunoprecipitation (RIP) from embryonic gonads. GST-tagged DND1 has been purified from bacteria (Fig. 28) and injected into both a guinea pig and chicken in hopes of producing a functional polyclonal antibody.

Another critical experiment is determining a comprehensive set of RNA targets for DND1. This will provide a new set of genes to investigate in the *Dnd1*^{Ter} model and will allow for alignment studies to elucidate a better consensus binding site for DND1. There is a lot of debate about the best way to identify targets of RBPs from whole tissue. We propose to use both a yeast-three hybrid (Y3H) screen and also a RIP approach in parallel. Each of these methods has advantages and disadvantages.

The Y3H system provides a relatively inexpensive approach to scan a relevant library of mRNAs from the endogenous tissue encompassing the range of stages pertinent to teratoma formation (for review see (Hook et al., 2005)). Additionally, a screen with a fully represented library will not be affected as much by low endogenous levels of expression of a particular target (because each individual clone is screened equally), which would be difficult/impossible to achieve in a RIP experiment. The steps for performing a Y3H screen are outlined in Figure 29.

Figure 29 – Experimental plan for identification of relevant RNA targets of DND1 by using a yeast three-hybrid screen. **(A)** RNA extracted from E11.5-E14.5 XX and XY gonads has been used to generate a cDNA library enriched for transcripts expressed by germ cells at a critical transition point during development and potentially bound by DND1. This library was transferred to a modified Y3H vector pIIIA/MS2-2/Att by using the Gateway™ Technology. **(B)** The library was transformed into the YBZ1 strain of yeast along with a fusion DND1-GAL4 expression vector, specially optimized for the Y3H screen to increase sensitivity and reduce background. **(C)** Putative targets will be sequenced and the interaction with DND1 will be verified and functionally validated. Potential targets will be assayed for increased three-hybrid activity with DND1α as compared to other control RBPs, DND1-ΔRRM and MVH, to ensure binding specificity. Protein expression of targets passing all of these tests will then be examined in *Dnd1*$^{Ter/Ter}$ mutant germ cells. Genuine interactions should display misregulation of target protein in mutant germ cells compared to wild type.

Figure 29

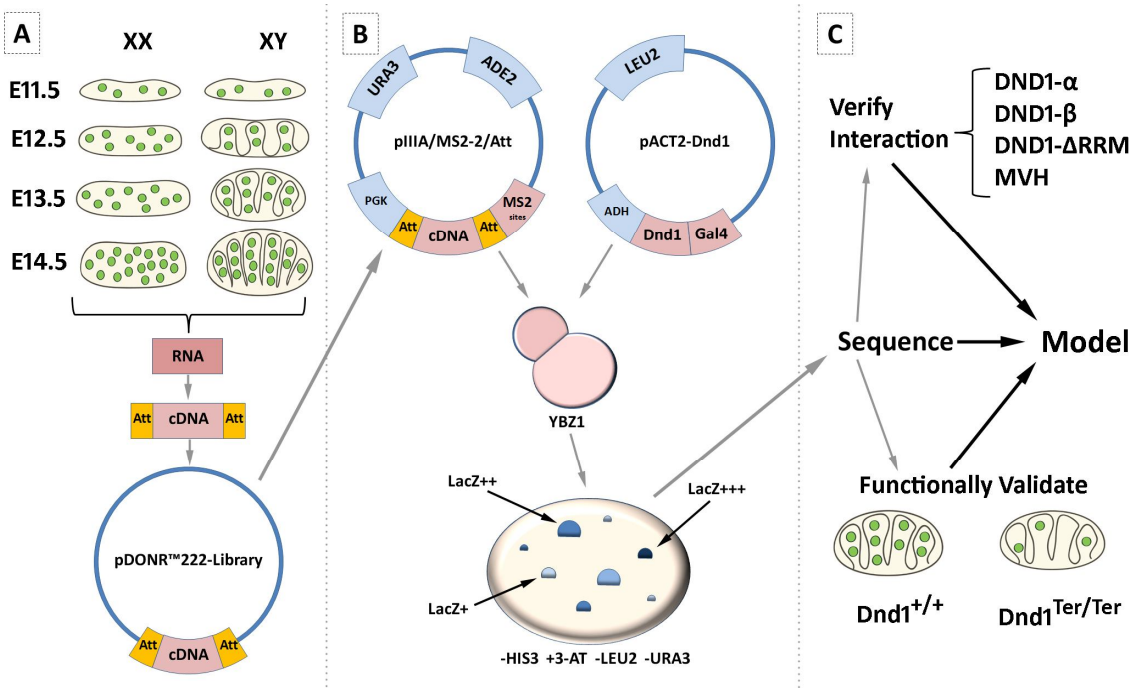
A
XX
XY
E11.5
E12.5
E13.5
E14.5
RNA
Att
cDNA
Att
pDONR™222-Library
Att
cDNA
Att
B
URA3
ADE2
pIIIA/MS2-2/Att
PGK
Att
cDNA
Att
MS2
sites
LEU2
pACT2-Dnd1
ADH
Dnd1
Gal4
YBZ1
LacZ++
LacZ+++
LacZ+
-HIS3 +3-AT -LEU2 -URA3
C
Verify
Interaction
DND1-α
DND1-β
DND1-ΔRRM
MVH
Sequence
Model
Functionally Validate
Dnd1+/+
Dnd1Ter/Ter

Figure 30 – Construction of modified gateway vector for custom library creation. The original Y3H vector provided by the Wickens laboratory (Sengupta et al., 1999; Zhang et al., 1999) is ideal for expression of short RNAs using an RNA polymerase III promoter (Stumpf et al., 2008). To generate a complete library that will express full-length cDNAs it was necessary to replace the transcription promoter and terminator with RNA polymerase II sequences. The tandem MS2 binding sites for the hybrid RNAX were also moved into the new vector with the gateway destination cassette. This vector allows for efficient sub-cloning from an entry library into the custom destination vector with appropriate tagging.

Figure 30

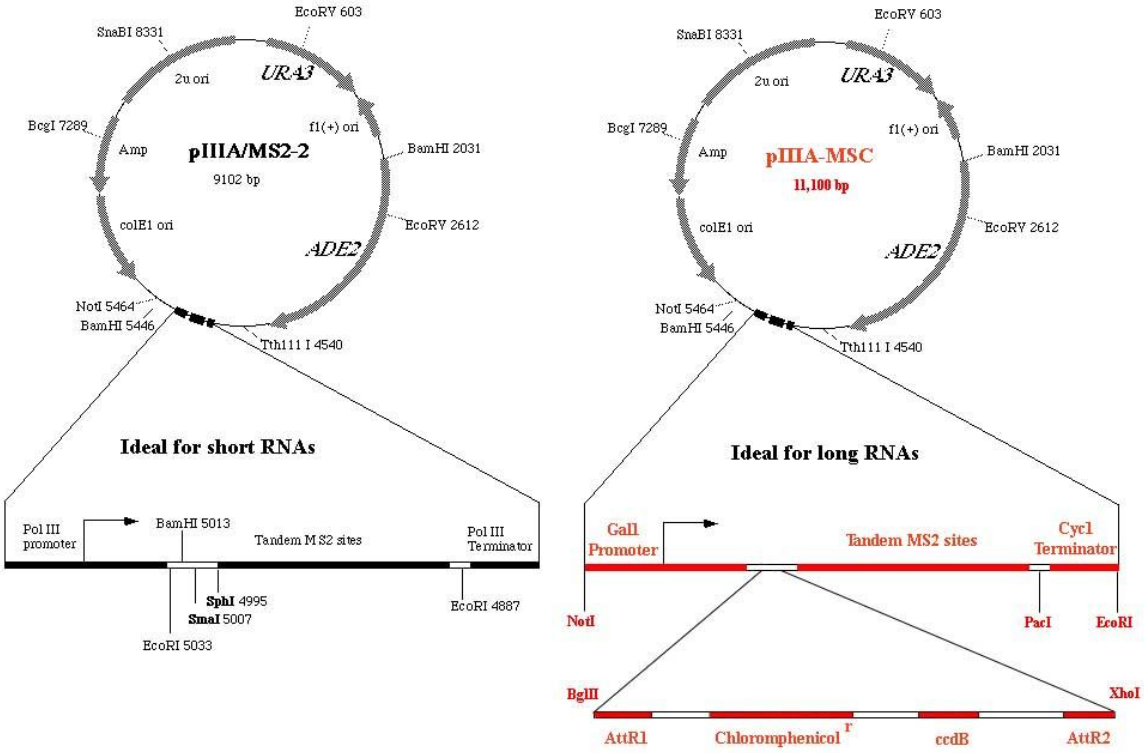
EcoRV 603
SnaBI 8331
2u ori
URA3
BcgI 7289
f1(+) ori
Amp
pIIIA/MS2-2
9102 bp
BamHI 2031
colE1 ori
EcoRV 2612
ADE2
NotI 5464
BamHI 5446
Tth111 I 4540
Ideal for short RNAs
Pol III promoter
BamHI 5013
Tandem MS2 sites
Pol III Terminator
SphI 4995
SmaI 5007
EcoRI 4887
EcoRI 5033
EcoRV 603
SnaBI 8331
2u ori
URA3
BcgI 7289
f1(+) ori
Amp
pIIIA-MSC
11,100 bp
BamHI 2031
colE1 ori
EcoRV 2612
ADE2
NotI 5464
BamHI 5446
Tth111 I 4540
Ideal for long RNAs
Gal1 Promoter
Tandem MS2 sites
Cyc1 Terminator
NotI
PacI
EcoRI
BglII
XhoI
AttR1
Chloromphenicol r
ccdB
AttR2

Figure 31 – Y3H positive control with known target *Lats2*. The yeast strain YBZ-1 was first transformed with either DND1-GAL4 or the IRP-GAL4 positive control and selected on –Leu media (1 and 2 left panel). Positive clones were grown up and DND1-GAL4 YBZ-1 was transformed with *Lats2-MS2* (4), MS2 (5), or nothing (2) and grown on selective media (middle panels). Only colonies appeared on the *Lats2-MS2* plate. Positive clones were picked and streaked out to verify growth with the positive control IRP-IRE (right panel).

Figure 31

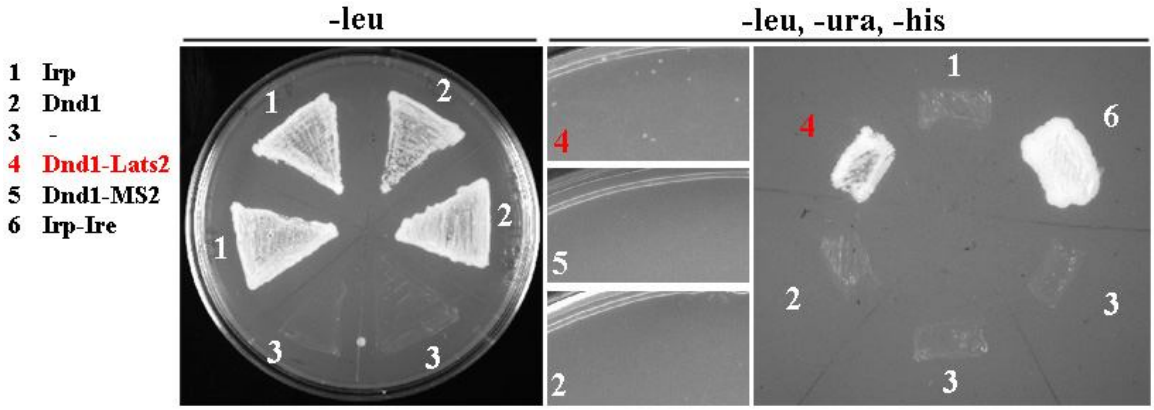

I generated the novel vector necessary for creation of the library (Fig. 30), made and validated the library, and shown that yeast carrying a known target of DND1 (*Lats2*) can grow on selective medium (Fig. 31). A full screen was performed and 44 total colonies were obtained – 31 of these were RNA-dependent and Beta-gal positive. These clones have been grown up and are ready for DNA extraction and sequencing to determine their identities.

The advantage to a Y3H screen is that it allows the screening of a library containing transcripts from the endogenous population of germ cells; however interactions are artificially constructed and may not detect interactions in vivo. As a second approach, I have performed RIP from the P19 teratocarcinoma cell line and am preparing to perform microarrays (RIP-Chip) to determine the outcome. We have been unable to perform these assays in endogenous germ cells as numbers of germ cells are limiting and a decent antibody against native DND1 is lacking. However, a RIP approach performed on the in vivo population of germ cells would be optimal. With a good antibody to endogenous DND1, or a functional fusion protein produced by a targeted allele, we plan to employ a RIP-Seq analysis – a technique better suited to limiting material than RIP-Chip – to obtain data directly from germ cells.

Understanding strain-specific expression differences, both in wildtype and mutant germ cells, is essential to solving the mystery of teratoma penetrance. We plan to isolate wild type and mutant germ cells at E14.5 from both susceptible (129/SvJ) and

non-susceptible (C57BL/6J) strains using the *Oct4-EGFP* reporter to obtain global expression profiles that can be functionally integrated with DND1 target data to determine the mechanism of tumor initiation and strain-sensitivity. It will be important to integrate our knowledge of direct DND1 targets obtained from the Y3H and RIP, with differences in the transcriptome within germ cells. This will provide a much clearer picture of how DND1 functions. The successful incorporation of RIP-Chip and transcriptional array data to develop a comprehensive mechanism of tumorigenesis based on the role of HuR in an *in vivo* model of breast cancer has been published previously (Mazan-Mamczarz et al., 2008).

RBPs exert their function through binding RNA targets; but the proteins with which they interact can be essential to this function. To determine what possible other roles DND1 might have in the cell, we have performed a comprehensive screen for protein partners using a yeast-two hybrid (Y2H). E9.5 and E10.5 whole embryo cDNA libraries were screened against DND1. A total of 1295 positive interactors were detected (Fig. 32 left panel). These were replica-plated onto 50mM 3-AT selection and many colonies still maintained robust growth (Fig. 32 right panel). One hundred of these colonies were randomly selected and grown up – they are currently ready for DNA extraction and sequencing to determine their identities.

Finally, to test whether DND1 is essential for adult germ cell spermatogenesis or maintenance of the spermatogonial stem cell (SSC), we are generating a conditional

allele of *Dnd1* so that we can use tissue and temporally-restricted Cre recombinase lines to delete *Dnd1* at various stages. It will be interesting to see if loss of *Dnd1* in adult 129/SvJ testes will lead to tumor formation and whether it is essential for adult spermatogenesis. Data suggesting this is the case are presented in Appendix 6.1.

Figure 32 – Y2H yields 1295 clones, many of which are interactors in the presence of strong selection. 1295 positive clones detected from the Y2H were streaked out to verify growth and positive interaction (left panel). Each clone was replica plated to media with strong selection (50mM 3-AT) and many still had growth (right panel).

Figure 32

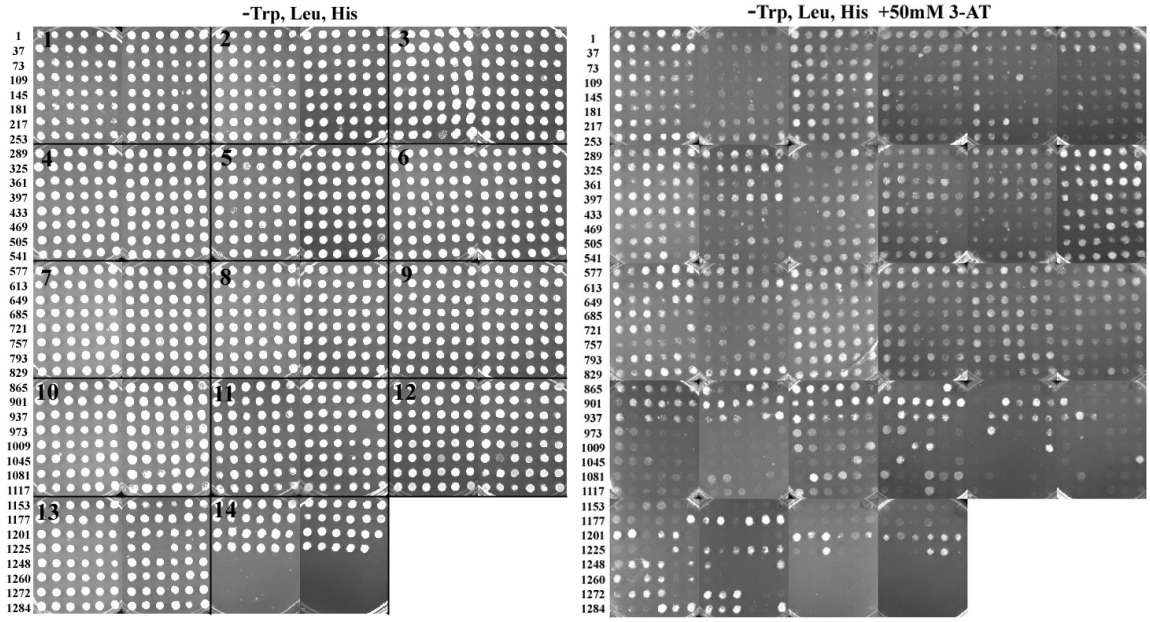

6. Appendix

Unfortunately many of the experiments that are performed during the course of graduate studies are inconclusive, yield negative results, or produce results that do not fit neatly into a particular storyline or dataset. Work on *Dnd1* is no different. Here I have only chosen to share three of the more complete sets of stories I have collected – none of these easily fit under either of the two broader headings covered in the previous chapters of this dissertation. The first concerns a long-standing issue in the field of laterality in tumor formation of 129/SvJ mice and then explores an old phenotype with new tools. The second set of data demonstrates that overexpression of DND1 in F9 and P19 cells did not directly antagonize pluripotency at the transcriptional or translational levels. The third and final set of results indicates a potentially novel role for Akt signaling in mitotically arresting male germ cells.

6.1 Laterality in teratoma formation and testis atrophy

Surprisingly, spontaneous tumor formation does not occur symmetrically in the 129/SvJ strain of mice. This is also somewhat true in humans as, even though the left testis is more likely to be undescended, neoplasms are slightly more common on the right (Wein et al., 2007). The original publication in which Leroy Stevens described the newly founded 129 strain revealed that "of forty cases where laterality is known, 30 teratomas occurred in the left testis" (Stevens and Little, 1954). Thirty years later it was shown that the *Ter* mutation segregated in Mendelian ratios to cause high rates of tumorigenesis in homozygous mutants (Noguchi and Noguchi, 1985). However, not since the 1950s has the laterality of tumor formation been revisited in the 129/SvJ strain or *Dnd1*^{Ter} mice.

To investigate whether our colony of mice maintains a bias in tumor formation, wildtype, heterozygous, and homozygous postnatal males were examined for testicular teratomas. The results can be found in Figure 33. Wildtype, heterozygous, and homozygous animals developed testicular teratomas at a rate of 6%, 32%, and 71% respectively. Interestingly, our rates of tumorigenesis are different than those reported originally for the *Dnd1*^{Ter} mice on a 129/SvJ background (1%, 17%, 94% respectively) (Noguchi and Noguchi, 1985). This is not surprising as the 129/SvJ strain is now known to be a contaminated strain and other groups have reported more variable penetrance of the tumor phenotype (Jiang and Nadeau, 2001; Threadgill et al., 1997).

In wildtype and heterozygous mice, the majority of tumors form unilaterally (100% in wildtype n=2 and 75% in heterozygotes n=32). Strikingly, of these unilateral tumors, the majority occur in the left testis (100% n=2 and 83% n=24 respectively). However, in *Dnd1*$^{Ter/Ter}$ homozygous mutants, only 33% of tumors are unilateral (n=42) and of those, there is an equal balance between the left and the right (50% n=14). This suggests that the left testis is more susceptible to testicular teratomas than the right testis unless there is a homozygous *Dnd1*$^{Ter/Ter}$ mutation. Are there gene expression differences between the left and the right testes? Is one testis more descended than another? Are there fewer germ cells in the right testis? Are there vascular differences between the left and right testes? The answers to these questions could reveal the cause of the laterality effect of tumor formation, but none have been investigated.

Supporting a model for intrinsic differences between the left and right testes, another phenotype on the 129/SvJ strain in heterozygotes involving atrophy of the testis is also biased towards the left (Figure 34). Interestingly, this same phenomenon was described by Stevens in the original publication on the 129/SvJ strain in 1954:

> In about 5% of strain 129 males, one testis is reduced in size. About 80% of these small testes occur on the left side. In most cases, a congenital hematoma in the testes is accompanied by degeneration of all or a fraction of the spermatogenic tubules. Examination of such small testes has failed to reveal teratomatous growths (Stevens and Little, 1954).

Figure 33 – Tumor incidence and laterality in our 129/SvJ *Dnd1*^{Ter} colony. Wildtype, heterozygous, and mutant males develop testicular teratomas at a rate of 6%, 32%, and 71% respectively (left table). In wildtype and heterozygous animals the majority of tumors occur unilaterally and the vast majority of these occur on the left (100% and 83% respectively). In homozygous mutants, only 33% of tumors are unilateral and of these, there is no bias to the right or left testis (right table).

Figure 33

	129/SvJ (n=)
Dnd1$^{+/+}$	**6%** (2/34)
Dnd1$^{Ter/+}$	**32%** (32/100)
Dnd1$^{Ter/Ter}$	**71%** (42/59)

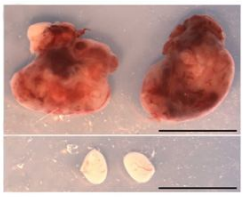

	Dnd1$^{+/+}$ (n=34)	Dnd1$^{Ter/+}$ (n=100)	Dnd1$^{Ter/Ter}$ (n=59)
Mice with Tumors	**6%**	**32%**	**71%**
Gonads with Tumors	**3%**	**20%**	**59%**
Unilateral Tumors	**100%**	**75%**	**33%**
Bilateral Tumors	**0%**	**25%**	**66%**
Left Tumor/Unilat.	**100%**	**83%**	**50%**
Right Tumor/Unilat.	**0%**	**17%**	**50%**
	Left Bias	Left Bias	No Bias

Figure 34 – 5% of 129/SvJ *Dnd1*$^{Ter/+}$ mice have left testis atrophy. While 32% of *Dnd1*$^{Ter/+}$ mice in our 129/SvJ colony develop testicular teratomas (either unilateral or bilateral), 5% present with a significantly smaller left testis at postnatal 90 days or later (right panel). This atrophy phenotype has yet to be observed for the right testis.

Figure 34

129/SvJ Het. Phenotypes

129/SvJ	Dnd1$^{Ter/+}$ (n=100)
Normal testes	**63%**
Tumor (Bil. Or Uni.)	**32%**
Smaller left testis	**5%**
Smaller right testis	**0%**

Left Bias for Smaller Testis

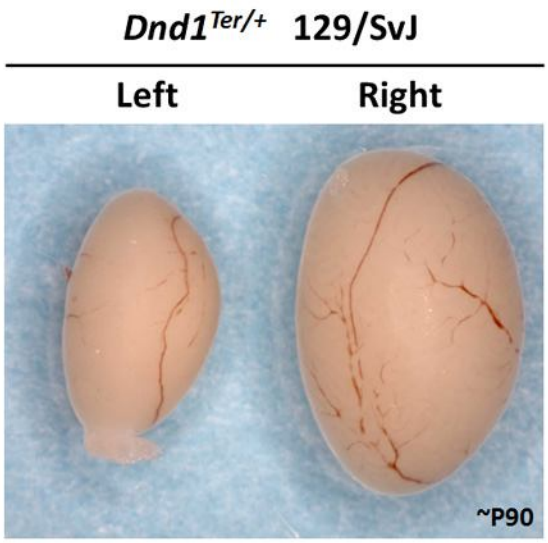

In our colony of heterozygous mice the rate of testis atrophy is approximately 5% and is biased to the left (Figure 34). To determine whether similar degeneration was observed in spermatogenic tubules of atrophied gonads in our colony, we collected several of these samples that had obviously smaller left testes and performed hematoxylin and eosin (H&E) stains (Figure 35). This revealed that the left testis had no mature spermatozoa and many tubules were empty of all germ cells whereas the right testis had developed normally and spermatogenesis was occurring properly.

While some tubules of the left testis were completely empty, others contained germ cells that appeared to be arrested. Staining with the germ cell markers MVH and germ cell nuclear antigen (GCNA) revealed lower levels of expression of these markers in the left testis and fewer total GCNA-positive germ cells suggesting spermatogonial stem cell loss (Fig. 36). To determine whether these fewer germ cells in the left testis were still cycling, sections were stained with the active cell cycle marker Ki67 (Fig. 37). None of the cells in the left testis were Ki67-positive whereas virtually all of the germ cells in the right testis expressed Ki67 robustly.

This evidence supports the idea that the left testis is intrinsically different from the right testis and more susceptible to testicular teratoma formation or atrophy. To better understand this difference, *Dnd1*^{Ter} heterozygous males were compared between the 129/SvJ and C57BL/6J background. Postnatal animals approximately 90 days old were sacrificed and the testes were dissected. Testes that had no tumors and were of

roughly equal size (no atrophy) were weighed and compared to the contralateral testis. Left:right testis weight ratios were calculated and plotted to determine if there are any strain specific differences in testis weights (Fig. 38). In heterozygous animals, the left:right testis weight ratios on the 129/SvJ strain compared to C57BL/6J were 95.62% and 103.68%, respectively. This difference was statistically significant and suggests that, in general, the left testis is slightly smaller than the right testis in 129/SvJ mice.

These data together warrant an investigation into the similarities and differences between the left and right testes of the 129/SvJ background. By comparing weights, sizes, descent, gene expression, vascularity, and histology we might shed light onto the enigmatic phenomenon of laterality of these particular phenotypes.

Figure 35 – Atrophied left testes contain degenerate spermatogenic tubules. By H&E staining the right testis (right panels) contains testis cords with many germ cells that produce mature spermatozoa. The left testis (left panels) contains testis cords with a greatly reduced population of germ cells and no mature spermatozoa.

Figure 35

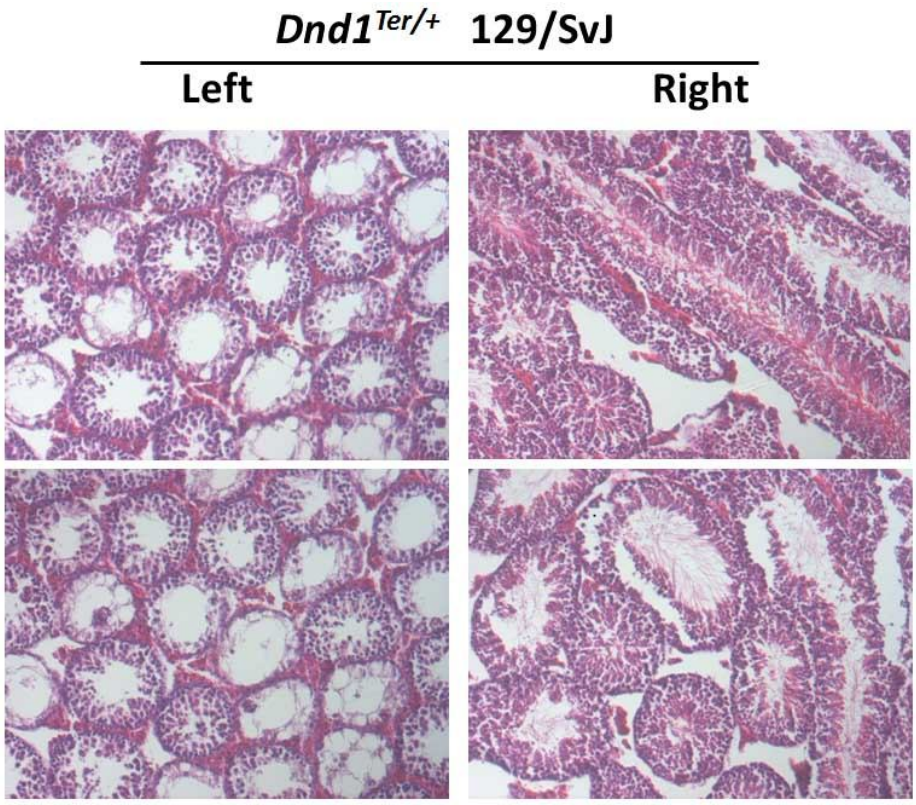

Figure 36 – Atrophied left testes contain fewer GCNA positive germ cells with less expression of MVH. GCNA (red) and MVH (green) immunostains reveal many germ cells in testis cords of the right testis (right panels). The atrophied left testis (left panels) contains many fewer GCNA positive germ cells and less expression of MVH.

Figure 36

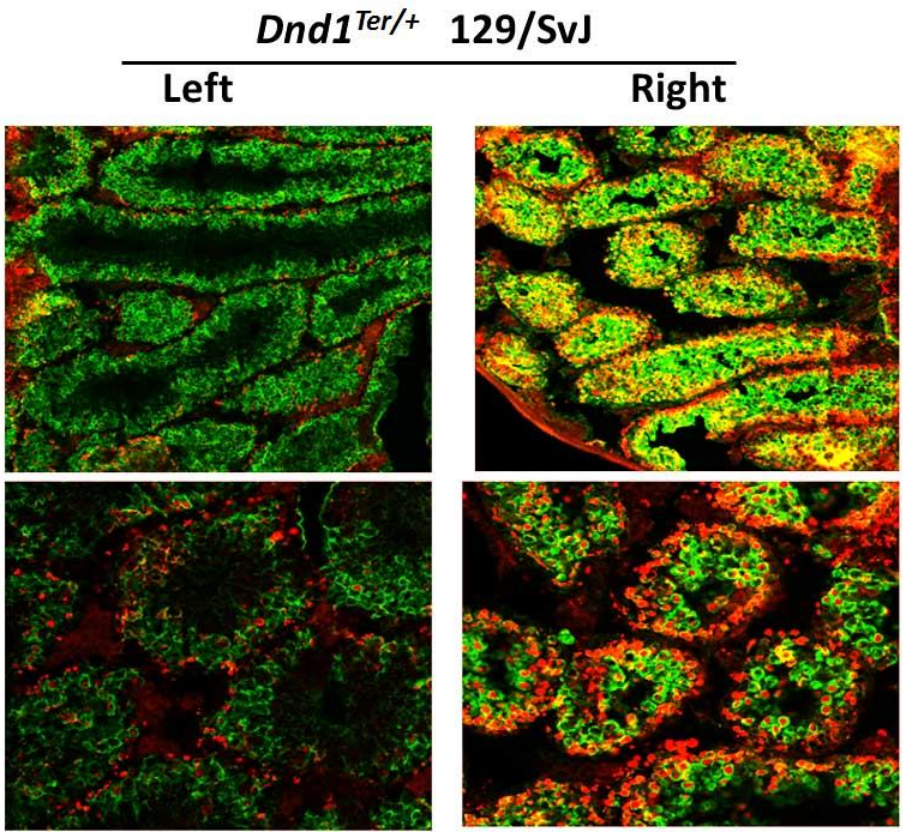

Figure 37 – Atrophied left testes contain no Ki67 positive germ cells. Immunostains using Ki67 (green - which labels active cell cycle) reveal that the right testis (right panels) has many positive germ cells. The left testis (left panels) has no detectable Ki67 expression in the testis cords, despite still have germ cells in many cases (Fig. 36). This indicates that the atrophied left testis germ cells have exited cell cycle and are not dividing.

Figure 37

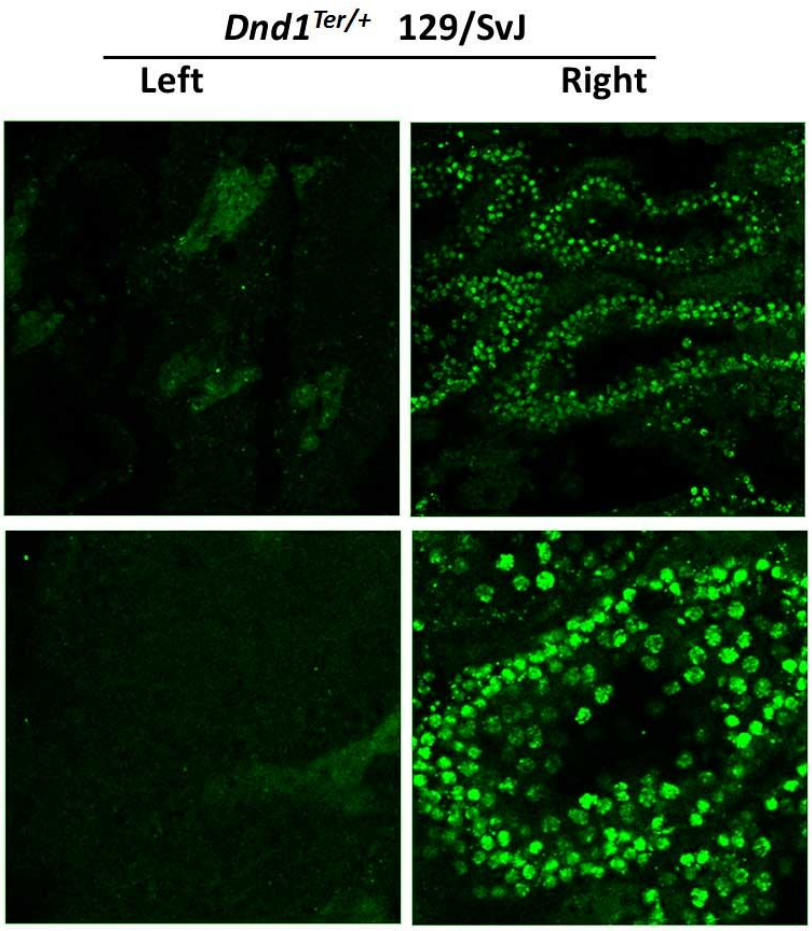

Figure 38 – The left testis is generally smaller than the right in 129/SvJ mice compared to C57BL/6J. Testes without tumors or obvious atrophy were compared for this analysis. The weight ratio of the left testis compared to the right at approximately 90 days of age in *Dnd1*$^{Ter/+}$ heterozygotes of the 129/SvJ (left column) and C57BL/6J (right column) strains. The average left:right testis weight ratios for 129/SvJ and C57BL/6J are 95.62% and 103.68%, respectively. This is a statistically significant difference with $p<0.05$. For the 129/SvJ strain, testes that were obviously atrophied were not included in this analysis

Figure 38

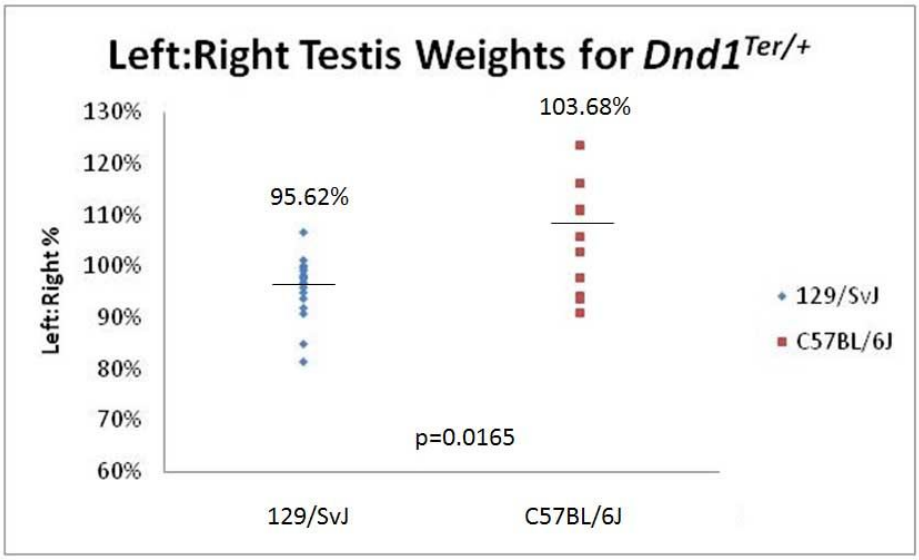
Left:Right Testis Weights for Dnd1Ter/+
130%
120%
110%
100%
90%
80%
70%
60%
Left:Right %
95.62%
103.68%
p=0.0165
129/SvJ
C57BL/6J
129/SvJ
C57BL/6J

6.2 DND1 does not directly antagonize pluripotency

Dnd1 is upregulated in male germ cells during the time they enter mitotic arrest and reprogram as pro-spermatogonia (Fig. 24D). The downregulation of the pluripotency markers *Nanog* and *Sox2* is concomitant with this important transition. These data suggest that DND1 may directly antagonize pluripotency at this stage of differentiation. Further supporting this idea are data showing that stable TAP-DND1α transfected lines of EG cells silence expression of the transgene in all cases tested (Fig. 39).

To test whether overexpression of *Dnd1* can directly antagonize a pluripotent program, two teratocarcinoma cell lines (F9 and P19) were transiently transfected with GFP-DND1α constructs. Using antibodies to stain for OCT4, NANOG, and SOX2, GFP-DND1α transfected cells were compared to GFP alone. All three pluripotent markers were expressed robustly at the protein level in GFP-DND1α transfected cells compared to GFP alone (Fig. 40 and data not shown). This suggests that over-expression of DND1 does not alter protein expression of these pluripotent markers. However, subtle changes might be detected by qRT-PCR. To test this possibility, transfected cells were trypsinized and pelleted, and then RNA was extracted for cDNA synthesis and qPCR. In both F9 and P19 cells *Dnd1* was over-expressed more than 2000- and 3000-fold, respectively compared to controls (Fig. 41A). Expression levels of *Oct4*, *Nanog*, *Sox2*, $p27^{Kip1}$, *Lats2*, and $p21^{Cip1}$ were tested and no significant difference was found for any of

them, though there was a slight increase trend for *p21^{Cip1}* expression in the GFP-DND1α cells (Fig. 41B). These data reveal that while Dnd1 may be important for the process of differentiation and cell cycle arrest in male germ cells at the time that pluripotency markers are downregulated, it does not directly antagonize pluripotent gene expression in cell lines. Other proteins may be required for DND1 to exert its effects on pluripotency. To determine what other protein interactors may be important, a yeast-two hybrid (Y2H) has been carried out and 1295 positive clones have been discovered (Fig. 32 and see Future Directions).

Figure 39 – EG cells silence expression of *Dnd1α* transgene. (A) Out of twelve independently derived stable lines transfected with *TAP-Dnd1α*, ten express the transcript (2 and 7 do not). **(B)** Of five lines that express the transcript, none express TAP-DND1α protein.

Figure 39

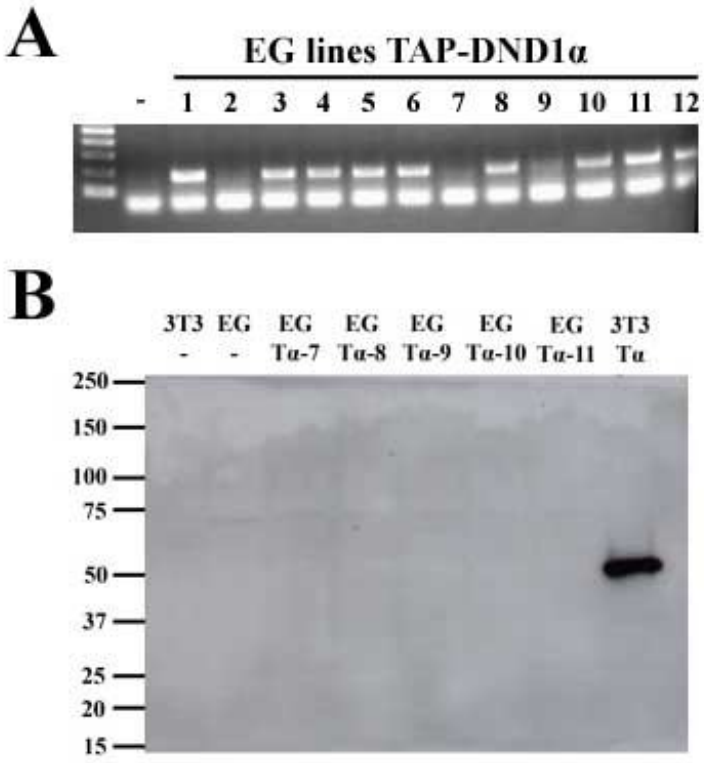
A
EG lines TAP-DND1α
- 1 2 3 4 5 6 7 8 9 10 11 12
B
3T3 - EG - EG Tα-7 EG Tα-8 EG Tα-9 EG Tα-10 EG Tα-11 3T3 Tα
250
150
100
75
50
37
25
20
15

Figure 40 – DND1α does not directly antagonize pluripotent gene protein expression in F9 and P19 cells. GFP-DND1α transfected F9 cells (bottom row) stained for OCT4 show robust expression similar to controls (top row). Scale bars represent 50 m.

Figure 40

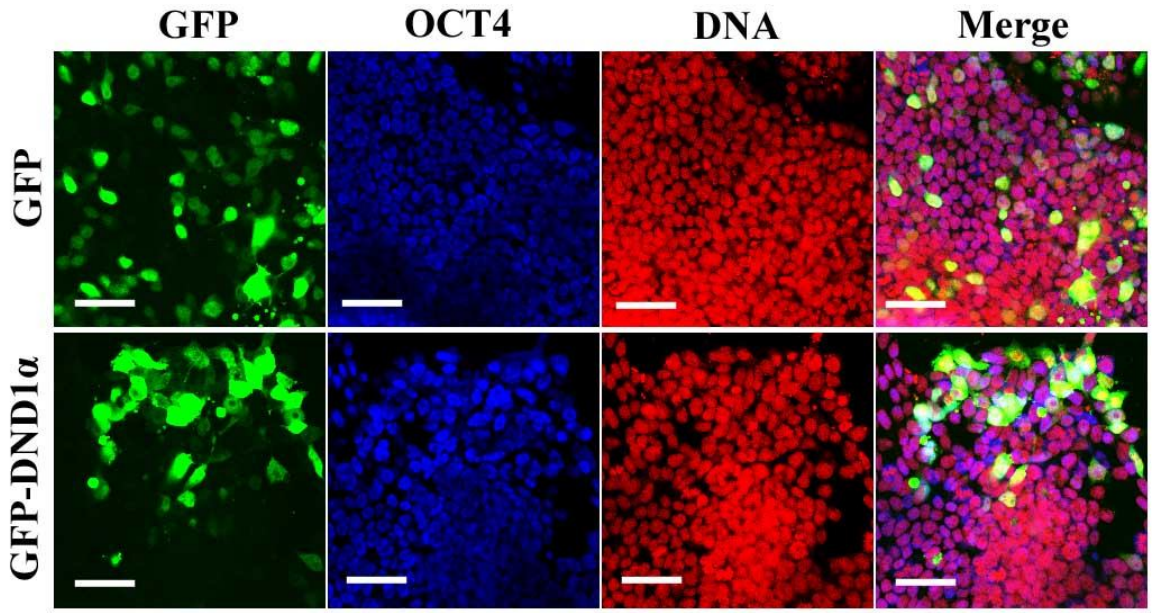

Figure 41 – DND1α does not directly antagonize pluripotent gene transcript levels in F9 and P19 cells. **(A)** GFP-DND1α was over-expressed in F9 and P19 cells more than 2000- and 3000-fold, respectively. **(B)** Transcript levels of *Oct4*, *Sox2*, *Nanog*, $p27^{Kip1}$, *Lats2*, and $p21^{Cip1}$ were not significantly altered in GFP-DND1α transfected cells compared to controls.

Figure 41

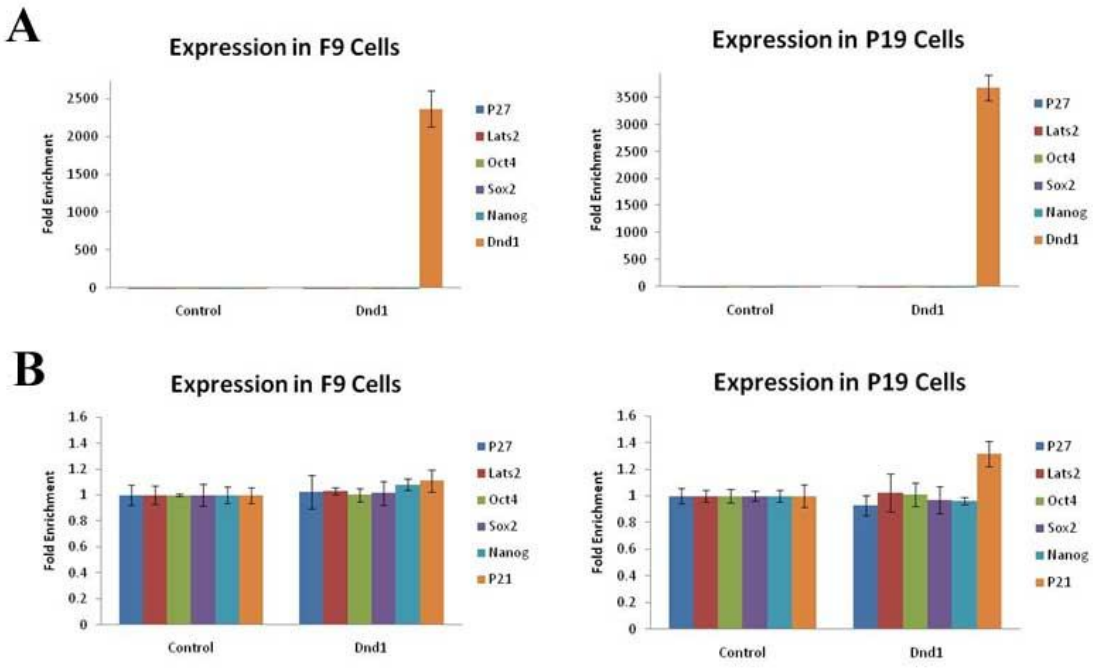
A
Expression in F9 Cells
Fold Enrichment
2500
2000
1500
1000
500
0
Control
Dnd1
P27
Lats2
Oct4
Sox2
Nanog
Dnd1
Expression in P19 Cells
Fold Enrichment
3500
3000
2500
2000
1500
1000
500
0
Control
Dnd1
P27
Lats2
Oct4
Sox2
Nanog
Dnd1
B
Expression in F9 Cells
Fold Enrichment
1.6
1.4
1.2
1
0.8
0.6
0.4
0.2
0
Control
Dnd1
P27
Lats2
Oct4
Sox2
Nanog
P21
Expression in P19 Cells
Fold Enrichment
1.6
1.4
1.2
1
0.8
0.6
0.4
0.2
0
Control
Dnd1
P27
Lats2
Oct4
Sox2
Nanog
P21

6.3 Akt signaling is active as germ cells mitotically arrest

Misregulation of Akt signaling is well-known to be an important modifier of tumor penetrance on many genetic backgrounds (Jiang and Liu, 2009). Mutations in PI3Kinase or PTEN, which regulate Akt, commonly result in various kinds of tumors. In mouse, conditional deletion of PTEN (which antagonizes Akt signaling) in germ cells results in testicular teratomas 100% of the time on a mixed genetic background (Kimura et al., 2003). This is in contrast to *Dnd1*^{Ter} teratomas which only arise on a 129/SvJ genetic background (in the absence of a second mutation in *Bax*). However, *Pten* tumors develop as early neoplasias at approximately E15.5, the same as in *Dnd1*$^{Ter/Ter}$ mutants. This suggests that PTEN activity is important in germ cell mitotic arrest and tumor prevention regardless of strain background. This is consistent with a model where Akt signaling is important during PGC colonization of the gonad but must be downregulated to promote mitotic arrest and prevent teratoma initiation.

Another property of migratory PGCs is that they can be explanted to form embryonic germ (EG) cells prior to the stage when they reach the gonad and commit to their sex-specific fate (Cheng et al., 1994; Donovan and de Miguel, 2003; Labosky et al., 1994a). This transition is coincident with the upregulation of PTEN, thus Akt signaling has been implicated in PGC proliferation and derivation of EG cells. Furthermore, EG cells can be derived more efficiently from migratory PGCs with a constitutively active form of Akt (Kimura et al., 2008).

Figure 42 – Model of Akt signaling in germ cells based on the literature. **(A)** E11.5 germ cells colonizing the gonad are still actively proliferating and have active Akt signaling (C top). **(B)** E14.5 germ cells have organized into testis cords, entered mitotic arrest, and blocked Akt signaling (C bottom). **(C)** Schematic of Akt signaling presumed to be taking place in E11.5 and E14.5 germ cells.

Figure 42

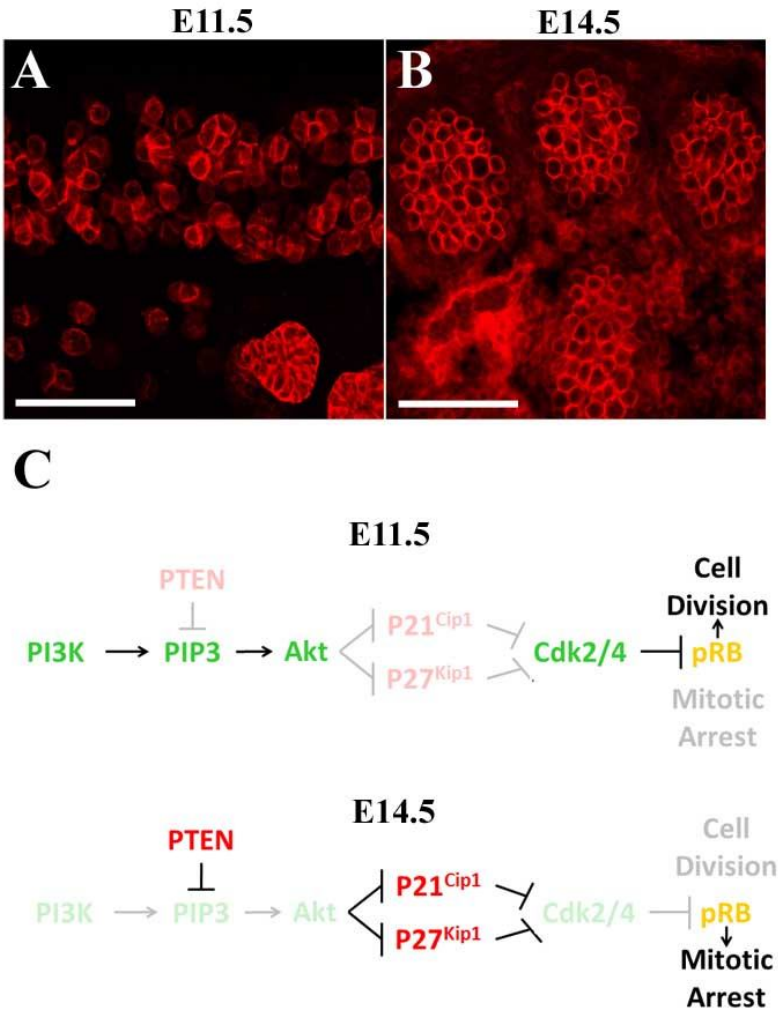
E11.5
E14.5
A
B
C
E11.5
PTEN
PI3K
PIP3
Akt
P21Cip1
P27Kip1
Cdk2/4
pRB
Cell Division
Mitotic Arrest
E14.5
PTEN
PI3K
PIP3
Akt
P21Cip1
P27Kip1
Cdk2/4
pRB
Cell Division
Mitotic Arrest

These genetic data, along with other data characterizing male germ cell mitotic arrest (Western et al., 2008), suggest that Akt signaling is active in PGCs as they colonize the gonad at E11.5 (Fig. 42A) but is suppressed by E14.5 (Fig. 42B) in male germ cells once they have entered mitotic arrest (Fig. 42C). Based on these data, one hypothesis is that Akt signaling in E14.5 *Dnd1*$^{Ter/Ter}$ mutant germ cells is maintained, which blocks cell cycle arrest and contributes to transformation.

To determine whether Akt signaling is misregulated in *Dnd1*$^{Ter/Ter}$ germ cells, antibodies to phosphorylated Akt-308 and Akt-473 were used to stain wildtype and mutant samples. Phosphorylated Akt indicates active Akt signaling and cannot distinguish between the three different *Akt* genes. Surprisingly, phospho-Akt-308 was not expressed in E11.5 germ cells (Fig. 43 left panels) but was upregulated as they entered mitotic arrest E14.5 (Fig. 43 middle and right panels). Phospho-Akt-308 staining was consistently nuclear. Staining for phospho-Akt-473 was also upregulated from E11.5 to E14.5 in arresting germ cells (Fig. 44 first three columns). Interestingly, phospho-Akt-473 staining was cytoplasmic and near the membrane. Consistently, *Dnd1*$^{Ter/Ter}$ mutant germ cells did not stain positive for phospho-Akt-473 and instead resembled E11.5 wildtype germ cells indicating their failure to reprogram and exit the migratory state (Fig. 44 right panels).

Figure 43 – phospho-Akt-308 is upregulated as male germ cells mitotically arrest. E11.5 germ cells (red, first column) are negative for pAkt-308 staining (green). E13.5 and E14.5 germ cells (middle and right columns) upregulate pAkt-308. Scale bars represent 50 m.

Figure 43

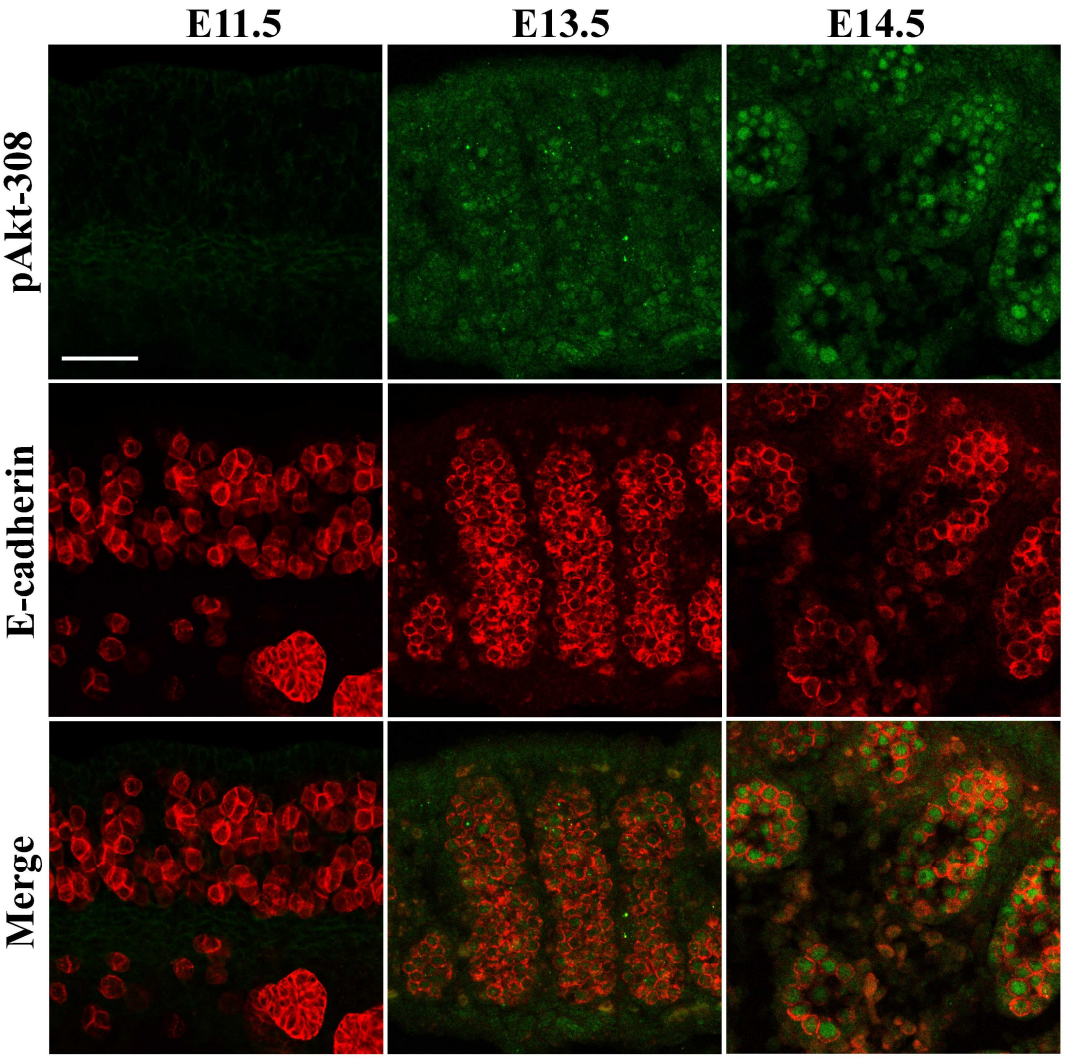

Figure 44 – phospho-Akt-473 is upregulated as male germ cells mitotically arrest. E11.5 germ cells (red, first column) are negative for pAkt-473 staining (green). E13.5 and E14.5 germ cells (middle columns) upregulate pAkt-308. E14.5 *Dnd1*$^{Ter/Ter}$ mutant germ cells do not upregulate pAkt-473 (right column) and resemble E11.5 wildtype germ cells. Scale bars represent 50 m.

Figure 44

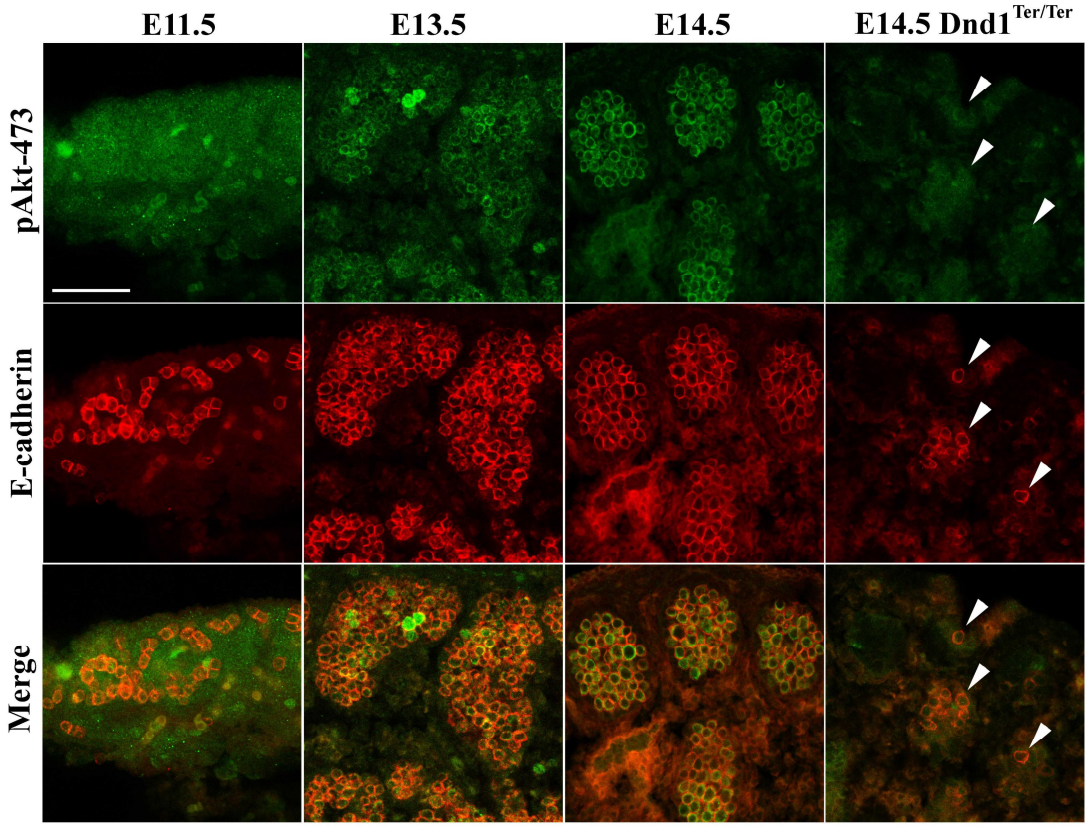

These data are the exact opposite of what was expected – phospho-Akt expressed at E14.5 and off at E11.5 instead of on at E11.5 and off at E14.5. After repeating these stains multiple times to validate the results, germ cells were isolated from E12.5-E14.5 testes and examined for expression of the three *Akt* genes (Fig. 45A). While *Akt1* levels did not change much during this time period, *Akt2* and *Akt3* were upregulated during the transition into mitotic arrest, especially *Akt3*. This suggests that *Akt2* and *Akt3* may be important in male germ cells as they exit cycle. Additionally, qPCR on mutant gonads (which contain very few germ cells) at E14.5 revealed a statistically significant decrease in *Akt3* levels compared to controls (Fig. 45B) suggesting that *Akt3* is mainly expressed in germ cells at this stage and is probably the important Akt signal relevant for this transition.

To determine whether phospho-Akt is functionally significant during mitotic arrest, XY gonads were cultured for 48 hours in the presence of the PI3Kinase inhibitor LY294002. It was first validated that phospho-Akt-308 is PI3Kinase dependent, as treatment with 25uM LY294002 antagonized phospho-Akt-308 expression but not phospho-Akt-473 (Fig. 46). Importantly, expression of $P27^{Kip1}$ and cell cycle arrest were unaffected with this treatment (Fig. 47). When gonads were cultured for 24 hours with an increased dose of LY294002 (100uM) testis cords hollowed out and it appeared that germ cell death was occurring. Stains for active Caspase-3 indicated that, at this particular dosage, most of the gonad cells undergo active cell death, which may be

responsible for the germ cell effect (Fig. 48), though specific effects on germ cells could not be ruled out.

LY294002 is a broad inhibitor of Akt signaling as its mechanism of action is to block PI3Kinase, which affects multiple signaling pathways. Another inhibitor, Akt Inhibitor V, blocks only Akt (Akt1, 2, and 3) and not PI3Kinase. XY gonads cultured with varying concentrations of Akt Inhibitor V revealed a similar germ cell phenotype (Fig. 49) at lower concentrations (10uM) without expansive cell death of the somatic cells (Fig. 49E). These preliminary data suggest that blocking Akt has a specific effect on germ cells.

Based on these data, we hypothesize that Akt signaling (specifically *Akt3*) plays a novel role in male germ cells as they enter mitotic arrest. This hypothesis has been unexplored until now, as most of the historical genetic data lead to the opposite hypothesis: that Akt signaling is important in migratory germ cells but must be downregulated for mitotic arrest (Kimura et al., 2003; Kimura et al., 2008). Perhaps phospho-Akt is necessary to prevent male germ cells from undergoing apoptosis as many cell cycle inhibitors such as *Pten*, $p27^{Kip1}$, $p21^{Cip1}$, $p57^{Kip2}$, and *p53*, known to cause senescence and apoptosis in other cell types, are upregulated in male germ cells as they enter mitotic arrest. Many questions still remain. For example, it is not clear whether apoptotic germ cells fail to express $P27^{Kip1}$ and undergo mitotic arrest prior to entering an apoptotic pathway. To further test whether phospho-Akt-473 is functionally

important, gonads will be cultured with Rapamycin to block mTOR activity which is known to phosphorylate Akt at residue 473. Additionally, both Akt Inhibitor V and Rapamycin will be used together at lower concentrations to block phosphorylation of Akt at both sites to test whether there is a synergistic effect on germ cells. Treated gonads will be examined at six hour intervals to determine whether Akt activity is upstream or downstream of mitotic arrest.

Figure 45 – *Akt3* is mainly expressed in germ cells and is upregulated as male germ cells enter mitotic arrest. **(A)** Isolated populations of E12.5-E14.5 germ cells were subjected to qRT-PCR. While *Akt1* expression does not change over this time period, both *Akt2* and *Akt3* are upregulated, especially *Akt3*. **(B)** Akt expression was quantified in control and *Dnd1*$^{Ter/Ter}$ mutant gonads at E14.5. Only *Akt3* showed a statistically significant drop in expression, along with germ cells, indicating that germ cell expression of *Akt3* represents a significant proportion of overall *Akt3* expression in the gonad at E14.5.

Figure 45

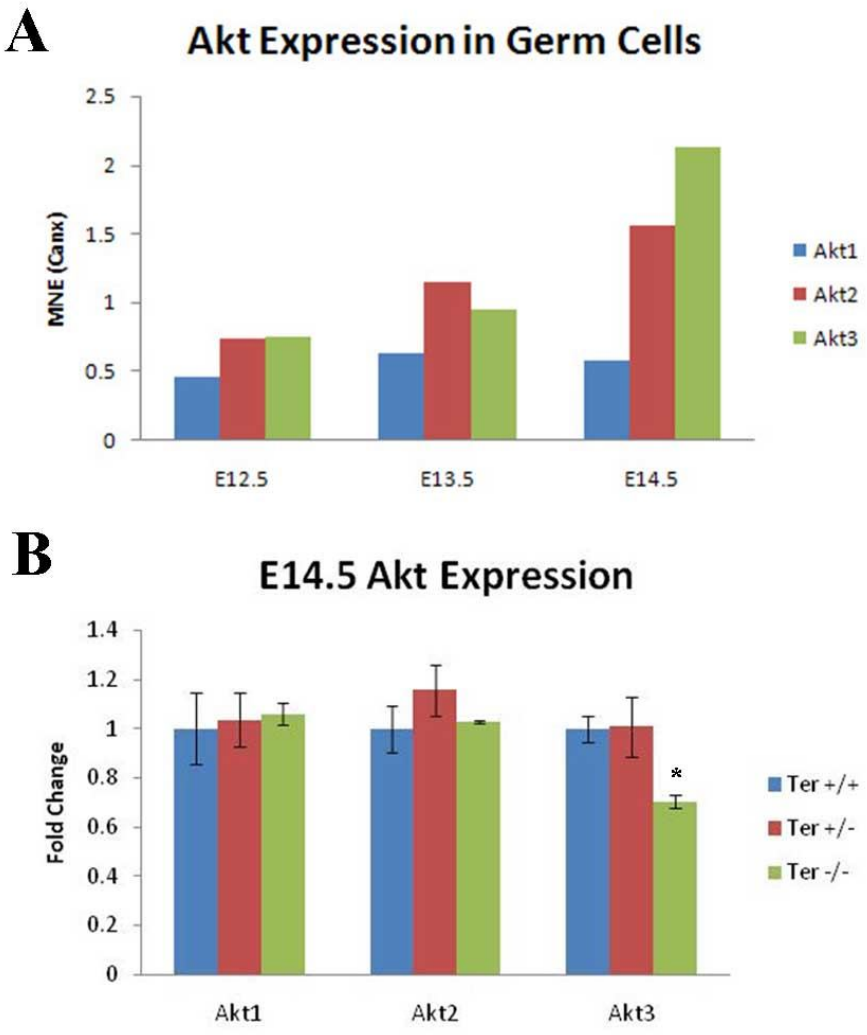
A
Akt Expression in Germ Cells
MNE (Canx)
2.5
2
1.5
1
0.5
0
E12.5
E13.5
E14.5
Akt1
Akt2
Akt3
B
E14.5 Akt Expression
Fold Change
1.4
1.2
1
0.8
0.6
0.4
0.2
0
*
Akt1
Akt2
Akt3
Ter +/+
Ter +/-
Ter -/-

Figure 46 – phospho-Akt-308 is PI3Kinase dependent. (Top section) E13.5 XY testes cultured for 48 hours in 25uM LY294002 (bottom row) lose expression of pAkt-308 compared to controls (top row). **(Bottom section)** E13.5 XY testes cultured for 48 hours in 25uM LY294002 (bottom row) do not lose expression of pAkt-473 compared to controls (top row). Scale bars represent 50μm.

Figure 46

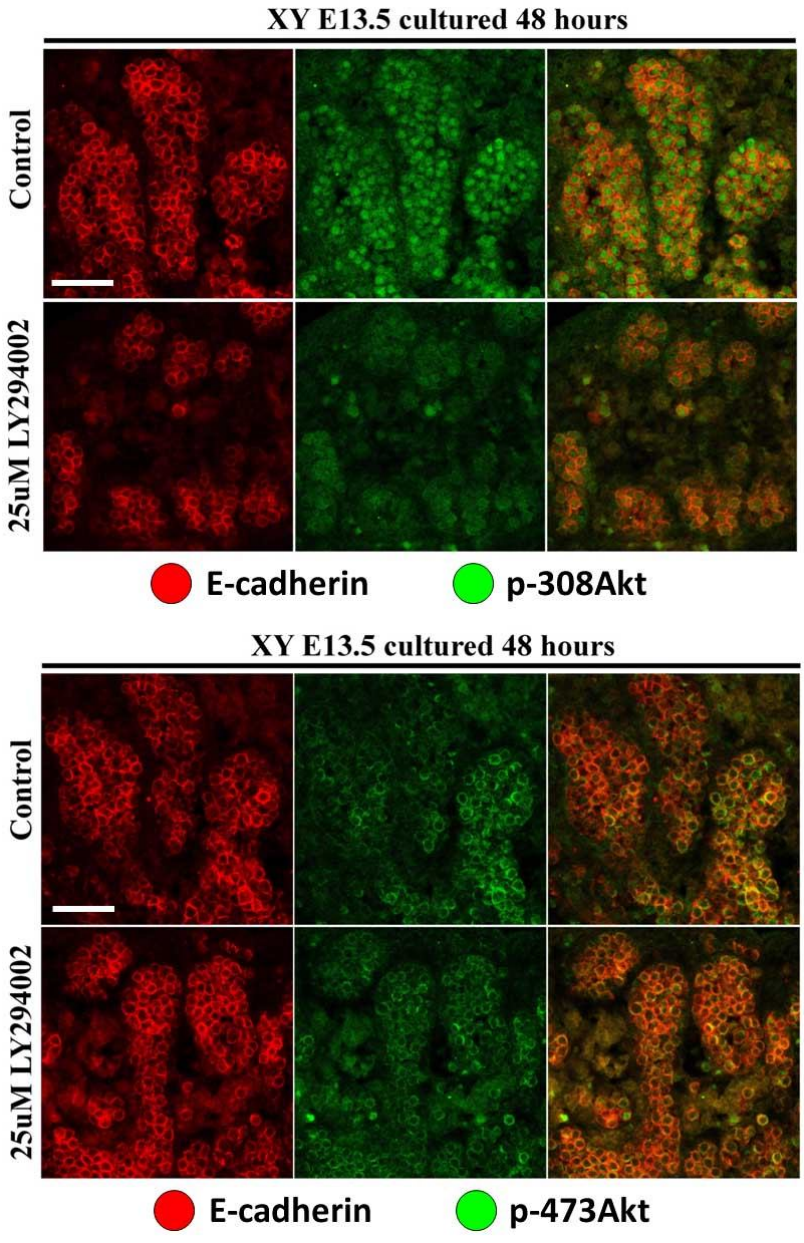
XY E13.5 cultured 48 hours
Control
25uM LY294002
E-cadherin
p-308Akt
XY E13.5 cultured 48 hours
Control
25uM LY294002
E-cadherin
p-473Akt

Figure 47 – PI3Kinase inhibition does not affect P27^{Kip1} expression or cell cycle arrest. **(Top section)** E13.5 XY testes cultured for 48 hours in 25uM LY294002 (bottom row) do not lose expression of P27^{Kip1} compared to controls (top row). **(Bottom section)** E13.5 XY testes cultured for 48 hours in 25uM LY294002 (bottom row) do not gain expression of Ki67 compared to controls (top row). Scale bars represent 50μm.

Figure 47

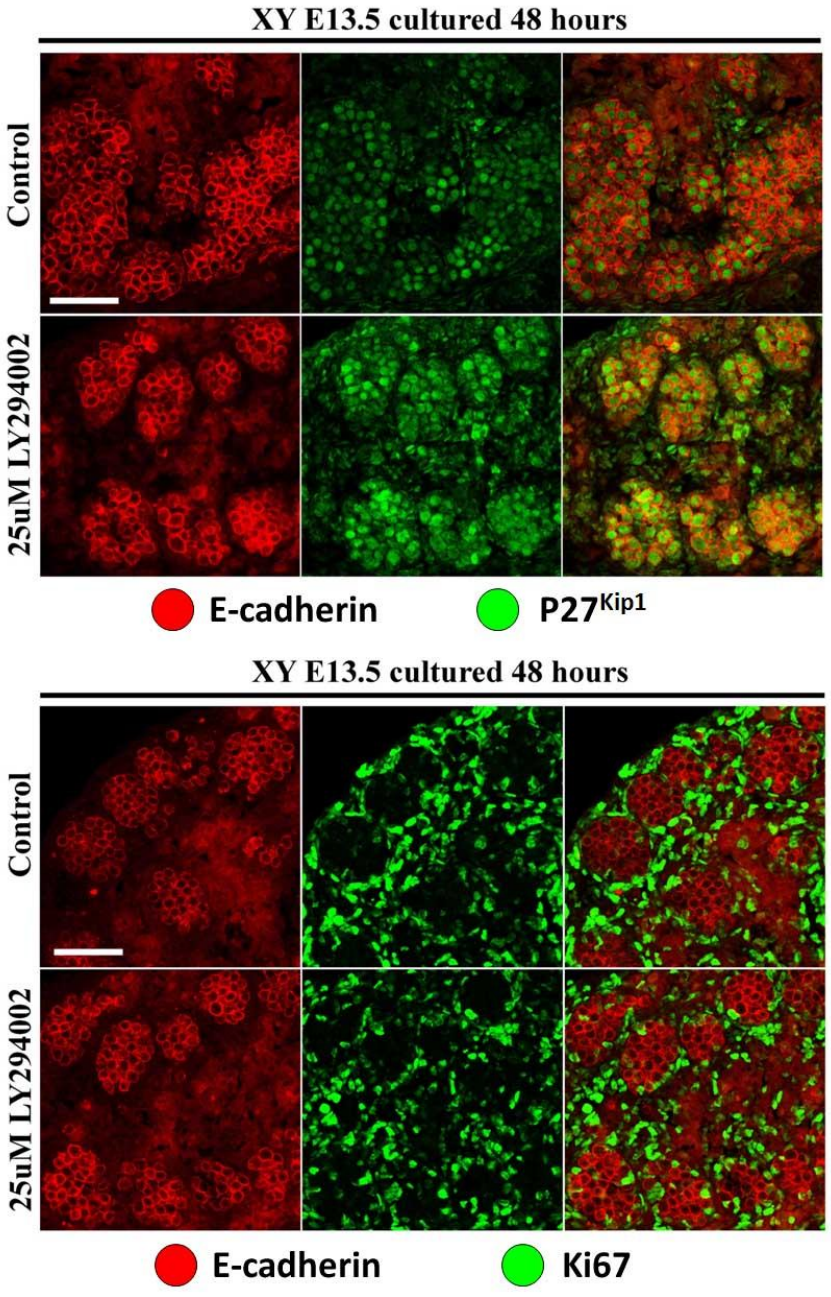
XY E13.5 cultured 48 hours
Control
25uM LY294002
E-cadherin
P27Kip1
XY E13.5 cultured 48 hours
Control
25uM LY294002
E-cadherin
Ki67

Figure 48 – Increased inhibition of PI3Kinase causes a germ cell phenotype and somatic cell death. (Top section) E13.5 XY testes cultured for 24 hours in 100uM LY294002 (bottom row) show hollow testis cords compared to controls (top row). **(Bottom section)** E13.5 XY testes cultured for 24 hours in 100uM LY294002 (bottom row) show a significant increase in active Caspase-3 (green) staining compared to controls (top row). Interestingly Caspase-3 staining does not appear in the remaining germ cells (red) in the periphery of the cords. Scale bars represent 50μm.

Figure 48

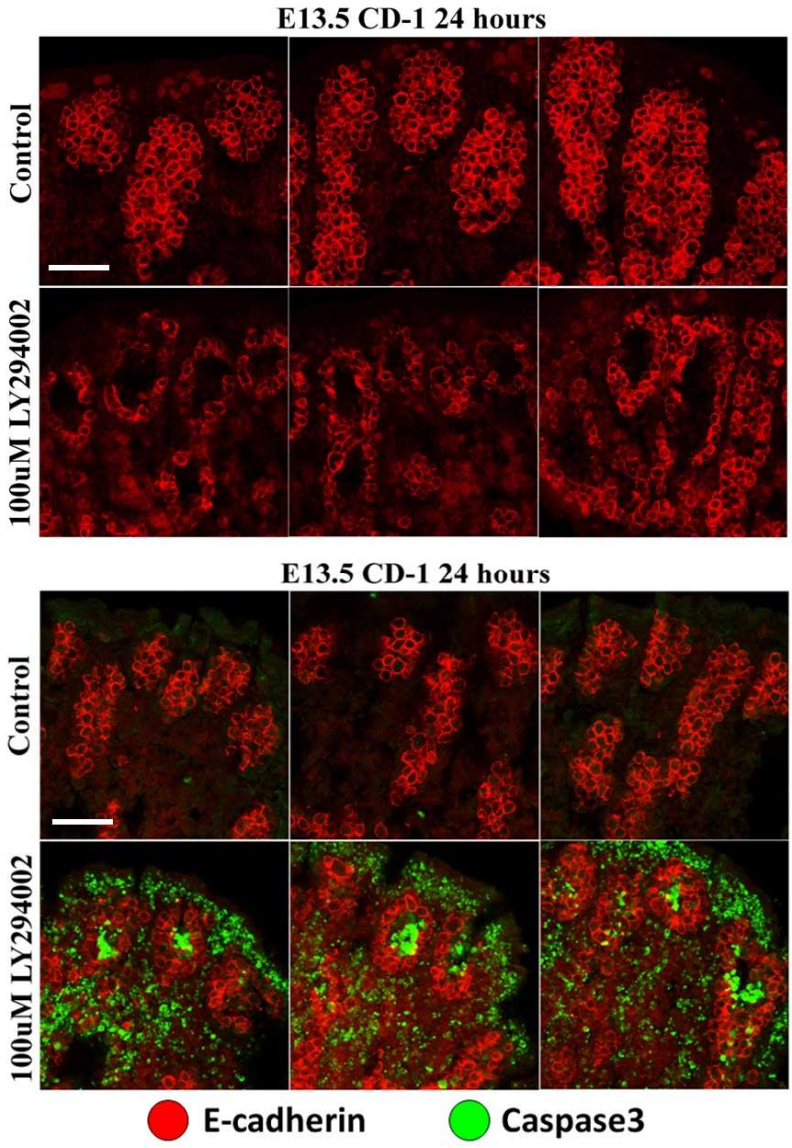
E13.5 CD-1 24 hours
Control
100uM LY294002
E13.5 CD-1 24 hours
Control
100uM LY294002
E-cadherin
Caspase3

Figure 49 – Akt Inhibitor V induces a germ cell phenotype without widespread cell death. **(A-C)** E13.5 XY control testes cultured for 24 hours. **(D-F)** E13.5 XY testes cultured for 24 hours in **(D)** 100uM, **(E)** 10uM, and **(F)** 1uM Akt Inhibitor V. 10uM of the inhibitor causes germ cell loss (red) and testis cord disorganization with minimal Caspase-3 activity (green) compared to controls. Few (if any) germ cells remain in the 100uM treated cultures and the 1uM cultures seem relatively unaffected.

Figure 49

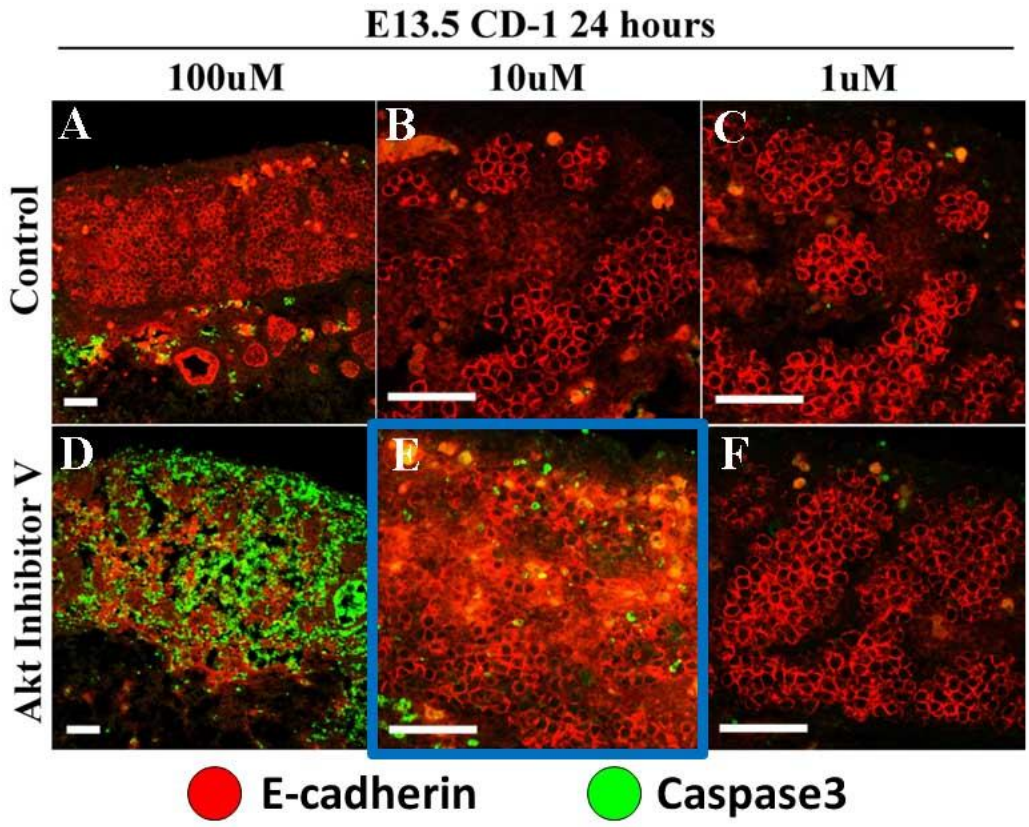
E13.5 CD-1 24 hours
100uM
10uM
1uM
A
B
C
D
E
F
Control
Akt Inhibitor V
E-cadherin
Caspase3

References

Abdelmohsen, K., Lal, A., Kim, H.H., and Gorospe, M. (2007). Posttranscriptional orchestration of an anti-apoptotic program by HuR. Cell Cycle *6*, 1288-1292.

Ancelin, K., Lange, U.C., Hajkova, P., Schneider, R., Bannister, A.J., Kouzarides, T., and Surani, M.A. (2006). Blimp1 associates with Prmt5 and directs histone arginine methylation in mouse germ cells. Nat Cell Biol *8*, 623-630.

Aramaki, S., Kubota, K., Soh, T., Yamauchi, N., and Hattori, M.A. (2009). Chicken Dead End Homologue Protein is a Nucleoprotein of Germ Cells Including Primordial Germ Cells. J Reprod Dev.

Batlle-Morera, L., Smith, A., and Nichols, J. (2008). Parameters influencing derivation of embryonic stem cells from murine embryos. Genesis *46*, 758-767.

Beck, A.R.P., Miller, I.J., Anderson, P., and Streuli, M. (1998). RNA-binding protein TIAR is essential for primordial germ cell development. Proceedings of the National Academy of Sciences of the United States of America *95*, 2331-2336.

Best, D., Sahlender, D.A., Walther, N., Peden, A.A., and Adams, I.R. (2008). Sdmg1 is a conserved transmembrane protein associated with germ cell sex determination and germline-soma interactions in mice. Development *135*, 1415-1425.

Bhattacharya, C., Aggarwal, S., Zhu, R., Kumar, M., Zhao, M., Meistrich, M.L., and Matin, A. (2007). The mouse dead-end gene isoform alpha is necessary for germ cell and embryonic viability. Biochemical and Biophysical Research Communications *355*, 194-199.

Biedermann, B., Wright, J., Senften, M., Kalchhauser, I., Sarathy, G., Lee, M.H., and Ciosk, R. (2009). Translational repression of cyclin E prevents precocious mitosis and embryonic gene activation during C. elegans meiosis. Dev Cell *17*, 355-364.

Bowles, J., Knight, D., Smith, C., Wilhelm, D., Richman, J., Mamiya, S., Yashiro, K., Chawengsaksophak, K., Wilson, M.J., Rossant, J., *et al.* (2006). Retinoid signaling determines germ cell fate in mice. Science *312*, 596-600.

Bowles, J., and Koopman, P. (2007). Retinoic acid, meiosis and germ cell fate in mammals. Development *134*, 3401-3411.

Brown, L.M., Pottern, L.M., and Hoover, R.N. (1987). Testicular Cancer in Young Men - the Search for Causes of the Epidemic Increase in the United-States. Journal of Epidemiology and Community Health *41*, 349-354.

Brown, L.M., Pottern, L.M., Hoover, R.N., Devesa, S.S., Aselton, P., and Flannery, J.T. (1986). Testicular Cancer in the United-States - Trends in Incidence and Mortality. International Journal of Epidemiology *15*, 164-170.

Buehr, M., McLaren, A., Bartley, A., and Darling, S. (1993). Proliferation and migration of primordial germ cells in We/We mouse embryos. Dev-Dyn *198*, 182-189 issn: 1058-8388.

Cheng, L., Gearing, D.P., White, L.S., Compton, D.L., Schooley, K., and Donovan, P.J. (1994). Role of leukemia inhibitory factor and its receptor in mouse primordial germ cell growth. Development *120*, 3145-3153.

Cook, M.S., Coveney, D., Batchvarov, I., Nadeau, J.H., and Capel, B. (2009). BAX-mediated cell death affects early germ cell loss and incidence of testicular teratomas in Dnd1Ter/Ter mice. Dev Biol *328*, 377-383.

DiNapoli, L., Batchvarov, J., and Capel, B. (2006). FGF9 promotes survival of germ cells in the fetal testis. Development *133*, 1519-1527.

Donovan, P.J., and de Miguel, M.P. (2003). Turning germ cells into stem cells. Curr Opin Genet Dev *13*, 463-471.

Durcova-Hills, G., Ainscough, J., and McLaren, A. (2001). Pluripotential stem cells derived from migrating primordial germ cells. Differentiation *68*, 220-226.

Durcova-Hills, G., and Capel, B. (2008). Chapter 6 development of germ cells in the mouse. Curr Top Dev Biol *83*, 185-212.

Forbes, A., and Lehmann, R. (1998). Nanos and Pumilio have critical roles in the development and function of Drosophila germline stem cells. Development *125*, 679-690.

Fujii, T., Mitsunaga-Nakatsubo, K., Saito, I., Iida, H., Sakamoto, N., Akasaka, K., and Yamamoto, T. (2006). Developmental expression of HpNanos, the Hemicentrotus pulcherrimus homologue of nanos. Gene Expr Patterns *6*, 572-577.

Fujiwara, Y., Komiya, T., Kawabata, H., Sato, M., Fujimoto, H., Furusawa, M., and Noce, T. (1994). Isolation of a DEAD-family protein gene that encodes a murine homolog of

Drosophila vasa and its specific expression in germ cell lineage. Proc Natl Acad Sci U S A *91*, 12258-12262.

Gidekel, S., Pizov, G., Bergman, Y., and Pikarsky, E. (2003). Oct-3/4 is a dose-dependent oncogenic fate determinant. Cancer Cell *4*, 361-370.

Godin, I., Wylie, C., and Heasman, J. (1990). Genital ridges exert long-range effects on mouse primordial germ cell numbers and direction of migration in culture. Development *108*, 357-363.

Guan, K., Nayernia, K., Maier, L.S., Wagner, S., Dressel, R., Lee, J.H., Nolte, J., Wolf, F., Li, M., Engel, W., *et al.* (2006). Pluripotency of spermatogonial stem cells from adult mouse testis. Nature *440*, 1199-1203.

Hammond, S., Zhu, R., Youngren, K.K., Lam, J., Anderson, P., and Matin, A. (2007). Chromosome X modulates incidence of testicular germ cell tumors in Ter mice. Mamm Genome *18*, 832-838.

Hayashi, K., Chuva de Sousa Lopes, S.M., Kaneda, M., Tang, F., Hajkova, P., Lao, K., O'Carroll, D., Das, P.P., Tarakhovsky, A., Miska, E.A., *et al.* (2008). MicroRNA biogenesis is required for mouse primordial germ cell development and spermatogenesis. PLoS ONE *3*, e1738.

Heaney, J.D., Michelson, M.V., Youngren, K.K., Lam, M.Y., and Nadeau, J.H. (2009). Deletion of eIF2beta suppresses testicular cancer incidence and causes recessive lethality in agouti-yellow mice. Hum Mol Genet.

Henrique, D., Adam, J., Myat, A., Chitnis, A., Lewis, J., and Ish-Horowicz, D. (1995). Expression of a Delta homologue in prospective neurons in the chick. Nature *375*, 787-790.

Hook, B., Bernstein, D., Zhang, B., and Wickens, M. (2005). RNA-protein interactions in the yeast three-hybrid system: affinity, sensitivity, and enhanced library screening. RNA *11*, 227-233.

Horvay, K., Claussen, M., Katzer, M., Landgrebe, J., and Pieler, T. (2006). Xenopus Dead end mRNA is a localized maternal determinant that serves a conserved function in germ cell development. Dev Biol *291*, 1-11.

Hosokawa, M., Shoji, M., Kitamura, K., Tanaka, T., Noce, T., Chuma, S., and Nakatsuji, N. (2007). Tudor-related proteins TDRD1/MTR-1, TDRD6 and TDRD7/TRAP: domain

composition, intracellular localization, and function in male germ cells in mice. Dev Biol *301*, 38-52.

Hussain, S.A., Ma, Y.T., Palmer, D.H., Hutton, P., and Cullen, M.H. (2008). Biology of testicular germ cell tumors. Expert Rev Anticancer Ther *8*, 1659-1673.

Ishii, M., Tachiwana, T., Hoshino, A., Tsunekawa, N., Hiramatsu, R., Matoba, S., Kanai-Azuma, M., Kawakami, H., Kurohmaru, M., and Kanai, Y. (2007). Potency of testicular somatic environment to support spermatogenesis in XX/Sry transgenic male mice. Development *134*, 449-454.

Jaruzelska, J., Kotecki, M., Kusz, K., Spik, A., Firpo, M., and Reijo Pera, R.A. (2003). Conservation of a Pumilio-Nanos complex from Drosophila germ plasm to human germ cells. Dev Genes Evol *213*, 120-126.

Jiang, B.H., and Liu, L.Z. (2009). PI3K/PTEN signaling in angiogenesis and tumorigenesis. Adv Cancer Res *102*, 19-65.

Jiang, L.I., and Nadeau, J.H. (2001). 129/Sv mice--a model system for studying germ cell biology and testicular cancer. Mamm Genome *12*, 89-94.

Kadyrova, L.Y., Habara, Y., Lee, T.H., and Wharton, R.P. (2007). Translational control of maternal Cyclin B mRNA by Nanos in the Drosophila germline. Development *134*, 1519-1527.

Kanatsu-Shinohara, M., Inoue, K., Lee, J., Yoshimoto, M., Ogonuki, N., Miki, H., Baba, S., Kato, T., Kazuki, Y., Toyokuni, S., *et al.* (2004). Generation of pluripotent stem cells from neonatal mouse testis. Cell *119*, 1001-1012.

Kanatsu-Shinohara, M., Lee, J., Inoue, K., Ogonuki, N., Miki, H., Toyokuni, S., Ikawa, M., Nakamura, T., Ogura, A., and Shinohara, T. (2008a). Pluripotency of a single spermatogonial stem cell in mice. Biol Reprod *78*, 681-687.

Kanatsu-Shinohara, M., Takehashi, M., and Shinohara, T. (2008b). Brief History, Pitfalls, and Prospects of Mammalian Spermatogonial Stem Cell Research. Cold Spring Harb Symp Quant Biol.

Kedde, M., and Agami, R. (2008). Interplay between microRNAs and RNA-binding proteins determines developmental processes. Cell Cycle *7*, 899-903.

Kedde, M., Strasser, M.J., Boldajipour, B., Oude Vrielink, J.A., Slanchev, K., le Sage, C., Nagel, R., Voorhoeve, P.M., van Duijse, J., Orom, U.A., *et al.* (2007a). RNA-binding protein Dnd1 inhibits microRNA access to target mRNA. Cell *131*, 1273-1286.

Kedde, M., Strasser, M.J., Boldajipour, B., Vrielink, J.A., Slanchev, K., le Sage, C., Nagel, R., Voorhoeve, P.M., van Duijse, J., Orom, U.A., *et al.* (2007b). RNA-binding protein Dnd1 inhibits microRNA access to target mRNA. Cell *131*, 1273-1286.

Keene, J.D. (2007). RNA regulons: coordination of post-transcriptional events. Nat Rev Genet *8*, 533-543.

Keene, J.D., Komisarow, J.M., and Friedersdorf, M.B. (2006). RIP-Chip: the isolation and identification of mRNAs, microRNAs and protein components of ribonucleoprotein complexes from cell extracts. Nat Protoc *1*, 302-307.

Kim, Y., Kobayashi, A., Sekido, R., DiNapoli, L., Brennan, J., Chaboissier, M.C., Poulat, F., Behringer, R.R., Lovell-Badge, R., and Capel, B. (2006). Fgf9 and Wnt4 act as antagonistic signals to regulate mammalian sex determination. PLoS Biol *4*, e187.

Kimble, J., and Crittenden, S.L. (2005). Germline proliferation and its control In The Celegans Research Community, WormBook.

Kimura, T., Suzuki, A., Fujita, Y., Yomogida, K., Lomeli, H., Asada, N., Ikeuchi, M., Nagy, A., Mak, T.W., and Nakano, T. (2003). Conditional loss of PTEN leads to testicular teratoma and enhances embryonic germ cell production. Development *130*, 1691-1700.

Kimura, T., Tomooka, M., Yamano, N., Murayama, K., Matoba, S., Umehara, H., Kanai, Y., and Nakano, T. (2008). AKT signaling promotes derivation of embryonic germ cells from primordial germ cells. Development *135*, 869-879.

Koprunner, M., Thisse, C., Thisse, B., and Raz, E. (2001). A zebrafish nanos-related gene is essential for the development of primordial germ cells. Genes Dev *15*, 2877-2885.

Krentz, A.D., Murphy, M.W., Kim, S., Cook, M.S., Capel, B., Zhu, R., Matin, A., Sarver, A.L., Parker, K.L., Griswold, M.D., *et al.* (2009). The DM domain protein DMRT1 is a dose-sensitive regulator of fetal germ cell proliferation and pluripotency. Proc Natl Acad Sci U S A.

Krentz, A.D., Murphy, M. W., Zhu, R., Matin, A., Cook, M. S., Capel, B., Sarver, A. L., Parker, K. L., Looijenga, L. H. J., Griswold, M. D., Bardwell, V. J., Zarkower, D. (2009). The DM domain protein DMRT1 is a dose-sensitive regulator of embryonic germ cell pluripotency and proliferation. Proc Natl Acad Sci U S A.

Labosky, P.A., Barlow, D.P., and Hogan, B.L. (1994a). Embryonic germ cell lines and their derivation from mouse primordial germ cells. Ciba Found Symp *182*, 157-168.

Labosky, P.A., Barlow, D.P., and Hogan, B.L. (1994b). Mouse embryonic germ (EG) cell lines: transmission through the germline and differences in the methylation imprint of insulin-like growth factor 2 receptor (Igf2r) gene compared with embryonic stem (ES) cell lines. Development *120*, 3197-3204.

Lam, M.Y., Heaney, J.D., Youngren, K.K., Kawasoe, J.H., and Nadeau, J.H. (2007). Trans-generational epistasis between Dnd1Ter and other modifier genes controls susceptibility to testicular germ cell tumors. Hum Mol Genet *16*, 2233-2240.

Lam, M.Y., and Nadeau, J.H. (2003). Genetic control of susceptibility to spontaneous testicular germ cell tumors in mice. APMIS *111*, 184-190; discussion 191.

Lawson, K.A., Dunn, N.R., Roelen, B.A., Zeinstra, L.M., Davis, A.M., Wright, C.V., Korving, J.P., and Hogan, B.L. (1999). Bmp4 is required for the generation of primordial germ cells in the mouse embryo. Genes Dev *13*, 424-436.

Lehmann, R., and Nusslein-Volhard, C. (1991). The maternal gene nanos has a central role in posterior pattern formation of the Drosophila embryo. Development *112*, 679-691.

Lin, Y., and Page, D.C. (2005). Dazl deficiency leads to embryonic arrest of germ cell development in XY C57BL/6 mice. Dev Biol *288*, 309-316.

Linger, R., Dudakia, D., Huddart, R., Easton, D., Bishop, D.T., Stratton, M.R., and Rapley, E.A. (2007). A physical analysis of the Y chromosome shows no additional deletions, other than Gr/Gr, associated with testicular germ cell tumour. Br J Cancer *96*, 357-361.

Looijenga, L.H. (2009). Human testicular (non)seminomatous germ cell tumours: the clinical implications of recent pathobiological insights. Journal of Pathology.

Massague, J. (2004). G1 cell-cycle control and cancer. Nature *432*, 298-306.

Matsui, Y. (1998). Developmental fates of the mouse germ cell line. Int J Dev Biol *42*, 1037.

Mazan-Mamczarz, K., Hagner, P.R., Corl, S., Srikantan, S., Wood, W.H., Becker, K.G., Gorospe, M., Keene, J.D., Levenson, A.S., and Gartenhaus, R.B. (2008). Post-transcriptional gene regulation by HuR promotes a more tumorigenic phenotype. Oncogene *27*, 6151-6163.

McLaren, A. (1984). Meiosis and differentiation of mouse germ cells. Symp Soc Exp Biol *38*, 7-23.

McLaren, A. (1988). Somatic and germ-cell sex in mammals. Philos Trans R Soc Lond B Biol Sci *322*, 3-9.

McLaren, A. (2001). Mammalian germ cells: birth, sex, and immortality. Cell Struct Funct *26*, 119-122.

McLaren, A., and Southee, D. (1997). Entry of mouse embryonic germ cells into meiosis. Dev Biol *187*, 107-113.

Mintz, B., and Russell, E.S. (1957). Gene-induced embryological modifications of primordial germ cells in the mouse. J Exp Zool *134*, 207-237.

Mishima, Y., Giraldez, A.J., Takeda, Y., Fujiwara, T., Sakamoto, H., Schier, A.F., and Inoue, K. (2006). Differential regulation of germline mRNAs in soma and germ cells by zebrafish miR-430. Curr Biol *16*, 2135-2142.

Molyneaux, K.A., Zinszner, H., Kunwar, P.S., Schaible, K., Stebler, J., Sunshine, M.J., O'Brien, W., Raz, E., Littman, D., Wylie, C., *et al.* (2003). The chemokine SDF1/CXCL12 and its receptor CXCR4 regulate mouse germ cell migration and survival. Development *130*, 4279-4286.

Munger, S.A., D.L. Syed, H.A. Magwene, P.M. Threadgill, D.W. Capel, B. (2009). Elucidation of the transcription network governing mammalian sex determination by exploiting strain-specific susceptibility to sex reversal Genes Dev *23*.

Noguchi, M., Watanabe, C., Kobayashi, T., Kuwashima, M., Sakurai, T., Katoh, H., and Moriwaki, K. (1996). The ter mutation responsible for germ cell deficiency but not testicular nor ovarian teratocarcinogenesis in ter/ter congenic mice. Development Growth & Differentiation *38*, 59-69.

Noguchi, T., and Noguchi, M. (1985). A recessive mutation (ter) causing germ cell deficiency and a high incidence of congenital testicular teratomas in 129/Sv-ter mice. J Natl Cancer Inst *75*, 385-392.

Ohbo, K., Yoshida, S., Ohmura, M., Ohneda, O., Ogawa, T., Tsuchiya, H., Kuwana, T., Kehler, J., Abe, K., Scholer, H.R., *et al.* (2003). Identification and characterization of stem cells in prepubertal spermatogenesis in mice small star, filled. Dev Biol *258*, 209-225.

Ohinata, Y., Ohta, H., Shigeta, M., Yamanaka, K., Wakayama, T., and Saitou, M. (2009). A signaling principle for the specification of the germ cell lineage in mice. Cell *137*, 571-584.

Ohinata, Y., Seki, Y., Payer, B., O'Carroll, D., Surani, M.A., and Saitou, M. (2006). Germline recruitment in mice: a genetic program for epigenetic reprogramming. Ernst Schering Res Found Workshop, 143-174.

Oosterhuis, J.W., and Looijenga, L.H. (2005). Testicular germ-cell tumours in a broader perspective. Nat Rev Cancer *5*, 210-222.

Raymond, C.S.M.M.W.O.S.M.G.B.V.J.Z.D. (2000). Dmrt1, a gene related to worm and fly sexual regulators, is required for mammalian testis differentiation. Genes Dev *14*, 2587.

Raz, E. (2000). The function and regulation of vasa-like genes in germ-cell development. Genome Biol *1*, REVIEWS1017.

Rivers, E.N., and Hamilton, D.W. (1986). Morphologic analysis of spontaneous teratocarcinogenesis in developing testes of strain 129/Sv-ter mice. Am J Pathol *124*, 263-280.

Sada, A., Suzuki, A., Suzuki, H., and Saga, Y. (2009). The RNA-binding protein NANOS2 is required to maintain murine spermatogonial stem cells. Science *325*, 1394-1398.

Saga, Y. (2008). Mouse germ cell development during embryogenesis. Curr Opin Genet Dev *18*, 337-341.

Saitou, M. (2009). Germ cell specification in mice. Curr Opin Genet Dev.

Sakurai, T., Iguchi, T., Moriwaki, K., and Noguchi, M. (1995a). The ter mutation first causes primordial germ cell deficiency in ter/ter mouse embryos at 8 days of gestation. Development Growth & Differentiation *37*, 293-302.

Sakurai, T., Iguchi, T., Moriwaki, K., and Noguchi, M. (1995b). The ter mutation first causes primordial germ clel deficiency in ter/ter mouse embryos at 8 days of gestation. Development Growth Differentiation *37*, 293-302.

Sekido, R., Bar, I., Narvaez, V., Penny, G., and Lovell-Badge, R. (2004). SOX9 is up-regulated by the transient expression of SRY specifically in Sertoli cell precursors. Dev Biol *274*, 271-279.

Sekido, R., and Lovell-Badge, R. (2008). Sex determination involves synergistic action of SRY and SF1 on a specific Sox9 enhancer. Nature *453*, 930-934.

Sengupta, D.J., Wickens, M., and Fields, S. (1999). Identification of RNAs that bind to a specific protein using the yeast three-hybrid system. RNA *5*, 596-601.

Seydoux, G., and Braun, R.E. (2006). Pathway to totipotency: lessons from germ cells. Cell *127*, 891-904.

Shen, R., Weng, C., Yu, J., and Xie, T. (2009). eIF4A controls germline stem cell self-renewal by directly inhibiting BAM function in the Drosophila ovary. Proc Natl Acad Sci U S A *106*, 11623-11628.

Slanchev, K., Stebler, J., Goudarzi, M., Cojocaru, V., Weidinger, G., and Raz, E. (2008). Control of Dead end localization and activity - Implications for the function of the protein in antagonizing miRNA function. Mech Dev.

Solter, D. (2006). From teratocarcinomas to embryonic stem cells and beyond: a history of embryonic stem cell research. Nat Rev Genet *7*, 319-327.

Stallock, J., Molyneaux, K., Schaible, K., Knudson, C.M., and Wylie, C. (2003). The pro-apoptotic gene Bax is required for the death of ectopic primordial germ cells during their migration in the mouse embryo. Development *130*, 6589-6597.

Stevens, L.C. (1970a). The development of transplantable teratocarcinomas from intratesticular grafts of pre- and postimplantation mouse embryos. Dev-Biol *21*, 364-382 issn: 0012-1606.

Stevens, L.C. (1970b). Environmental influence on experimental teratocarcinogenesis in testes of mice. J-Exp-Zool *174*, 407-414 issn: 0022-0104x.

Stevens, L.C. (1973). A new inbred subline of mice (129-terSv) with a high incidence of spontaneous congenital testicular teratomas. J-Natl-Cancer-Inst *50*, 235-242 issn: 0027-8874.

Stevens, L.C. (1981). Genetic influences on teratocarcinogenesis and parthenogenesis. Prog Clin Biol Res *45*, 93-104.

Stevens, L.C., and Little, C.C. (1954). Spontaneous Testicular Teratomas in an Inbred Strain of Mice. Proc Natl Acad Sci U S A *40*, 1080-1087.

Strome, S., and Lehmann, R. (2007). Germ versus soma decisions: lessons from flies and worms. Science *316*, 392-393.

Stumpf, C.R., Opperman, L., and Wickens, M. (2008). Chapter 14. Analysis of RNA-protein interactions using a yeast three-hybrid system. Methods Enzymol *449*, 295-315.

Suzuki, A., and Saga, Y. (2008). Nanos2 suppresses meiosis and promotes male germ cell differentiation. Genes Dev *22*, 430-435.

Suzuki, H., Tsuda, M., Kiso, M., and Saga, Y. (2008). Nanos3 maintains the germ cell lineage in the mouse by suppressing both Bax-dependent and -independent apoptotic pathways. Dev Biol *318*, 133-142.

Takabayashi, S., Sasaoka, Y., Yamashita, M., Tokumoto, T., Ishikawa, K., and Noguchi, M. (2001). Novel growth factor supporting survival of murine primordial germ cells: evidence from conditioned medium of ter fetal gonadal somatic cells. Mol Reprod Dev *60*, 384-396.

Takeuchi, Y., Molyneaux, K., Runyan, C., Schaible, K., and Wylie, C. (2005). The roles of FGF signaling in germ cell migration in the mouse. Development *132*, 5399-5409.

Tanaka, S.S., Toyooka, Y., Akasu, R., Katoh-Fukui, Y., Nakahara, Y., Suzuki, R., Yokoyama, M., and Noce, T. (2000). The mouse homolog of Drosophila Vasa is required for the development of male germ cells. Genes Dev *14*, 841-853.

Tang, H., Ross, A., and Capel, B. (2008). Expression and functional analysis of Gm114, a putative mammalian ortholog of Drosophila bam. Dev Biol *318*, 73-81.

Threadgill, D.W., Yee, D., Matin, A., Nadeau, J.H., and Magnuson, T. (1997). Genealogy of the 129 inbred strains: 129/SvJ is a contaminated inbred strain. Mamm Genome *8*, 390-393.

Tsuda, M., Kiso, M., and Saga, Y. (2006). Implication of nanos2-3'UTR in the expression and function of nanos2. Mech Dev *123*, 440-449.

Tsuda, M., Sasoaka, Y., Kiso, M., Abe, K., Haraguchi, S., Kobayashi, S., and Saga, Y. (2003). Conserved Role of nanos Proteins in Germ Cell Development. Science *301*, 1239-1241.

Urano, J., Fox, M.S., and Reijo Pera, R.A. (2005). Interaction of the conserved meiotic regulators, BOULE (BOL) and PUMILIO-2 (PUM2). Mol Reprod Dev *71*, 290-298.

Weidinger, G., Stebler, J., Slanchev, K., Dumstrei, K., Wise, C., Lovell-Badge, R., Thisse, C., Thisse, B., and Raz, E. (2003). dead end, a novel vertebrate germ plasm component, is

required for zebrafish primordial germ cell migration and survival. Curr Biol *13*, 1429-1434.

Wein, A.J., Kavoussi, L.R., Novick, A.C., Partin, A.W., and Peters, C.A. (2007). Campbell-Walsh Urology, 9th edn (WB Saunders Co.).

Western, P. (2009). Foetal germ cells: striking the balance between pluripotency and differentiation. Int J Dev Biol *53*, 393-409.

Western, P.S., Miles, D.C., van den Bergen, J.A., Burton, M., and Sinclair, A.H. (2008). Dynamic regulation of mitotic arrest in fetal male germ cells. Stem Cells *26*, 339-347.

Yabuta, Y., Kurimoto, K., Ohinata, Y., Seki, Y., and Saitou, M. (2006). Gene expression dynamics during germline specification in mice identified by quantitative single-cell gene expression profiling. Biol Reprod *75*, 705-716.

Yamanaka, S. (2009). Elite and stochastic models for induced pluripotent stem cell generation. Nature *460*, 49-52.

Youngren, K.K., Coveney, D., Peng, X., Bhattacharya, C., Schmidt, L.S., Nickerson, M.L., Lamb, B.T., Deng, J.M., Behringer, R.R., Capel, B., *et al.* (2005). The Ter mutation in the dead end gene causes germ cell loss and testicular germ cell tumours. Nature *435*, 360-364.

Zhang, B., Kraemer, B., SenGupta, D., Fields, S., and Wickens, M. (1999). Yeast three-hybrid system to detect and analyze interactions between RNA and protein. Methods Enzymol *306*, 93-113.

Zhao, G.Q., and Garbers, D.L. (2002). Male germ cell specification and differentiation. Dev Cell *2*, 537-547.

Biography

Matthew Simon Cook was born at 11:29AM on March 28th, 1983 in Wilson, NC to the parents of Simon Hoy Cooke Jr. and Donna Louise Rogers Cook. The majority of his childhood was spent in eastern North Carolina, growing up in a small town called Nashville (not to be confused with the bigger one in Tennessee, which has more stoplights and a bigger music scene). After graduating from Northern Nash Senior High School in 2001 with an International Baccalaureate Diploma (and as an Eagle Scout), Matthew attended East Carolina University in Greenville, NC on a full scholarship from the EC scholars program. At ECU he majored in Biology and minored in Hispanic Studies. During this time he studied abroad for six months in Sevilla, España at La Universidad de Sevilla. After graduation, he matriculated into the Cell and Molecular Biology Program at Duke University in 2005. He joined Blanche Capel's laboratory and the Department of Cell Biology in 2006.

Publications:

Cook M. S., Nadeau J. H., Capel B. The RNA binding protein DND1 regulates pluripotency, cell cycle, and male differentiation in germ cells of the fetal testis. In preparation.

Cook, M. S., Capel, B., 2010. Shifting gears and putting on the brakes: Female germ cells transition into meiosis. Cell Cycle. 9.

Krentz, A. D., Murphy, M. W., Kim, S., **Cook, M. S.**, Capel, B., Zhu, R., Matin, A., Sarver, A. L., Parker, K. L., Griswold, M. D., Looijenga, L. H., Bardwell, V. J., Zarkower,

D., 2009. The DM domain protein DMRT1 is a dose-sensitive regulator of fetal germ cell proliferation and pluripotency. Proc Natl Acad Sci U S A.

Cook, M. S., Coveney, D., Batchvarov, I., Nadeau, J. H., Capel, B., 2009. BAX-mediated cell death affects early germ cell loss and incidence of testicular teratomas in Dnd1Ter/Ter mice. Developmental Biology. 328**,** 377-383.

Stiller, J. W., **Cook, M. S.**, 2004. Functional unit of the RNA polymerase II C-terminal domain lies within heptapeptide pairs. Eukaryot Cell. 3**,** 735-40.

Awards:

Alexander and Margaret Stewart Trust fellowship recipient

Vertebrate Sex Determination meeting travel fellowship

Member of the Society for Developmental Biology

Teacher and Scientist Coalition (TASC) fellowship from Glaxo-Smith-Kline

BOOST summer immersion education fellowship